© Copyright Princeton University Press. No part of this book may be distributed, posted, or reproduced in any form by digital or mechanical means without prior written permission of the publisher.

CONTENTS

List of Boxes xiii

Preface xv

Contents of *Modern Classical Physics*, volumes 1–5 xxiii

PART IV ELASTICITY 565

11 Elastostatics 567

11.1 Overview 567

11.2 Displacement and Strain 570

11.2.1 Displacement Vector and Its Gradient 570

11.2.2 Expansion, Rotation, Shear, and Strain 571

11.3 Stress, Elastic Moduli, and Elastostatic Equilibrium 577

11.3.1 Stress Tensor 577

11.3.2 Realm of Validity for Hooke's Law 580

11.3.3 Elastic Moduli and Elastostatic Stress Tensor 580

11.3.4 Energy of Deformation 582

11.3.5 Thermoelasticity 584

11.3.6 Molecular Origin of Elastic Stress; Estimate of Moduli 585

11.3.7 Elastostatic Equilibrium: Navier-Cauchy Equation 587

11.4 Young's Modulus and Poisson's Ratio for an Isotropic Material: A Simple Elastostatics Problem 589

11.5 Reducing the Elastostatic Equations to 1 Dimension for a Bent Beam: Cantilever Bridge, Foucault Pendulum, DNA Molecule, Elastica 592

11.6 Buckling and Bifurcation of Equilibria 602

11.6.1 Elementary Theory of Buckling and Bifurcation 602

11.6.2 Collapse of the World Trade Center Buildings 605

11.6.3 Buckling with Lateral Force; Connection to Catastrophe Theory 606

11.6.4 Other Bifurcations: Venus Fly Trap, Whirling Shaft, Triaxial Stars, and Onset of Turbulence 607

T2 Track Two; see page xvii

For general queries contact webmaster@press.princeton.edu.

© Copyright Princeton University Press. No part of this book may be distributed, posted, or reproduced in any form by digital or mechanical means without prior written permission of the publisher.

11.7 Reducing the Elastostatic Equations to 2 Dimensions for a Deformed Thin Plate: Stress Polishing a Telescope Mirror 609
11.8 Cylindrical and Spherical Coordinates: Connection Coefficients and Components of the Gradient of the Displacement Vector 614 T2
11.9 Solving the 3-Dimensional Navier-Cauchy Equation in Cylindrical Coordinates 619 T2
11.9.1 Simple Methods: Pipe Fracture and Torsion Pendulum 619 T2
11.9.2 Separation of Variables and Green's Functions: Thermoelastic Noise in Mirrors 622 T2
Bibliographic Note 627

12 Elastodynamics 629

12.1 Overview 629
12.2 Basic Equations of Elastodynamics; Waves in a Homogeneous Medium 630
12.2.1 Equation of Motion for a Strained Elastic Medium 630
12.2.2 Elastodynamic Waves 636
12.2.3 Longitudinal Sound Waves 637
12.2.4 Transverse Shear Waves 638
12.2.5 Energy of Elastodynamic Waves 640
12.3 Waves in Rods, Strings, and Beams 642
12.3.1 Compression Waves in a Rod 643
12.3.2 Torsion Waves in a Rod 643
12.3.3 Waves on Strings 644
12.3.4 Flexural Waves on a Beam 645
12.3.5 Bifurcation of Equilibria and Buckling (Once More) 647
12.4 Body Waves and Surface Waves—Seismology and Ultrasound 648
12.4.1 Body Waves 650
12.4.2 Edge Waves 654
12.4.3 Green's Function for a Homogeneous Half-Space 658
12.4.4 Free Oscillations of Solid Bodies 661
12.4.5 Seismic Tomography 663
12.4.6 Ultrasound; Shock Waves in Solids 663
12.5 The Relationship of Classical Waves to Quantum Mechanical Excitations 667 T2
Bibliographic Note 670

PART V FLUID DYNAMICS 671

13 Foundations of Fluid Dynamics 675

13.1 Overview 675
13.2 The Macroscopic Nature of a Fluid: Density, Pressure, Flow Velocity; Liquids versus Gases 677

For general queries contact webmaster@press.princeton.edu.

© Copyright Princeton University Press. No part of this book may be distributed, posted, or reproduced in any form by digital or mechanical means without prior written permission of the publisher.

13.3 Hydrostatics 681
13.3.1 Archimedes' Law 684
13.3.2 Nonrotating Stars and Planets 686
13.3.3 Rotating Fluids 689
13.4 Conservation Laws 691
13.5 The Dynamics of an Ideal Fluid 695
13.5.1 Mass Conservation 696
13.5.2 Momentum Conservation 696
13.5.3 Euler Equation 697
13.5.4 Bernoulli's Theorem 697
13.5.5 Conservation of Energy 704
13.6 Incompressible Flows 709
13.7 Viscous Flows with Heat Conduction 710
13.7.1 Decomposition of the Velocity Gradient into Expansion, Vorticity, and Shear 710
13.7.2 Navier-Stokes Equation 711
13.7.3 Molecular Origin of Viscosity 713
13.7.4 Energy Conservation and Entropy Production 714
13.7.5 Reynolds Number 716
13.7.6 Pipe Flow 716
13.8 Relativistic Dynamics of a Perfect Fluid 719 T2
13.8.1 Stress-Energy Tensor and Equations of Relativistic Fluid Mechanics 719 T2
13.8.2 Relativistic Bernoulli Equation and Ultrarelativistic Astrophysical Jets 721 T2
13.8.3 Nonrelativistic Limit of the Stress-Energy Tensor 723 T2
Bibliographic Note 726

14 Vorticity 729

14.1 Overview 729
14.2 Vorticity, Circulation, and Their Evolution 731
14.2.1 Vorticity Evolution 734
14.2.2 Barotropic, Inviscid, Compressible Flows: Vortex Lines Frozen into Fluid 736
14.2.3 Tornados 738
14.2.4 Circulation and Kelvin's Theorem 739
14.2.5 Diffusion of Vortex Lines 741
14.2.6 Sources of Vorticity 744
14.3 Low-Reynolds-Number Flow—Stokes Flow and Sedimentation 746
14.3.1 Motivation: Climate Change 748
14.3.2 Stokes Flow 749
14.3.3 Sedimentation Rate 754
14.4 High-Reynolds-Number Flow—Laminar Boundary Layers 757
14.4.1 Blasius Velocity Profile Near a Flat Plate: Stream Function and Similarity Solution 758
14.4.2 Blasius Vorticity Profile 763

For general queries contact webmaster@press.princeton.edu.

© Copyright Princeton University Press. No part of this book may be distributed, posted, or reproduced in any form by digital or mechanical means without prior written permission of the publisher.

14.4.3 Viscous Drag Force on a Flat Plate 763
14.4.4 Boundary Layer Near a Curved Surface: Separation 764
14.5 Nearly Rigidly Rotating Flows—Earth's Atmosphere and Oceans 766
14.5.1 Equations of Fluid Dynamics in a Rotating Reference Frame 767
14.5.2 Geostrophic Flows 770
14.5.3 Taylor-Proudman Theorem 771
14.5.4 Ekman Boundary Layers 772
14.6 Instabilities of Shear Flows—Billow Clouds and Turbulence in the Stratosphere 778 T2
14.6.1 Discontinuous Flow: Kelvin-Helmholtz Instability 778 T2
14.6.2 Discontinuous Flow with Gravity 782 T2
14.6.3 Smoothly Stratified Flows: Rayleigh and Richardson Criteria for Instability 784 T2
Bibliographic Note 786

15 Turbulence 787

15.1 Overview 787
15.2 The Transition to Turbulence—Flow Past a Cylinder 789
15.3 Empirical Description of Turbulence 798
15.3.1 The Role of Vorticity in Turbulence 799
15.4 Semiquantitative Analysis of Turbulence 800
15.4.1 Weak-Turbulence Formalism 800
15.4.2 Turbulent Viscosity 804
15.4.3 Turbulent Wakes and Jets; Entrainment; the Coanda Effect 805
15.4.4 Kolmogorov Spectrum for Fully Developed, Homogeneous, Isotropic Turbulence 810
15.5 Turbulent Boundary Layers 817
15.5.1 Profile of a Turbulent Boundary Layer 818
15.5.2 Coanda Effect and Separation in a Turbulent Boundary Layer 820
15.5.3 Instability of a Laminar Boundary Layer 822
15.5.4 Flight of a Ball 823
15.6 The Route to Turbulence—Onset of Chaos 825
15.6.1 Rotating Couette Flow 825
15.6.2 Feigenbaum Sequence, Poincaré Maps, and the Period-Doubling Route to Turbulence in Convection 828
15.6.3 Other Routes to Turbulent Convection 831
15.6.4 Extreme Sensitivity to Initial Conditions 832
Bibliographic Note 834

16 Waves 835

16.1 Overview 835
16.2 Gravity Waves on and beneath the Surface of a Fluid 837
16.2.1 Deep-Water Waves and Their Excitation and Damping 840

For general queries contact webmaster@press.princeton.edu.

© Copyright Princeton University Press. No part of this book may be distributed, posted, or reproduced in any form by digital or mechanical means without prior written permission of the publisher.

16.2.2 Shallow-Water Waves 840
16.2.3 Capillary Waves and Surface Tension 844
16.2.4 Helioseismology 848
16.3 Nonlinear Shallow-Water Waves and Solitons 850
16.3.1 Korteweg–de Vries (KdV) Equation 850
16.3.2 Physical Effects in the KdV Equation 853
16.3.3 Single-Soliton Solution 854
16.3.4 Two-Soliton Solution 855
16.3.5 Solitons in Contemporary Physics 856
16.4 Rossby Waves in a Rotating Fluid 858
16.5 Sound Waves 862
16.5.1 Wave Energy 863
16.5.2 Sound Generation 865
16.5.3 Radiation Reaction, Runaway Solutions, and Matched Asymptotic Expansions 869
Bibliographic Note 874

17 Compressible and Supersonic Flow 875

17.1 Overview 875
17.2 Equations of Compressible Flow 877
17.3 Stationary, Irrotational, Quasi-1-Dimensional Flow 880
17.3.1 Basic Equations; Transition from Subsonic to Supersonic Flow 880
17.3.2 Setting up a Stationary, Transonic Flow 883
17.3.3 Rocket Engines 887
17.4 1-Dimensional, Time-Dependent Flow 891
17.4.1 Riemann Invariants 891
17.4.2 Shock Tube 895
17.5 Shock Fronts 897
17.5.1 Junction Conditions across a Shock; Rankine-Hugoniot Relations 898
17.5.2 Junction Conditions for Ideal Gas with Constant γ 904
17.5.3 Internal Structure of a Shock 906
17.5.4 Mach Cone 907
17.6 Self-Similar Solutions—Sedov-Taylor Blast Wave 908
17.6.1 The Sedov-Taylor Solution 909
17.6.2 Atomic Bomb 912
17.6.3 Supernovae 914
Bibliographic Note 916

18 Convection 917

18.1 Overview 917
18.2 Diffusive Heat Conduction—Cooling a Nuclear Reactor; Thermal Boundary Layers 918

T2

For general queries contact webmaster@press.princeton.edu.

© Copyright Princeton University Press. No part of this book may be distributed, posted, or reproduced in any form by digital or mechanical means without prior written permission of the publisher.

18.3 Boussinesq Approximation 923
18.4 Rayleigh-Bénard Convection 925
18.5 Convection in Stars 933
18.6 Double Diffusion—Salt Fingers 937
Bibliographic Note 941

App. A Newtonian Physics: Geometric Viewpoint 943

1.1 Introduction 943
1.1.1 The Geometric Viewpoint on the Laws of Physics 943
1.1.2 Purposes of This Chapter 945
1.1.3 Overview of This Chapter 945
1.2 Foundational Concepts 946
1.3 Tensor Algebra without a Coordinate System 948
1.4 Particle Kinetics and Lorentz Force in Geometric Language 951
1.5 Component Representation of Tensor Algebra 954
1.5.1 Slot-Naming Index Notation 955
1.5.2 Particle Kinetics in Index Notation 957
1.6 Orthogonal Transformations of Bases 958
1.7 Differentiation of Scalars, Vectors, and Tensors; Cross Product and Curl 960
1.8 Volumes, Integration, and Integral Conservation Laws 964
1.8.1 Gauss's and Stokes' Theorems 965
1.9 The Stress Tensor and Momentum Conservation 967
1.9.1 Examples: Electromagnetic Field and Perfect Fluid 968
1.9.2 Conservation of Momentum 969
1.10 Geometrized Units and Relativistic Particles for Newtonian Readers 971
1.10.1 Geometrized Units 971
1.10.2 Energy and Momentum of a Moving Particle 972
Bibliographic Note 973

References 975
Name Index 983
Subject Index 985
Contents of the Unified Work, *Modern Classical Physics* 997
Preface to *Modern Classical Physics* 1005
Acknowledgments for *Modern Classical Physics* 1013

For general queries contact webmaster@press.princeton.edu.

© Copyright Princeton University Press. No part of this book may be distributed, posted, or reproduced in any form by digital or mechanical means without prior written permission of the publisher.

CHAPTER ELEVEN

11

Elastostatics

Ut tensio, sic vis

ROBERT HOOKE (1678)

11.1 Overview

11.1

From the viewpoint of continuum mechanics, a *solid* is a substance that recovers its original shape after the application and removal of any small stress. Note the requirement that this be true for *any* small stress. Many fluids (e.g., water) satisfy our definition as long as the applied stress is isotropic, but they will deform permanently under a shear stress. Other materials (e.g., Earth's crust) are only solid for limited times but undergo plastic flow when a small stress is applied for a long time.

We focus our attention in this chapter on solids whose deformation (quantified by a *tensorial strain*) is linearly proportional to the applied, small, *tensorial stress*. This linear, 3-dimensional stress-strain relationship, which we develop and explore in this chapter, generalizes Hooke's famous 1-dimensional law, which states that if an elastic wire or rod is stretched by an applied force F (Fig. 11.1a), its fractional change of length (its strain) is proportional to the force, $\Delta\ell/\ell \propto F$.

Hooke's law

Hooke's law turns out to be one component of a 3-dimensional stress-strain relation, but to understand it deeply in that language, we must first define and understand the *strain tensor* and the *stress tensor*. Our approach to these tensors follows the geometric, frame-independent philosophy introduced in Chap. 1. Some readers may wish to review that philosophy and mathematics by rereading or browsing Chap. 1.

We begin our development of elasticity theory in Sec. 11.2 by introducing, in a frame-independent way, the vectorial displacement field $\boldsymbol{\xi}(\mathbf{x})$ inside a stressed body (Fig. 11.1b), and its gradient $\nabla\boldsymbol{\xi}$, whose symmetric part is the strain tensor $\mathbf{S}$. We then express the strain tensor as the sum of an expansion Θ that represents volume changes and a shear $\boldsymbol{\Sigma}$ that represents shape changes.

In Sec. 11.3.1, we introduce the stress tensor, and in Sec. 11.3.2, we discuss the realms in which there is a linear relationship between stress and strain, and ways in which linearity can fail. In Sec. 11.3.3, assuming linearity, we discuss how the material resists volume change by developing an opposing isotropic stress, with a stress/strain ratio that is equal to the *bulk modulus* K. We discuss how the material also

For general queries contact webmaster@press.princeton.edu.

© Copyright Princeton University Press. No part of this book may be distributed, posted, or reproduced in any form by digital or mechanical means without prior written permission of the publisher.

BOX 11.1. READERS' GUIDE

- This chapter relies heavily on the geometric view of Newtonian physics (including vector and tensor analysis) laid out in Chap. 1.
- Chapter 12 (Elastodynamics) is an extension of this chapter; to understand it, this chapter must be mastered.
- The idea of the irreducible tensorial parts of a tensor, and its most important example, decomposition of the gradient of a displacement vector into expansion, rotation, and shear (Sec. 11.2.2 and Box 11.2) will be encountered again in Part V (Fluid Dynamics), Part VI (Plasma Physics), and Part VII (General Relativity).
- Differentiation of vectors and tensors with the help of connection coefficients (Sec. 11.8; Track Two) will be used occasionally in Part V (Fluid Dynamics) and Part VI (Plasma Physics), and will be generalized to nonorthonormal bases in Part VII (General Relativity), where it will become Track One and will be used extensively.
- No other portions of this chapter are important for subsequent parts of this book.

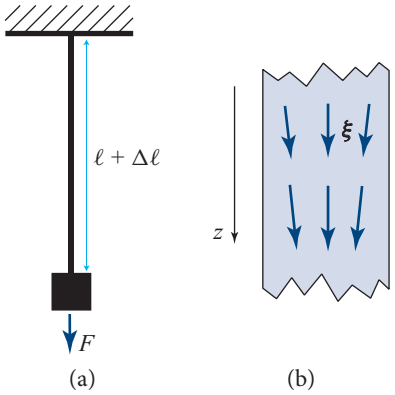

FIGURE 11.1 (a) Hooke's 1-dimensional law for a rod stretched by a force F: $\Delta\ell/\ell \propto F$. (b) The 3-dimensional displacement vector $\boldsymbol{\xi}(\mathbf{x})$ inside the stretched rod.

resists a shear-type strain by developing an opposing shear stress with a stress/strain ratio equal to twice the shear modulus 2μ. In Sec. 11.3.4, we evaluate the energy density stored in elastostatic strains; in Sec. 11.3.5, we explore the influence of thermal expansion on the stress-strain relationship; and in Sec. 11.3.6, we discuss the atomic-force origin of the elastostatic stresses and use atomic considerations to estimate

For general queries contact webmaster@press.princeton.edu.

© Copyright Princeton University Press. No part of this book may be distributed, posted, or reproduced in any form by digital or mechanical means without prior written permission of the publisher.

the magnitudes of the bulk and shear moduli. Then in Sec. 11.3.7, we compute the elastic force density inside a linear material as the divergence of the sum of its elastic stresses, and we formulate the law of elastostatic stress balance (the Navier-Cauchy equation) as the vanishing sum of the material's internal elastic force density and any other force densities that may act (usually a gravitational force density due to the weight of the elastic material). We discuss the analogy between this elastostatic stress-balance equation and Maxwell's electrostatic and magnetostatic equations. We describe how mathematical techniques common in electrostatics can also be applied to solve the Navier-Cauchy equation, subject to boundary conditions that describe external forces.

In Sec. 11.4, as a simple example, we use our 3-dimensional formulas to deduce Hooke's law for the 1-dimensional longitudinal stress and strain in a stretched wire.

When the elastic body that one studies is very thin in two dimensions compared to the third (e.g., a wire or rod), we can reduce the 3-dimensional elastostatic equations to a set of coupled 1-dimensional equations by taking moments of the elastostatic equations. We illustrate this technique in Sec. 11.5, where we treat the bending of beams and other examples.

Elasticity theory, as developed in this chapter, is an example of a common (some would complain far too common) approach to physics problems, namely, to linearize them. Linearization may be acceptable when the distortions are small. However, when deformed by sufficiently strong forces, elastic media may become unstable to small displacements, which can then grow to large amplitude, causing rupture. We study an example of this in Sec. 11.6: the buckling of a beam when subjected to a sufficiently large longitudinal stress. Buckling is associated with *bifurcation of equilibria,* a phenomenon that is common to many physical systems, not just elastostatic ones. We illustrate bifurcation in Sec. 11.6 using our beam under a compressive load, and we explore its connection to catastrophe theory.

In Sec. 11.7, we discuss dimensional reduction by the method of moments for bodies that are thin in only 1 dimension, not two, such as plates and thin mirrors. In such bodies, the 3-dimensional elastostatic equations are reduced to 2 dimensions. We illustrate our 2-dimensional formalism by the stress polishing of telescope mirrors.

Because elasticity theory entails computing gradients of vectors and tensors, and practical calculations are often best performed in cylindrical or spherical coordinate systems, we present a mathematical digression in Track-Two Sec. 11.8—an introduction to how one can perform practical calculations of gradients of vectors and tensors in the orthonormal bases associated with curvilinear coordinate systems, using the concept of a connection coefficient.

As illustrative examples of both connection coefficients and elastostatic force balance, in Track-Two Sec. 11.9 and various exercises, we give practical examples of solutions of the elastostatic force-balance equation in cylindrical coordinates using two common techniques of elastostatics and electrostatics: separation of variables (text of Sec. 11.9.2) and Green's functions (Ex. 11.27).

For general queries contact webmaster@press.princeton.edu.

© Copyright Princeton University Press. No part of this book may be distributed, posted, or reproduced in any form by digital or mechanical means without prior written permission of the publisher.

11.2 Displacement and Strain

We begin our study of elastostatics by introducing the elastic displacement vector, its gradient, and the irreducible tensorial parts of its gradient. We then identify the strain as the symmetric part of the displacement's gradient.

11.2.1 Displacement Vector and Its Gradient

Elasticity provides a major application of the tensorial techniques we developed in Chap. 1. Label the position of a *point* (a tiny bit of solid) in an unstressed body, relative to some convenient origin in the body, by its position vector $\mathbf{x}$. Let a force be applied, so the body deforms and the point moves from $\mathbf{x}$ to $\mathbf{x} + \boldsymbol{\xi}(\mathbf{x})$; we call $\boldsymbol{\xi}$ the point's *displacement vector* (Fig. 11.1b). If $\boldsymbol{\xi}$ were constant (i.e., if its components in a Cartesian coordinate system were independent of location in the body), then the body would simply be translated and would undergo no deformation. To produce a deformation, we must make the displacement $\boldsymbol{\xi}$ change from one location to another. The most simple, coordinate-independent way to quantify those changes is by the gradient of $\boldsymbol{\xi}$, $\boldsymbol{\nabla}\boldsymbol{\xi}$. This gradient is a second-rank tensor field, which we denote by $\mathbf{W}$:

displacement vector

$$\boxed{\mathbf{W} \equiv \boldsymbol{\nabla}\boldsymbol{\xi}.} \tag{11.1a}$$

This tensor is a geometric object, defined independently of any coordinate system in the manner described in Sec. 1.7. In slot-naming index notation (Sec. 1.5), it is denoted

$$W_{ij} = \xi_{i;j}, \tag{11.1b}$$

where the index j after the semicolon is the name of the gradient slot.

In a Cartesian coordinate system the components of the gradient are always just partial derivatives [Eq. (1.15c)], and therefore the Cartesian components of $\mathbf{W}$ are

$$W_{ij} = \frac{\partial \xi_i}{\partial x_j} = \xi_{i\,,\,j}. \tag{11.1c}$$

(Recall that indices following a comma represent partial derivatives.) In Sec. 11.8, we learn how to compute the components of the gradient in cylindrical and spherical coordinates.

In any small neighborhood of any point $\mathbf{x}_o$ in a deformed body, we can reconstruct the displacement vector $\boldsymbol{\xi}$ from its gradient $\mathbf{W}$ up to an additive constant. Specifically, in Cartesian coordinates, by virtue of a Taylor-series expansion, $\boldsymbol{\xi}$ is given by

$$\begin{aligned} \xi_i(\mathbf{x}) &= \xi_i(\mathbf{x}_o) + (x_j - x_{oj})(\partial \xi_i/\partial x_j) + \dots \\ &= \xi_i(\mathbf{x}_o) + (x_j - x_{oj}) W_{ij} + \dots . \end{aligned} \tag{11.2}$$

If we place the origin of Cartesian coordinates at $\mathbf{x}_o$ and let the origin move with the point there as the body deforms [so $\boldsymbol{\xi}(\mathbf{x}_o) = 0$], then Eq. (11.2) becomes

$$\xi_i = W_{ij} x_j \quad \text{when } |\mathbf{x}| \text{ is sufficiently small.} \tag{11.3}$$

For general queries contact webmaster@press.princeton.edu.

© Copyright Princeton University Press. No part of this book may be distributed, posted, or reproduced in any form by digital or mechanical means without prior written permission of the publisher.

We have derived this as a relationship between components of $\boldsymbol{\xi}$, $\mathbf{x}$, and $\mathbf{W}$ in a Cartesian coordinate system. However, the indices can also be thought of as the names of slots (Sec. 1.5) and correspondingly, Eq. (11.3) can be regarded as a geometric, coordinate-independent relationship among the vectors and tensor $\boldsymbol{\xi}$, $\mathbf{x}$, and $\mathbf{W}$.

In Ex. 11.2, we use Eq. (11.3) to gain insight into the displacements associated with various parts of the gradient $\mathbf{W}$.

11.2.2 Expansion, Rotation, Shear, and Strain

11.2.2

irreducible tensorial parts of a tensor

In Box 11.2, we introduce the concept of the irreducible tensorial parts of a tensor, and we state that in physics, when one encounters an unfamiliar tensor, it is often useful to identify the tensor's irreducible parts. The gradient of the displacement vector, $\mathbf{W} = \nabla\boldsymbol{\xi}$, is an important example. It is a second-rank tensor. Therefore, as discussed in Box 11.2, its irreducible tensorial parts are its trace $\Theta \equiv \mathrm{Tr}(\mathbf{W}) = W_{ii} = \boldsymbol{\nabla}\cdot\boldsymbol{\xi}$, which is called the deformed body's *expansion* (for reasons we shall explore below); its symmetric, trace-free part $\boldsymbol{\Sigma}$, which is called the body's *shear;* and its antisymmetric part $\mathbf{R}$, which is called the body's *rotation:*

expansion, shear, and rotation

$$\boxed{\Theta = W_{ii} = \boldsymbol{\nabla}\cdot\boldsymbol{\xi},} \tag{11.4a}$$

$$\boxed{\Sigma_{ij} = \frac{1}{2}(W_{ij} + W_{ji}) - \frac{1}{3}\Theta g_{ij} = \frac{1}{2}(\xi_{i;j} + \xi_{j;i}) - \frac{1}{3}\xi_{k;k}\, g_{ij},} \tag{11.4b}$$

$$\boxed{R_{ij} = \frac{1}{2}(W_{ij} - W_{ji}) = \frac{1}{2}(\xi_{i;j} - \xi_{j;i}).} \tag{11.4c}$$

Here g_{ij} is the metric, which has components $g_{ij} = \delta_{ij}$ (Kronecker delta) in Cartesian coordinates, and repeated indices [the ii in Eq. (11.4a)] are to be summed [Eq. (1.9b) and subsequent discussion].

We can reconstruct $\mathbf{W} = \boldsymbol{\nabla}\boldsymbol{\xi}$ from these irreducible tensorial parts in the following manner [Eq. (4) of Box 11.2, rewritten in abstract notation]:

$$\boxed{\boldsymbol{\nabla}\boldsymbol{\xi} = \mathbf{W} = \frac{1}{3}\Theta\mathbf{g} + \boldsymbol{\Sigma} + \mathbf{R}.} \tag{11.5}$$

Let us explore the physical effects of the three separate parts of $\mathbf{W}$ in turn. To understand expansion, consider a small 3-dimensional piece $\mathcal{V}$ of a deformed body (a *volume element*). When the deformation $\mathbf{x} \to \mathbf{x} + \boldsymbol{\xi}$ occurs, a much smaller element of area[1] $d\boldsymbol{\Sigma}$ on the surface $\partial\mathcal{V}$ of $\mathcal{V}$ gets displaced through the vectorial distance $\boldsymbol{\xi}$ and in the process sweeps out a volume $\boldsymbol{\xi}\cdot d\boldsymbol{\Sigma}$. Therefore, the change in the volume element's volume, produced by $\boldsymbol{\xi}$, is

$$\delta V = \int_{\partial\mathcal{V}} d\boldsymbol{\Sigma}\cdot\boldsymbol{\xi} = \int_{\mathcal{V}} dV\,\boldsymbol{\nabla}\cdot\boldsymbol{\xi} = \boldsymbol{\nabla}\cdot\boldsymbol{\xi}\int_{\mathcal{V}} dV = (\boldsymbol{\nabla}\cdot\boldsymbol{\xi})\, V. \tag{11.6}$$

1. Note that we use $\boldsymbol{\Sigma}$ for a vectorial area and $\boldsymbol{\Sigma}$ for the shear tensor. There should be no confusion.

For general queries contact webmaster@press.princeton.edu.

© Copyright Princeton University Press. No part of this book may be distributed, posted, or reproduced in any form by digital or mechanical means without prior written permission of the publisher.

BOX 11.2. IRREDUCIBLE TENSORIAL PARTS OF A SECOND-RANK TENSOR IN 3-DIMENSIONAL EUCLIDEAN SPACE

In quantum mechanics, an important role is played by the *rotation group:* the set of all rotation matrices, viewed as a mathematical entity called a group (e.g., Mathews and Walker, 1970, Chap. 16). Each tensor in 3-dimensional Euclidean space, when rotated, is said to generate a specific *representation* of the rotation group. Tensors that are "big" (in a sense to be discussed later in this box) can be broken down into a sum of several tensors that are "as small as possible." These smallest tensors are said to generate *irreducible representations* of the rotation group. All this mumbo-jumbo is really simple, when one thinks about tensors as geometric, frame-independent objects.

As an example, consider an arbitrary second-rank tensor W_{ij} in 3-dimensional, Euclidean space. In the text W_{ij} is the gradient of the displacement vector. From this tensor we can construct the following "smaller" tensors by linear operations that involve only W_{ij} and the metric g_{ij}. (As these smaller tensors are enumerated, the reader should think of the notation used as the basis-independent, frame-independent, slot-naming index notation of Sec. 1.5.1.) The smaller tensors are the contraction (i.e., trace) of W_{ij},

$$\Theta \equiv W_{ij}g_{ij} = W_{ii}; \tag{1}$$

the antisymmetric part of W_{ij},

$$R_{ij} \equiv \frac{1}{2}(W_{ij} - W_{ji}); \tag{2}$$

and the symmetric, trace-free part of W_{ij},

$$\Sigma_{ij} \equiv \frac{1}{2}(W_{ij} + W_{ji}) - \frac{1}{3}g_{ij}W_{kk}. \tag{3}$$

It is straightforward to verify that the original tensor W_{ij} can be reconstructed from these three smaller tensors plus the metric g_{ij} as follows:

$$W_{ij} = \frac{1}{3}\Theta g_{ij} + R_{ij} + \Sigma_{ij}. \tag{4}$$

One way to see the sense in which Θ, R_{ij}, and Σ_{ij} are smaller than W_{ij} is by counting the number of independent real numbers required to specify their components in an arbitrary basis. (Think of the index notation as components on a chosen basis.) The original tensor W_{ij} has three $\times$ three = nine components (W_{11}, W_{12}, W_{13}, W_{21}, . . . W_{33}), all of which are independent. By contrast, the scalar Θ has just one. The antisymmetric

(continued)

For general queries contact webmaster@press.princeton.edu.

© Copyright Princeton University Press. No part of this book may be distributed, posted, or reproduced in any form by digital or mechanical means without prior written permission of the publisher.

BOX 11.2. (continued)

tensor R_{ij} has just three independent components, R_{12}, R_{23}, and R_{31}. Finally, the nine components of Σ_{ij} are not independent; symmetry requires that $\Sigma_{ij} \equiv \Sigma_{ji}$, which reduces the number of independent components from nine to six; being trace-free, $\Sigma_{ii} = 0$, reduces it further from six to five. Therefore, (five independent components in Σ_{ij}) + (three independent components in R_{ij}) + (one independent component in Θ) $= 9 =$ (number of independent components in W_{ij}).

The number of independent components (one for Θ, three for R_{ij}, and five for Σ_{ij}) is a geometric, basis-independent concept: It is the same, regardless of the basis used to count the components; and for each of the smaller tensors that make up W_{ij}, it is easily deduced without introducing a basis at all (think here in slot-naming index notation): The scalar Θ is clearly specified by just one real number. The antisymmetric tensor R_{ij} contains precisely the same amount of information as the vector

$$\phi_i \equiv -\frac{1}{2}\epsilon_{ijk}R_{jk}, \tag{5}$$

as can be seen from the fact that Eq. (5) can be inverted to give

$$R_{ij} = -\epsilon_{ijk}\phi_k; \tag{6}$$

and the vector ϕ_i can be characterized by its direction in space (two numbers) plus its length (a third). The symmetric, trace-free tensor Σ_{ij} can be characterized geometrically by the ellipsoid $(g_{ij} + \varepsilon\Sigma_{ij})\zeta_i\zeta_j = 1$, where ε is an arbitrary number $\ll 1$, and ζ_i is a vector whose tail sits at the center of the ellipsoid and whose head moves around on the ellipsoid's surface. Because Σ_{ij} is trace-free, this ellipsoid has unit volume. Therefore, it is specified fully by the direction of its longest principal axis (two numbers) plus the direction of a second principal axis (a third number) plus the ratio of the length of the second axis to the first (a fourth number) plus the ratio of the length of the third axis to the first (a fifth number).

Each of the tensors Θ, R_{ij} (or equivalently, ϕ_i), and Σ_{ij} is irreducible in the sense that one cannot construct any smaller tensors from it, by any linear operation that involves only it, the metric, and the Levi-Civita tensor. Irreducible tensors in 3-dimensional Euclidean space always have an odd number of components. It is conventional to denote this number by $2l + 1$, where the integer l is called the "order of the irreducible representation of the

(continued)

For general queries contact webmaster@press.princeton.edu.

© Copyright Princeton University Press. No part of this book may be distributed, posted, or reproduced in any form by digital or mechanical means without prior written permission of the publisher.

BOX 11.2. (continued)

rotation group" that the tensor generates. For Θ, R_{ij} (or equivalently, ϕ_i), and Σ_{jk}, l is 0, 1, and 2, respectively. These three tensors can be mapped into the spherical harmonics of order $l = 0,\ 1,\ 2$; and their $2l + 1$ components correspond to the $2l + 1$ values of the quantum number $m = -l,\ -l + 1 \ldots, l - 1,\ l$. (For details see, e.g., Thorne, 1980, Sec. II.C.)

In physics, when one encounters a new tensor, it is often useful to identify the tensor's irreducible parts. They almost always play important, independent roles in the physical situation one is studying. We meet one example in this chapter, another when we study fluid dynamics (Chap. 13), and a third in general relativity (Box 25.2).

Here we have invoked Gauss's theorem in the second equality, and in the third we have used the smallness of $\mathcal{V}$ to infer that $\nabla \cdot \boldsymbol{\xi}$ is essentially constant throughout $\mathcal{V}$ and so can be pulled out of the integral. Therefore, the fractional change in volume is equal to the trace of the stress tensor (i.e., the expansion):

expansion as fractional volume change

$$\boxed{\frac{\delta V}{V} = \nabla \cdot \boldsymbol{\xi} = \Theta.} \tag{11.7}$$

See Fig. 11.2 for a simple example.

shearing displacements

The shear tensor $\boldsymbol{\Sigma}$ produces the shearing displacements illustrated in Figs. 11.2 and 11.3. As the tensor has zero trace, there is no volume change when a body undergoes a pure shear deformation. The shear tensor has five independent components (Box 11.2). However, by rotating our Cartesian coordinates appropriately, we can transform away all the off-diagonal elements, leaving only the three diagonal elements Σ_{xx}, Σ_{yy}, and Σ_{zz}, which must sum to zero. This is known as a *principal-axis transformation*. Each element produces a stretch ($\Sigma_{..} > 0$) or squeeze ($\Sigma_{..} < 0$) along its

shear's stretch and squeeze along principal axes

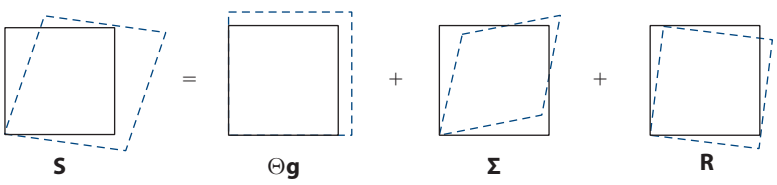

FIGURE 11.2 A simple example of the decomposition of a 2-dimensional distortion **S** of a square body into an expansion Θ, a shear $\boldsymbol{\Sigma}$, and a rotation **R**.

For general queries contact webmaster@press.princeton.edu.

© Copyright Princeton University Press. No part of this book may be distributed, posted, or reproduced in any form by digital or mechanical means without prior written permission of the publisher.

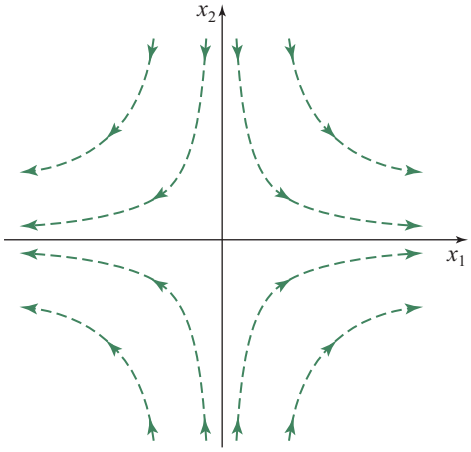

FIGURE 11.3 Shear in 2 dimensions. The displacement of points in a solid undergoing pure shear is the vector field $\boldsymbol{\xi}(\mathbf{x})$ given by Eq. (11.3) with W_{ji} replaced by Σ_{ji}: $\xi_j = \Sigma_{ji}x_i = \Sigma_{j1}x_1 + \Sigma_{j2}x_2$. The integral curves of this vector field are plotted in this figure. The figure is drawn using principal axes, which are Cartesian, so $\Sigma_{12} = \Sigma_{21} = 0$ and $\Sigma_{11} = -\Sigma_{22}$, which means that $\xi_1 = \Sigma_{11}x_1$ and $\xi_2 = -\Sigma_{11}x_2$; or, equivalently, $\xi_x = \Sigma_{xx}x$ and $\xi_y = -\Sigma_{xx}y$. The integral curves of this simple vector field are the hyperbolas shown. Note that the displacement increases linearly with distance from the origin. The shear shown in Fig. 11.2 is the same as this, but with the axes rotated counterclockwise by 45°.

axis,[2] and their vanishing sum (the vanishing trace of $\boldsymbol{\Sigma}$) means that there is no net volume change. The components of the shear tensor in any Cartesian coordinate system can be written down immediately from Eq. (11.4b) by substituting the Kronecker delta δ_{ij} for the components of the metric tensor g_{ij} and treating all derivatives as partial derivatives:

$$\Sigma_{xx} = \frac{2}{3}\frac{\partial \xi_x}{\partial x} - \frac{1}{3}\left(\frac{\partial \xi_y}{\partial y} + \frac{\partial \xi_z}{\partial z}\right), \quad \Sigma_{xy} = \frac{1}{2}\left(\frac{\partial \xi_x}{\partial y} + \frac{\partial \xi_y}{\partial x}\right), \tag{11.8}$$

and similarly for the other components. The analogous equations in spherical and cylindrical coordinates are given in Sec. 11.8.

The third term $\mathbf{R}$ in Eq. (11.5) describes a pure rotation, which does not deform the solid. To verify this, write $\boldsymbol{\xi} = \boldsymbol{\phi} \times \mathbf{x}$, where $\boldsymbol{\phi}$ is a small rotation of magnitude ϕ about an axis parallel to the direction of $\boldsymbol{\phi}$. Using Cartesian coordinates in 3-dimensional Euclidean space, we can demonstrate by direct calculation that the symmetric part of $\mathbf{W} = \nabla\boldsymbol{\xi}$ vanishes (i.e., $\Theta = \boldsymbol{\Sigma} = 0$) and that

rotation vector

$$R_{ij} = -\epsilon_{ijk}\phi_k, \quad \phi_i = -\frac{1}{2}\epsilon_{ijk}R_{jk}. \tag{11.9a}$$

2. More explicitly, $\Sigma_{xx} > 0$ produces a stretch along the x-axis, $\Sigma_{yy} < 0$ produces a squeeze along the y-axis, etc.

For general queries contact webmaster@press.princeton.edu.

© Copyright Princeton University Press. No part of this book may be distributed, posted, or reproduced in any form by digital or mechanical means without prior written permission of the publisher.

Therefore, the elements of the tensor $\mathbf{R}$ in a Cartesian coordinate system just involve the vectorial rotation angle $\boldsymbol{\phi}$. Note that expression (11.9a) for $\boldsymbol{\phi}$ and expression (11.4c) for R_{ij} imply that $\boldsymbol{\phi}$ is half the curl of the displacement vector:

$$\boldsymbol{\phi} = \frac{1}{2}\boldsymbol{\nabla} \times \boldsymbol{\xi}. \tag{11.9b}$$

A simple example of rotation is shown in the last picture in Fig. 11.2.

Elastic materials resist expansion Θ and shear $\boldsymbol{\Sigma}$, but they don't mind at all having their orientation in space changed (i.e., they do not resist rotations $\mathbf{R}$). Correspondingly, in elasticity theory a central focus is on expansion and shear. For this reason the symmetric part of the gradient of $\boldsymbol{\xi}$,

strain tensor

$$S_{ij} \equiv \frac{1}{2}(\xi_{i;j} + \xi_{j;i}) = \Sigma_{ij} + \frac{1}{3}\Theta g_{ij}, \tag{11.10}$$

which includes the expansion and shear but omits the rotation, is given a special name—the *strain*—and is paid great attention.

Let us consider some examples of strains that arise in physical systems.

1. Understanding how materials deform under various *loads* (externally applied forces) is central to mechanical, civil, and structural engineering. As we learn in Sec. 11.3.2, all Hookean materials (materials with strain proportional to stress when the stress is small) crack or break when the load is so great that any component of their strain exceeds $\sim$0.1, and almost all crack or break at strains $\sim$0.001. For this reason, in our treatment of elasticity theory (this chapter and the next), we focus on strains that are small compared to unity.
2. Continental drift can be measured on the surface of Earth using very long baseline interferometry, a technique in which two or more radio telescopes are used to detect interferometric fringes using radio waves from an astronomical point source. (A similar technique uses the Global Positioning System to achieve comparable accuracy.) By observing the fringes, it is possible to detect changes in the spacing between the telescopes as small as a fraction of a wavelength ($\sim$1 cm). As the telescopes are typically 1,000 km apart, this means that dimensionless strains $\sim 10^{-8}$ can be measured. The continents drift apart on a timescale $\lesssim 10^8$ yr, so it takes roughly a year for these changes to grow large enough to be measured. Such techniques are also useful for monitoring earthquake faults.
3. The smallest time-varying strains that have been measured so far involve laser interferometer gravitational-wave detectors, such as LIGO. In each arm of a LIGO interferometer, two mirrors hang freely, separated by 4 km. In 2015 their separations were monitored (at frequencies of $\sim$100 Hz) to $\sim 4 \times 10^{-19}$ m, four ten-thousandths the radius of a nucleon. The associated strain is 1×10^{-22}. Although this strain is not associated with an elastic solid, it does indicate the high accuracy of optical measurement techniques.

For general queries contact webmaster@press.princeton.edu.

© Copyright Princeton University Press. No part of this book may be distributed, posted, or reproduced in any form by digital or mechanical means without prior written permission of the publisher.

EXERCISES

Exercise 11.1 *Derivation and Practice: Reconstruction of a Tensor from Its Irreducible Tensorial Parts*

Using Eqs. (1), (2), and (3) of Box 11.2, show that $\frac{1}{3}\Theta g_{ij} + \Sigma_{ij} + R_{ij}$ is equal to W_{ij}.

Exercise 11.2 *Example: Displacement Vectors Associated with Expansion, Rotation, and Shear*

(a) Consider a $\mathbf{W} = \nabla\boldsymbol{\xi}$ that is pure expansion: $W_{ij} = \frac{1}{3}\Theta g_{ij}$. Using Eq. (11.3) show that, in the vicinity of a chosen point, the displacement vector is $\xi_i = \frac{1}{3}\Theta x_i$. Draw this displacement vector field.

(b) Similarly, draw $\boldsymbol{\xi}(\mathbf{x})$ for a $\mathbf{W}$ that is pure rotation. [Hint: Express $\boldsymbol{\xi}$ in terms of the vectorial angle $\boldsymbol{\phi}$ with the aid of Eq. (11.9b).]

(c) Draw $\boldsymbol{\xi}(\mathbf{x})$ for a $\mathbf{W}$ that is pure shear. To simplify the drawing, assume that the shear is confined to the x-y plane, and make your drawing for a shear whose only nonzero components are $\Sigma_{xx} = -\Sigma_{yy}$. Compare your drawing with Fig. 11.3.

11.3 Stress, Elastic Moduli, and Elastostatic Equilibrium

11.3

11.3.1 Stress Tensor

11.3.1

The forces acting in an elastic solid are measured by a second-rank tensor, the *stress tensor* introduced in Sec. 1.9. Let us recall the definition of this stress tensor.

Consider two small, contiguous regions in a solid. If we take a small element of area $d\boldsymbol{\Sigma}$ in the contact surface with its positive sense[3] (same as the direction of $d\boldsymbol{\Sigma}$ viewed as a vector) pointing from the first region toward the second, then the first region exerts a force $d\mathbf{F}$ (not necessarily normal to the surface) on the second through this area. The force the second region exerts on the first (through the area $-d\boldsymbol{\Sigma}$) will, by Newton's third law, be equal and opposite to that force. The force and the area of contact are both vectors, and there is a linear relationship between them. (If we double the area, we double the force.) The two vectors therefore will be related by a second-rank tensor, the stress tensor $\mathbf{T}$:

$$\boxed{d\mathbf{F} = \mathbf{T}\cdot d\boldsymbol{\Sigma} = \mathbf{T}(\ldots, d\boldsymbol{\Sigma}); \quad dF_i = T_{ij}d\Sigma_j.} \tag{11.11}$$

stress tensor

Thus the tensor $\mathbf{T}$ is the net (vectorial) force per unit (vectorial) area that a body exerts on its surroundings. Be aware that many books on elasticity (e.g., Landau and Lifshitz, 1986) define the stress tensor with the opposite sign to that in Eq. (11.11). Also be careful not to confuse the shear tensor Σ_{jk} with the vectorial infinitesimal surface area $d\Sigma_j$.

3. For a discussion of area elements including their positive sense, see Sec. 1.8.

For general queries contact webmaster@press.princeton.edu.

© Copyright Princeton University Press. No part of this book may be distributed, posted, or reproduced in any form by digital or mechanical means without prior written permission of the publisher.

We often need to compute the total elastic force acting on some finite volume $\mathcal{V}$. To aid in this, we make an important assumption, discussed in Sec. 11.3.6: the stress is determined by local conditions and can be computed from the local arrangement of atoms. If this assumption is valid, then (as we shall see in Sec. 11.3.6), we can compute the total force acting on the volume element by integrating the stress over its surface $\partial\mathcal{V}$:

$$\mathbf{F} = -\int_{\partial\mathcal{V}} \mathbf{T}\cdot d\mathbf{\Sigma} = -\int_{\mathcal{V}} \nabla\cdot\mathbf{T} dV, \tag{11.12}$$

where we have invoked Gauss's theorem, and the minus sign is included because by convention, for a closed surface $\partial\mathcal{V}$, $d\mathbf{\Sigma}$ points out of $\mathcal{V}$ instead of into it.

Equation (11.12) must be true for arbitrary volumes, so we can identify the *elastic force density* $\mathbf{f}$ acting on an elastic solid as

elastic force density

$$\boxed{\mathbf{f} = -\nabla\cdot\mathbf{T}.} \tag{11.13}$$

In elastostatic equilibrium, this force density must balance all other volume forces acting on the material, most commonly the gravitational force density, so

force balance equation

$$\boxed{\mathbf{f} + \rho\mathbf{g} = 0,} \tag{11.14}$$

where $\mathbf{g}$ is the gravitational acceleration. (Again, there should be no confusion between the vector $\mathbf{g}$ and the metric tensor $\mathbf{g}$.) There are other possible external forces, some of which we shall encounter later in the context of fluids (e.g., an electromagnetic force density). These can be added to Eq. (11.14).

Just as for the strain, the stress tensor $\mathbf{T}$ can be decomposed into its irreducible tensorial parts, a pure trace (the *pressure* P) plus a symmetric trace-free part (the *shear stress*):

pressure and shear stress

$$\mathbf{T} = P\mathbf{g} + \mathbf{T}^{\text{shear}}; \quad P = \frac{1}{3}\,\text{Tr}(\mathbf{T}) = \frac{1}{3}T_{ii}. \tag{11.15}$$

There is no antisymmetric part, because the stress tensor is symmetric, as we saw in Sec. 1.9. Fluids at rest exert isotropic stresses: $\mathbf{T} = P\mathbf{g}$. They cannot exert shear stress when at rest, though when moving and shearing, they can exert a viscous shear stress, as we discuss extensively in Part V (initially in Sec. 13.7.2).

In SI units, stress is measured in units of Pascals, denoted Pa:

Pascal

$$1\,\text{Pa} = 1\,\text{N m}^{-2} = 1\frac{\text{kg m s}^{-2}}{\text{m}^2}, \tag{11.16}$$

or sometimes in GPa $= 10^9$ Pa. In cgs units, stress is measured in dyne cm^{-2}. Note that 1 Pa $= 10$ dyne cm^{-2}.

Now let us consider some examples of stresses.

1. Atmospheric pressure is equal to the weight of the air in a column of unit area extending above the surface of Earth, and thus is roughly $P \sim \rho g H \sim$

For general queries contact webmaster@press.princeton.edu.

© Copyright Princeton University Press. No part of this book may be distributed, posted, or reproduced in any form by digital or mechanical means without prior written permission of the publisher.

10^5 Pa, where $\rho \simeq 1\,\mathrm{kg\,m^{-3}}$ is the density of air, $g \simeq 10\,\mathrm{m\,s^{-2}}$ is the acceleration of gravity at Earth's surface, and $H \simeq 10\,\mathrm{km}$ is the atmospheric scale height [$H \equiv (d \ln P/dz)^{-1}$, with z the vertical distance]. Thus 1 atmosphere is $\sim 10^5$ Pa (or, more precisely, 1.01325×10^5 Pa). The stress tensor is isotropic.

2. Suppose we hammer a nail into a block of wood. The hammer might weigh $m \sim 0.3\,\mathrm{kg}$ and be brought to rest from a speed of $v \sim 10\,\mathrm{m\,s^{-1}}$ in a distance of, say, $d \sim 3\,\mathrm{mm}$. Then the average force exerted on the wood by the nail, as it is driven, is $F \sim mv^2/d \sim 10^4\,\mathrm{N}$. If this is applied over an effective area $A \sim 1\,\mathrm{mm^2}$, then the magnitude of the typical stress in the wood is $\sim F/A \sim 10^{10}$ Pa $\sim 10^5$ atmosphere. There is a large shear component to the stress tensor, which is responsible for separating the fibers in the wood as the nail is hammered.
3. Neutron stars are as massive as the Sun, $M \sim 2 \times 10^{30}\,\mathrm{kg}$, but have far smaller radii, $R \sim 10\,\mathrm{km}$. Their surface gravities are therefore $g \sim GM/R^2 \sim 10^{12}\,\mathrm{m\,s^{-2}}$, 10 billion times that encountered on Earth. They have solid crusts of density $\rho \sim 10^{16}\,\mathrm{kg\,m^{-3}}$ that are about 1 km thick. In the crusts, the main contribution to the pressure is from the degeneracy of relativistic electrons (see Sec. 3.5.3). The magnitude of the stress at the base of a neutron-star crust is $P \sim \rho g H \sim 10^{31}$ Pa! The crusts are solid, because the free electrons are neutralized by a lattice of ions. However, a crust's shear modulus is only a few percent of its bulk modulus.
4. As we discuss in Sec. 28.7.1, a popular cosmological theory called *inflation* postulates that the universe underwent a period of rapid, exponential expansion during its earliest epochs. This expansion was driven by the stress associated with a *false vacuum*. The action of this stress on the universe can be described quite adequately using a classical stress tensor. If the interaction energy is $E \sim 10^{15}\,\mathrm{GeV}$, the supposed scale of grand unification, and the associated lengthscale is the Compton wavelength associated with that energy, $l \sim \hbar c/E$, then the magnitude of the stress is $\sim E/l^3 \sim 10^{97}(E/10^{15}\,\mathrm{GeV})^4$ Pa.
5. Elementary particles interact through forces. Although it makes no sense to describe this interaction using classical elasticity, it is reasonable to make order-of-magnitude estimates of the associated stress. One promising model of these interactions involves *strings* with mass per unit length $\mu = g_s^2 c^2/(8\pi G) \sim 1$ Megaton/fermi (where Megaton is not the TNT equivalent!), and cross section of order the Planck length squared, ${L_P}^2 = \hbar G/c^3 \sim 10^{-70}\ \mathrm{m^2}$, and tension (negative pressure) $T_{zz} \sim \mu c^2/{L_P}^2 \sim 10^{110}$ Pa. Here $\hbar$, G, and c are Planck's reduced constant, Newton's gravitation constant, and the speed of light, and $g_s^2 \sim 0.025$ is the string coupling constant.

For general queries contact webmaster@press.princeton.edu.

© Copyright Princeton University Press. No part of this book may be distributed, posted, or reproduced in any form by digital or mechanical means without prior written permission of the publisher.

6. The highest possible stress is presumably associated with spacetime singularities, for example at the birth of the universe or inside a black hole. Here the characteristic energy is the Planck energy $E_P = (\hbar c^5/G)^{1/2} \sim 10^{19}$ GeV, the lengthscale is the Planck length $L_P = (\hbar G/c^3)^{1/2} \sim 10^{-35}$ m, and the associated ultimate stress is $\sim E_P/L_P^3 \sim 10^{114}$ Pa.

11.3.2

11.3.2 Realm of Validity for Hooke's Law

In elasticity theory, motivated by Hooke's Law (Fig. 11.1), we assume a linear relationship between a material's stress and strain tensors. Before doing so, however, we discuss the realm in which this linearity is true and some ways in which it can fail.

For this purpose, consider again the stretching of a rod by an applied force (Fig. 11.1a, shown again in Fig. 11.4a). For a sufficiently small stress $T_{zz} = F/A$ (with A the cross sectional area of the rod), the strain $S_{zz} = \Delta\ell/\ell$ follows Hooke's law (straight red line in Fig. 11.4b). However, at some point, called the *proportionality limit* (first big dot in Fig. 11.4b), the strain begins to depart from Hooke's law. Despite this deviation, if the stress is removed, the rod returns to its original length. At a somewhat larger stress, called the *elastic limit,* that ceases to be true; the rod is permanently stretched. At a still larger stress, called the *yield limit* or *yield point,* little or no increase in stress causes a large increase in strain, usually because the material begins to flow plasticly. At an even larger stress, the *rupture point,* the rod cracks or breaks. For a ductile substance like polycrystalline copper, the proportionality limit and elastic limit both occur at about the same rather low strain $\Delta\ell/\ell \sim 10^{-4}$, but yield and rupture do not occur until $\Delta\ell/\ell \sim 10^{-3}$. For a more resilient material like cemented tungsten carbide, strains can be proportional and elastic up to $\sim 3 \times 10^{-3}$. Rubber is non-Hookean (stress is not proportional to strain) at essentially all strains; its proportionality limit is exceedingly small, but it returns to its original shape from essentially all nonrupturing deformations, which can be as large as $\Delta\ell/\ell \sim 8$ (the yield and rupture points).[4] Especially significant is that in almost all solids except rubber, the proportionality, elastic, and yield limits are all small compared to unity.

proportionality limit

elastic limit

yield point

rupture point

11.3.3

11.3.3 Elastic Moduli and Elastostatic Stress Tensor

In realms where Hooke's law is valid, there is a corresponding linear relationship between the material's stress tensor and its strain tensor. The most general linear equation relating two second-rank tensors involves a fourth-rank tensor known as the *elastic modulus tensor* $\mathbf{Y}$. In slot-naming index notation,

elastic modulus tensor

$$T_{ij} = -Y_{ijkl} S_{kl}. \tag{11.17}$$

4. Rubber is made of long, polymeric molecules, and its elasticity arises from uncoiling of the molecules when a force is applied, which is a different mechanism than is found in crystalline materials (Xing, Goldbart, and Radzihovsky, 2007).

For general queries contact webmaster@press.princeton.edu.

© Copyright Princeton University Press. No part of this book may be distributed, posted, or reproduced in any form by digital or mechanical means without prior written permission of the publisher.

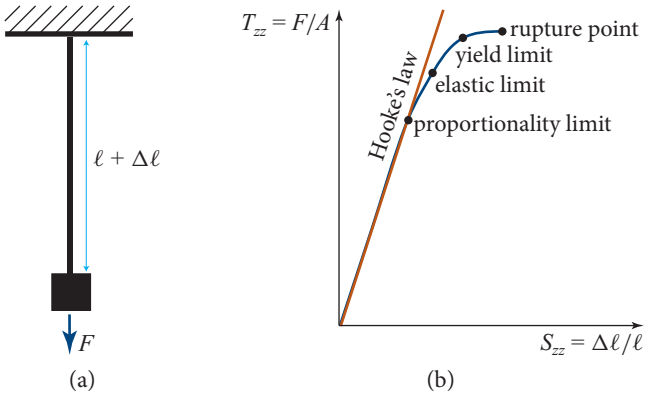

FIGURE 11.4 The stress-strain relation for a rod, showing special points at which the behavior of the rod's material changes.

Now, a general fourth-rank tensor in 3 dimensions has $3^4 = 81$ independent components. Elasticity can get complicated! However, the situation need not be so dire. There are several symmetries that we can exploit. Let us look first at the general case. As the stress and strain tensors are both symmetric, $\mathbf{Y}$ is symmetric in its first pair of slots, and we are free to choose it symmetric in its second pair: $Y_{ijkl} = Y_{jikl} = Y_{ijlk}$. There are therefore 6 independent components Y_{ijkl} for variable i, j and fixed k, l, and vice versa. In addition, as we will show, $\mathbf{Y}$ is symmetric under an interchange of its first and second pairs of slots: $Y_{ijkl} = Y_{klij}$. There are therefore $(6 \times 7)/2 = 21$ independent components in $\mathbf{Y}$. This is an improvement over 81. Many substances, notably crystals, exhibit additional symmetries, which can reduce the number of independent components considerably.

The simplest, and in fact most common, case arises when the medium is *isotropic*. In other words, there are no preferred directions in the material. This occurs when the solid is polycrystalline or amorphous and completely disordered on a scale large compared with the atomic spacing, but small compared with the solid's inhomogeneity scale.

If a medium is isotropic, then its elastic properties must be describable by scalars that relate the irreducible parts P and $\mathbf{T}^{\rm shear}$ of the stress tensor $\mathbf{T}$ to those, Θ and $\mathbf{\Sigma}$, of the strain tensor $\mathbf{S}$. The only mathematically possible, linear, coordinate-independent relationship between $\{P, \mathbf{T}^{\rm shear}\}$ and $\{\Theta, \mathbf{\Sigma}\}$ involving solely scalars is $P = -K\Theta$, $\mathbf{T}^{\rm shear} = -2\mu\mathbf{\Sigma}$, corresponding to a total stress tensor

$$\boxed{\mathbf{T} = -K\Theta\mathbf{g} - 2\mu\Sigma.} \tag{11.18}$$

bulk modulus, shear modulus, and stress tensor for isotropic elastic medium

Here K is called the *bulk modulus* and μ the *shear modulus*, and the factor 2 is included for purely historical reasons. The first minus sign (with $K > 0$) ensures that the isotropic part of the stress, $-K\Theta\mathbf{g}$, resists volume changes; the second minus sign (with $\mu > 0$) ensures that the symmetric, trace-free part, $-2\mu\mathbf{\Sigma}$, resists shape changes (resists shearing).

For general queries contact webmaster@press.princeton.edu.

© Copyright Princeton University Press. No part of this book may be distributed, posted, or reproduced in any form by digital or mechanical means without prior written permission of the publisher.

Hooke's law (Figs. 11.1 and 11.4) can be expressed in this same stress-proportional-to-strain form. The stress, when the rod is stretched, is the force F that does the stretching divided by the rod's cross sectional area A, the strain is the rod's fractional change of length $\Delta\ell/\ell$, and so Hooke's law takes the form

$$F/A = -E\Delta\ell/\ell, \tag{11.19}$$

with E an elastic coefficient called *Young's modulus*. In Sec. 11.4, we show that E is a combination of the bulk and shear moduli: $E = 9\mu K/(3K+\mu)$.

In many treatments and applications of elasticity, the shear tensor $\mathbf{\Sigma}$ is paid little attention. The focus instead is on the strain S_{ij} and its trace $S_{kk} = \Theta$, and the elastic stress tensor (11.18) is written as $\mathbf{T} = -\lambda\Theta\mathbf{g} - 2\mu\mathbf{S}$, where $\lambda \equiv K - \frac{2}{3}\mu$. In these treatments μ and λ are called the *first and second Lamé coefficients* and are used in place of μ and K. We shall not adopt this viewpoint.

Lamé coefficients

11.3.4 Energy of Deformation

Take a wire of length ℓ and cross sectional area A, and stretch it (e.g., via the "Hooke's-law experiment" of Figs. 11.1 and 11.4) by an amount ζ' that grows gradually from 0 to $\Delta\ell$. When the stretch is ζ', the force that does the stretching is [by Eq. (11.19)] $F' = EA(\zeta'/\ell) = (EV/\ell^2)\zeta'$; here $V = A\ell$ is the wire's volume, and E is its Young's modulus. As the wire is gradually lengthened, the stretching force F' does work

$$W = \int_0^{\Delta\ell} F' d\zeta' = \int_0^{\Delta\ell} (EV/\ell^2)\zeta' d\zeta'$$
$$= \frac{1}{2} EV(\Delta\ell/\ell)^2.$$

This tells us that the stored elastic energy per unit volume is

$$U = \frac{1}{2} E(\Delta\ell/\ell)^2. \tag{11.20}$$

To generalize this formula to a strained, isotropic, 3-dimensional medium, consider an arbitrary but small region $\mathcal{V}$ inside a body that has already been strained by a displacement vector field ξ_i and is thus already experiencing an elastic stress $T_{ij} = -K\Theta\delta_{ij} - 2\mu\Sigma_{ij}$ [Eq. (11.18)]. Imagine building up this displacement gradually from zero at the same rate everywhere in and around $\mathcal{V}$, so at some moment during the buildup the displacement field is $\xi_i' = \xi_i\epsilon$ (with the parameter ϵ gradually growing from 0 to 1). At that moment, the stress tensor (by virtue of the linearity of the stress-strain relation) is $T_{ij}' = T_{ij}\epsilon$. On the boundary $\partial\mathcal{V}$ of the region $\mathcal{V}$, this stress exerts a force $\Delta F_i' = -T_{ij}'\Delta\Sigma_j$ across any surface element $\Delta\Sigma_j$, from the exterior of ∂V to its interior. As the displacement grows, this surface force does the following amount of work on $\mathcal{V}$:

$$\Delta W_{\rm surf} = \int \Delta F_i' d\xi_i' = \int (-T_{ij}'\Delta\Sigma_j) d\xi_i' = -\int_0^1 T_{ij}\epsilon\Delta\Sigma_j\xi_i' d\epsilon = -\frac{1}{2} T_{ij}\Delta\Sigma_j\xi_i. \tag{11.21}$$

For general queries contact webmaster@press.princeton.edu.

© Copyright Princeton University Press. No part of this book may be distributed, posted, or reproduced in any form by digital or mechanical means without prior written permission of the publisher.

The total amount of work done can be computed by adding up the contributions from all the surface elements of $\partial\mathcal{V}$:

$$W_{\rm surf} = -\frac{1}{2}\int_{\partial\mathcal{V}} T_{ij}\xi_i d\Sigma_j = -\frac{1}{2}\int_{\mathcal{V}} (T_{ij}\xi_i)_{;j} dV = -\frac{1}{2}(T_{ij}\xi_i)_{;j}\, V. \qquad (11.22)$$

In the second step we have used Gauss's theorem, and in the third step we have used the smallness of the region $\mathcal{V}$ to infer that the integrand is very nearly constant and the integral is the integrand times the total volume V of $\mathcal{V}$.

Does $W_{\rm surf}$ equal the elastic energy stored in $\mathcal{V}$? The answer is "no," because we must also take account of the work done in the interior of $\mathcal{V}$ by gravity or any other nonelastic force that may be acting. Although it is not easy in practice to turn gravity off and then on, we must do so in the following thought experiment. In the volume's final deformed state, the divergence of its elastic stress tensor is equal to the gravitational force density, $\boldsymbol{\nabla}\cdot\mathbf{T} = \rho\mathbf{g}$ [Eqs. (11.13) and (11.14)]; and in the initial, undeformed and unstressed state, $\boldsymbol{\nabla}\cdot\mathbf{T}$ must be zero, whence so must $\mathbf{g}$. Therefore, we must imagine growing the gravitational force proportional to ϵ just like we grow the displacement, strain, and stress. During this growth, with $\mathbf{g}' = \epsilon\mathbf{g}$, the gravitational force $\rho\mathbf{g}'V$ does the following amount of work on our tiny region $\mathcal{V}$:

$$W_{\rm grav} = \int \rho V\mathbf{g}'\cdot d\boldsymbol{\xi}' = \int_0^1 \rho V\mathbf{g}\epsilon\cdot\boldsymbol{\xi} d\epsilon = \frac{1}{2}\rho V\mathbf{g}\cdot\boldsymbol{\xi} = \frac{1}{2}(\boldsymbol{\nabla}\cdot\mathbf{T})\cdot\boldsymbol{\xi}V = \frac{1}{2}T_{ij;j}\xi_i\, V. \qquad (11.23)$$

The total work done to deform $\mathcal{V}$ is the sum of the work done by the elastic force (11.22) on its surface and the gravitational force (11.23) in its interior, $W_{\rm surf} + W_{\rm grav} = -\frac{1}{2}(\xi_i T_{ij})_{;j}V + \frac{1}{2}T_{ij;j}\xi_i V = -\frac{1}{2}T_{ij}\xi_{i;j}V$. This work gets stored in $\mathcal{V}$ as elastic energy, so the energy density is $U = -\frac{1}{2}T_{ij}\xi_{i;j}$. Inserting (for an isotropic material) $T_{ij} = -K\Theta g_{ij} - 2\mu\Sigma_{ij}$ and $\xi_{i;j} = \frac{1}{3}\Theta g_{ij} + \Sigma_{ij} + R_{ij}$ in this equation for U and performing some simple algebra that relies on the symmetry properties of the expansion, shear, and rotation (Ex. 11.3), we obtain

$$\boxed{U = \frac{1}{2}K\Theta^2 + \mu\Sigma_{ij}\Sigma_{ij}.} \qquad (11.24)$$

elastic energy density at fixed temperature

Note that this elastic energy density is always positive if the elastic moduli are positive, as they must be for matter to be stable against small perturbations, and note that it is independent of the rotation R_{ij}, as it should be on physical grounds.

For the more general, anisotropic case, expression (11.24) becomes [by virtue of the stress-strain relation $T_{ij} = -Y_{ijkl}\xi_{k;l}$, Eq. (11.17)]

$$U = \frac{1}{2}\xi_{i;j}Y_{ijkl}\xi_{k;l}. \qquad (11.25)$$

The volume integral of the elastic energy density given by Eq. (11.24) or (11.25) can be used as an action from which to compute the stress, by varying the displacement (Ex. 11.4). Since only the part of $\mathbf{Y}$ that is symmetric under interchange of the first

For general queries contact webmaster@press.princeton.edu.

© Copyright Princeton University Press. No part of this book may be distributed, posted, or reproduced in any form by digital or mechanical means without prior written permission of the publisher.

and second pairs of slots contributes to U, only that part can affect the action-principle-derived stress. Therefore, it must be that $Y_{ijkl} = Y_{klij}$. This is the symmetry we asserted earlier.

EXERCISES

Exercise 11.3 *Derivation and Practice: Elastic Energy*
Beginning with $U = -\frac{1}{2} T_{ij} \xi_{i;j}$ [text following Eq. (11.23)], derive Eq. (11.24) for the elastic energy density inside a body.

Exercise 11.4 *Derivation and Practice: Action Principle for Elastic Stress*
For an anisotropic, elastic medium with elastic energy density $U = \frac{1}{2} \xi_{i;j} Y_{ijkl} \xi_{k;l}$, integrate this energy density over a 3-dimensional region $\mathcal{V}$ (not necessarily small) to get the total elastic energy E. Now consider a small variation $\delta\xi_i$ in the displacement field. Evaluate the resulting change δE in the elastic energy without using the relation $T_{ij} = -Y_{ijkl}\xi_{k;l}$. Convert to a surface integral over $\partial\mathcal{V}$, and thence infer the stress-strain relation $T_{ij} = -Y_{ijkl}\xi_{k;l}$.

11.3.5

11.3.5 Thermoelasticity

In our discussion of deformation energy, we tacitly assumed that the temperature of the elastic medium was held fixed during the deformation (i.e., we ignored the possibility of any thermal expansion). Correspondingly, the energy density U that we computed is actually the physical free energy per unit volume $\mathcal{F}$, at some chosen temperature T_0 of a heat bath. If we increase the bath's and material's temperature from T_0 to $T = T_0 + \delta T$, then the material wants to expand by $\Theta = \delta V / V = 3\alpha\delta T$ (i.e., it will have vanishing expansional elastic energy if Θ has this value). Here α is its coefficient of linear thermal expansion. (The factor 3 is because there are three directions into which it can expand: x, y, and z.) Correspondingly, the physical-free-energy density at temperature $T = T_0 + \delta T$ is

coefficient of linear thermal expansion

elastic physical free energy

$$\mathcal{F} = \mathcal{F}_0(T) + \frac{1}{2} K (\Theta - 3\alpha\delta T)^2 + \mu \Sigma_{ij}\Sigma_{ij}. \tag{11.26}$$

The stress tensor in this heated and strained state can be computed from $T_{ij} = -\partial\mathcal{F}/\partial S_{ij}$ [a formula most easily inferred from Eq. (11.25) with U reinterpreted as $\mathcal{F}$ and $\xi_{i;j}$ replaced by its symmetrization, S_{ij}]. Reexpressing Eq. (11.26) in terms of S_{ij} and computing the derivative, we obtain (not surprisingly!)

$$T_{ij} = -\frac{\partial \mathcal{F}}{\partial S_{ij}} = -K(\Theta - 3\alpha\delta T)\delta_{ij} - 2\mu\Sigma_{ij}. \tag{11.27}$$

What happens if we allow our material to expand *adiabatically* rather than at fixed temperature? Adiabatic expansion means expansion at fixed entropy S. Consider a small sample of material that contains mass M and has volume $V = M/\rho$. Its entropy

For general queries contact webmaster@press.princeton.edu.

© Copyright Princeton University Press. No part of this book may be distributed, posted, or reproduced in any form by digital or mechanical means without prior written permission of the publisher.

is $S = -[\partial(\mathcal{F}V)/\partial T]_V$ [cf. Eq. (5.33)], which, using Eq. (11.26), becomes

$$S = S_0(T) + 3\alpha K\Theta\, V\,. \tag{11.28}$$

Here we have neglected the term $-9\alpha^2 K\delta T$, which can be shown to be negligible compared to the temperature dependence of the elasticity-independent term $S_0(T)$. If our sample expands adiabatically by an amount $\Delta V = V\Delta\Theta$, then its temperature must go down by the amount $\Delta T < 0$ that keeps S fixed (i.e., that makes $\Delta S_0 = -3\alpha K V \Delta\Theta$). Noting that $T\Delta S_0$ is the change of the sample's thermal energy, which is $\rho c_V \Delta T$ (c_V is the specific heat per unit mass), we see that the temperature change is

$$\frac{\Delta T}{T} = \frac{-3\alpha K \Delta\Theta}{\rho c_V} \quad \text{for adiabatic expansion.} \tag{11.29}$$

temperature change in adiabatic expansion

This temperature change, accompanying an adiabatic expansion, alters slightly the elastic stress [Eq. (11.27)] and thence the bulk modulus K (i.e., it gives rise to an adiabatic bulk modulus that differs slightly from the isothermal bulk modulus K introduced in previous sections). However, the differences are so small that they are generally ignored. For further details, see Landau and Lifshitz (1986, Sec. 6).

11.3.6 Molecular Origin of Elastic Stress; Estimate of Moduli

It is important to understand the microscopic origin of the elastic stress. Consider an ionic solid in which singly ionized ions (e.g., positively charged sodium and negatively charged chlorine) attract their nearest (opposite-species) neighbors through their mutual Coulomb attraction and repel their *next* nearest (same-species) neighbors, and so on. Overall, there is a net electrostatic attraction on each ion, which is balanced by the short-range repulsion of its bound electrons against its neighbors' bound electrons. Now consider a thin slice of material of thickness intermediate between the inter-atomic spacing and the solid's inhomogeneity scale (Fig. 11.5).

Although the electrostatic force between individual pairs of ions is long range, the material is electrically neutral on the scale of several ions; as a result, when averaged

FIGURE 11.5 A thin slice of an ionic solid (between the dark lines) that interacts electromagnetically with ions outside it. The electrostatic force on the slice is dominated by interactions between ions lying in the two thin shaded areas, a few atomic layers thick, one on each side of the slice. The force is effectively a surface force rather than a volume force. In elastostatic equilibrium, the forces on the two sides are equal and opposite, if the slice is sufficiently thin.

For general queries contact webmaster@press.princeton.edu.

© Copyright Princeton University Press. No part of this book may be distributed, posted, or reproduced in any form by digital or mechanical means without prior written permission of the publisher.

TABLE 11.1: Density ρ; bulk, shear, and Young's moduli K, μ, and E, respectively; Poisson's ratio ν; and yield strain S_Y under tension, for various materials

Substance	ρ (kg m^{-3})	K (GPa)	μ (GPa)	E (GPa)	ν	S_Y	c_L (km s^{-1})	c_T (km s^{-1})
Carbon nanotube	1,300			∼1,000		0.05		
Steel	7,800	170	81	210	0.29	0.003	5.9	3.2
Copper	8,960	130	45	120	0.34	0.0006	4.6	2.2
Rock	3,000	70	40	100	0.25	0.001	6.0	3.5
Glass	2,500	47	28	70	0.25	0.0005	5.8	3.3
Rubber	1,200	10	0.0007	0.002	0.50	∼8	1.0	0.03
DNA molecule				0.3		∼0.1		

Notes: The final two columns are the longitudinal and transverse sound speeds c_L, c_T, defined in Chap. 12. The DNA molecule is discussed in Ex. 11.12.

over many ions, the net electric force is short range (Fig. 11.5). We can therefore treat the net force acting on the thin slice as a surface force, governed by local conditions in the material. This is essential if we are to be able to write down a localized linear stress-strain relation $T_{ij} = -Y_{ijkl}S_{kl}$ or $T_{ij} = -K\Theta\delta_{ij} - 2\mu\Sigma_{ij}$. This need not have been the case; there are other circumstances where the net electrostatic force is long range, not short. One example occurs in certain types of crystal (e.g., tourmaline), which develop internal, long-range *piezoelectric* fields when strained.

Our treatment so far has implicitly assumed that matter is continuous on all scales and that derivatives are mathematically well defined. Of course, this is not the case. In fact, we not only need to acknowledge the existence of atoms, we must also use them to compute the elastic moduli.

magnitudes of elastic moduli

We can estimate the elastic moduli in ionic or metallic materials by observing that, if a crystal lattice were to be given a dimensionless strain of order unity, then the elastic stress would be of order the electrostatic force between adjacent ions divided by the area associated with each ion. If the lattice spacing is $a \sim 2$ Å $= 0.2$ nm and the ions are singly charged, then K and $\mu \sim e^2/4\pi\epsilon_0 a^4 \sim 100$ GPa. This is about a million atmospheres. Covalently bonded compounds are less tightly bound and have somewhat smaller elastic moduli; exotic carbon nanotubes have larger moduli. See Table 11.1.

On the basis of this argument, it might be thought that crystals can be subjected to strains of order unity before they attain their elastic limits. However, as discussed in Sec. 11.3.2, most materials are only elastic for strains $\lesssim 10^{-3}$. The reason for this difference is that crystals are generally imperfect and are laced with *dislocations*. Relatively small stresses suffice for the dislocations to move through the solid and for the crystal thereby to undergo permanent deformation (Fig. 11.6).

For general queries contact webmaster@press.princeton.edu.

© Copyright Princeton University Press. No part of this book may be distributed, posted, or reproduced in any form by digital or mechanical means without prior written permission of the publisher.

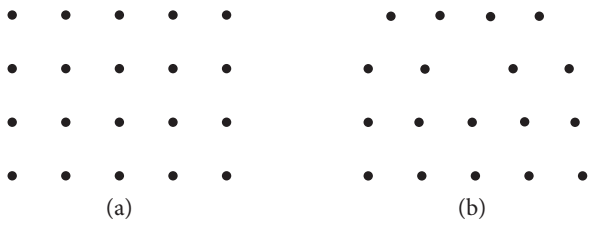

FIGURE 11.6 The ions in one layer of a crystal. In subsequent layers, going into each picture, the ion distribution is the same. (a) This perfect crystal, in which the atoms are organized in a perfectly repeating lattice, can develop very large shear strains without yielding. (b) Real materials contain dislocations that greatly reduce their rigidity. The simplest type of dislocation, shown here, is the *edge dislocation* (with the central vertical atomic layer having a terminating edge that extends into the picture). The dislocation will move transversely, and the crystal thereby will undergo inelastic deformation when the strain is typically greater than $\sim 10^{-3}$, which is $\sim 1\%$ of the yield shear strain for a perfect crystal.

EXERCISES

Exercise 11.5 *Problem: Order-of-Magnitude Estimates*

(a) What is the maximum size of a nonspherical asteroid? [Hint: If the asteroid is too large, its gravity will deform it into a spherical shape.]

(b) What length of steel wire can hang vertically without breaking? What length of carbon nanotube? What are the prospects for creating a tether that hangs to Earth's surface from a geostationary satellite?

(c) Can a helium balloon lift the tank used to transport its helium gas? (Purcell, 1983).

Exercise 11.6 *Problem: Jumping Heights*

Explain why all animals, from fleas to humans to elephants, can jump to roughly the same height. The field of science that deals with topics like this is called *allometry* (Ex. 11.18).

11.3.7 Elastostatic Equilibrium: Navier-Cauchy Equation

11.3.7

elastic force density

It is commonly the case that the elastic moduli K and μ are constant (i.e., independent of location in the medium), even though the medium is stressed in an inhomogeneous way. (This is because the strains are small and thus perturb the material properties by only small amounts.) If so, then from the elastic stress tensor $\mathbf{T} = -K\Theta\mathbf{g} - 2\mu\boldsymbol{\Sigma}$ and expressions (11.4a) and (11.4b) for the expansion and shear in terms of the displacement vector, we can deduce the following expression for the elastic force density $\mathbf{f}$ [Eq. (11.13)] inside the body:

$$\boxed{\mathbf{f} = -\nabla\cdot\mathbf{T} = K\nabla\Theta + 2\mu\nabla\cdot\boldsymbol{\Sigma} = \left(K + \frac{1}{3}\mu\right)\nabla(\nabla\cdot\boldsymbol{\xi}) + \mu\nabla^2\boldsymbol{\xi};} \quad (11.30)$$

For general queries contact webmaster@press.princeton.edu.

© Copyright Princeton University Press. No part of this book may be distributed, posted, or reproduced in any form by digital or mechanical means without prior written permission of the publisher.

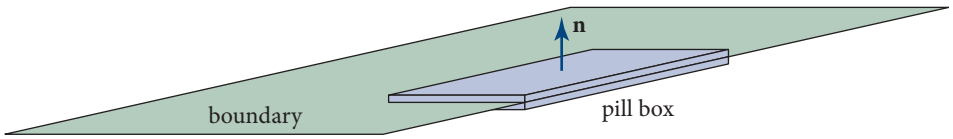

FIGURE 11.7 Pill box used to derive boundary conditions in electrostatics and elastostatics.

see Ex. 11.7. Here $\nabla \cdot \mathbf{\Sigma}$ in index notation is $\Sigma_{ij;j} = \Sigma_{ji;j}$. Extra terms must be added if we are dealing with anisotropic materials. However, in this book Eq. (11.30) will be sufficient for our needs.

If no other countervailing forces act in the interior of the material (e.g., if there is no gravitational force), and if, as in this chapter, the material is in a static, equilibrium state rather than vibrating dynamically, then this force density will have to vanish throughout the material's interior. This vanishing of $\mathbf{f} \equiv -\nabla \cdot \mathbf{T}$ is just a fancy version of Newton's law for static situations, $\mathbf{F} = m\mathbf{a} = 0$. If the material has density ρ and is pulled on by a gravitational acceleration $\mathbf{g}$, then the sum of the elastostatic force per unit volume and gravitational force per unit volume must vanish, $\mathbf{f} + \rho\mathbf{g} = 0$:

Navier-Cauchy equation for elastostatic equilibrium

$$\boxed{\mathbf{f} + \rho\mathbf{g} = \left(K + \frac{1}{3}\mu\right) \nabla(\nabla \cdot \boldsymbol{\xi}) + \mu\nabla^2\boldsymbol{\xi} + \rho\mathbf{g} = 0.} \tag{11.31}$$

This is often called the *Navier-Cauchy equation*.[5]

When external forces are applied to the surface of an elastic body (e.g., when one pushes on the face of a cylinder) and gravity acts on the interior, the distribution of the strain $\boldsymbol{\xi}(\mathbf{x})$ inside the body can be computed by solving the Navier-Cauchy equation (11.31) subject to boundary conditions provided by the applied forces.

In electrostatics, one can derive boundary conditions by integrating Maxwell's equations over the interior of a thin box (a "pill box") with parallel faces that snuggle up to the boundary (Fig. 11.7). For example, by integrating $\nabla \cdot \mathbf{E} = \rho_e/\epsilon_o$ over the interior of the pill box and then applying Gauss's law to convert the left-hand side to a surface integral, we obtain the junction condition that the discontinuity in the normal component of the electric field is equal $1/\epsilon_o$ times the surface charge density. Similarly, in elastostatics one can derive boundary conditions by integrating the elastostatic equation $\nabla \cdot \mathbf{T} = 0$ over the pill box of Fig. 11.7 and then applying Gauss's law:

$$0 = \int_{\mathcal{V}} \nabla \cdot \mathbf{T}\, dV = \int_{\partial\mathcal{V}} \mathbf{T} \cdot d\mathbf{\Sigma} = \int_{\partial\mathcal{V}} \mathbf{T} \cdot \mathbf{n}\, dA = [(\mathbf{T} \cdot \mathbf{n})_{\text{upper face}} - (\mathbf{T} \cdot \mathbf{n})_{\text{lower face}}]\, A. \tag{11.32}$$

Here in the next-to-last expression we have used $d\mathbf{\Sigma} = \mathbf{n}\, dA$, where dA is the scalar area element, and $\mathbf{n}$ is the unit normal to the pill-box face. In the last term we have

5. It was first written down by Claude-Louis Navier (in 1821) and in a more general form by Augustin-Louis Cauchy (in 1822).

For general queries contact webmaster@press.princeton.edu.

© Copyright Princeton University Press. No part of this book may be distributed, posted, or reproduced in any form by digital or mechanical means without prior written permission of the publisher.

assumed the pill box has a small face, so $\mathbf{T}\cdot\mathbf{n}$ can be treated as constant and be pulled outside the integral. The result is the boundary condition that

$$\mathbf{T}\cdot\mathbf{n} \quad \text{must be continuous across any boundary;} \tag{11.33}$$

boundary conditions for Navier-Cauchy equation

in index notation, $T_{ij}n_j$ is continuous.

Physically, this is nothing but the law of force balance across the boundary: the force per unit area acting from the lower side to the upper side must be equal and opposite to that acting from upper to lower. As an example, if the upper face is bounded by vacuum, then the solid's stress tensor must satisfy $T_{ij}n_j = 0$ at the surface. If a normal pressure P is applied by some external agent at the upper face, then the solid must respond with a normal force equal to P: $n_i T_{ij} n_j = P$. If a vectorial force per unit area $\mathcal{F}_i$ is applied at the upper face by some external agent, then it must be balanced: $T_{ij}n_j = -\mathcal{F}_i$.

Solving the Navier-Cauchy equation (11.32) for the displacement field $\boldsymbol{\xi}(\mathbf{x})$, subject to specified boundary conditions, is a problem in elastostatics analogous to solving Maxwell's equations for an electric field subject to boundary conditions in electrostatics, or for a magnetic field subject to boundary conditions in magnetostatics. The types of solution techniques used in electrostatics and magnetostatics can also be used here. See Box 11.3.

EXERCISES

Exercise 11.7 *Derivation and Practice: Elastic Force Density*
From Eq. (11.18) derive expression (11.30) for the elastostatic force density inside an elastic body.

Exercise 11.8 ***Practice: Biharmonic Equation*
A homogeneous, isotropic, elastic solid is in equilibrium under (uniform) gravity and applied surface stresses. Use Eq. (11.30) to show that the displacement inside it, $\boldsymbol{\xi}(\mathbf{x})$, is biharmonic, i.e., it satisfies the differential equation

$$\boxed{\nabla^2\nabla^2\boldsymbol{\xi} = 0.} \tag{11.34a}$$

Show also that the expansion Θ satisfies the Laplace equation

$$\boxed{\nabla^2\Theta = 0.} \tag{11.34b}$$

11.4 Young's Modulus and Poisson's Ratio for an Isotropic Material: A Simple Elastostatics Problem

11.4

As a simple example of an elastostatics problem, we explore the connection between our 3-dimensional theory of stress and strain and the 1-dimensional Hooke's law (Fig. 11.1).

For general queries contact webmaster@press.princeton.edu.

© Copyright Princeton University Press. No part of this book may be distributed, posted, or reproduced in any form by digital or mechanical means without prior written permission of the publisher.

BOX 11.3. METHODS OF SOLVING THE NAVIER-CAUCHY EQUATION

Many techniques have been devised to solve the Navier-Cauchy equation (11.31), or other equations equivalent to it, subject to appropriate boundary conditions. Among them are:

- Separation of variables. See Sec. 11.9.2.
- Green's functions. See Ex. 11.27 and Johnson (1985).
- Variational principles. See Marsden and Hughes (1986, Chap. 5) and Slaughter (2002, Chap. 10).
- Saint-Venant's principle. One changes the boundary conditions to something simpler, for which the Navier-Cauchy equation can be solved analytically, and then one uses linearity of the Navier-Cauchy equation to compute an approximate, additive correction that accounts for the difference in boundary conditions.[1]
- Dimensional reduction. This method reduces the theory to 2 dimensions in the case of thin plates (Sec. 11.7), and to 1 dimension for rods and for translation-invariant plates (Sec. 11.5).
- Complex variable methods. These are particularly useful in solving the 2-dimensional equations (Boresi and Chong, 1999, Appendix 5B).
- Numerical simulations on computers. These are usually carried out by the method of finite elements, in which one approximates stressed objects by a finite set of elementary, interconnected physical elements, such as rods; thin, triangular plates; and tetrahedra (Ugural and Fenster, 2012, Chap. 7).
- Replace Navier-Cauchy by equivalent equations. For example, and widely used in the engineering literature, write force balance $T_{ij;j} = 0$ in terms of the strain tensor S_{ij}, supplement this with an equation that guarantees S_{ij} can be written as the symmetrized gradient of a vector field (the displacement vector), and develop techniques to solve these coupled equations plus boundary conditions for S_{ij} [Ugural and Fenster (2012, Sec. 2.4); also large parts of Boresi and Chong (1999) and Slaughter (2002)].
- Mathematica or other computer software. These software packages can be used to perform complicated analytical analyses. One can then explore their predictions numerically (Constantinescu and Korsunsky, 2007).

1. In 1855 Barré de Saint-Venant had the insight to realize that, under suitable conditions, the correction will be significant only locally (near the altered boundary) and not globally. (See Boresi and Chong, 1999, pp. 288ff; Ugural and Fenster, 2012, Sec. 2.16, and references therein.)

For general queries contact webmaster@press.princeton.edu.

© Copyright Princeton University Press. No part of this book may be distributed, posted, or reproduced in any form by digital or mechanical means without prior written permission of the publisher.

Consider a thin rod of square cross section hanging along the $\mathbf{e}_z$ direction of a Cartesian coordinate system (Fig. 11.1). Subject the rod to a stretching force applied normally and uniformly at its ends. (It could just as easily be a rod under compression.) Its sides are free to expand or contract transversely, since no force acts on them: $dF_i = T_{ij}d\Sigma_j = 0$. As the rod is slender, vanishing of dF_i at its x and y sides implies to high accuracy that the stress components T_{ix} and T_{iy} will vanish throughout the interior; otherwise there would be a very large force density $T_{ij;j}$ inside the rod. Using $T_{ij} = -K\Theta g_{ij} - 2\mu\Sigma_{ij}$, we then obtain

$$T_{xx} = -K\Theta - 2\mu\Sigma_{xx} = 0, \tag{11.35a}$$

$$T_{yy} = -K\Theta - 2\mu\Sigma_{yy} = 0, \tag{11.35b}$$

$$T_{yz} = -2\mu\Sigma_{yz} = 0, \tag{11.35c}$$

$$T_{xz} = -2\mu\Sigma_{xz} = 0, \tag{11.35d}$$

$$T_{xy} = -2\mu\Sigma_{xy} = 0, \tag{11.35e}$$

$$T_{zz} = -K\Theta - 2\mu\Sigma_{zz}. \tag{11.35f}$$

From the first two of these equations and $\Sigma_{xx} + \Sigma_{yy} + \Sigma_{zz} = 0$, we obtain a relationship between the expansion and the nonzero components of the shear,

$$K\Theta = \mu\Sigma_{zz} = -2\mu\Sigma_{xx} = -2\mu\Sigma_{yy}; \tag{11.36}$$

and from this and Eq. (11.35f), we obtain $T_{zz} = -3K\Theta$. The decomposition of S_{ij} into its irreducible tensorial parts tells us that $S_{zz} = \xi_{z;z} = \Sigma_{zz} + \frac{1}{3}\Theta$, which becomes, on using Eq. (11.36), $\xi_{z;z} = [(3K + \mu)/(3\mu)]\Theta$. Combining with $T_{zz} = -3K\Theta$, we obtain Hooke's law and an expression for Young's modulus E in terms of the bulk and shear moduli:

Hooke's law and Young's modulus

$$\frac{-T_{zz}}{\xi_{z;z}} = \frac{9\mu K}{3K + \mu} = E. \tag{11.37}$$

It is conventional to introduce *Poisson's ratio* ν, which is minus the ratio of the lateral strain to the longitudinal strain during a deformation of this type, where the transverse motion is unconstrained. It can be expressed as a ratio of elastic moduli as follows:

Poisson's ratio

$$\nu \equiv -\frac{\xi_{x;x}}{\xi_{z;z}} = -\frac{\xi_{y;y}}{\xi_{z;z}} = -\frac{\Sigma_{xx} + \frac{1}{3}\Theta}{\Sigma_{zz} + \frac{1}{3}\Theta} = \frac{3K - 2\mu}{2(3K + \mu)}, \tag{11.38}$$

where we have used Eq. (11.36). We tabulate these relations and their inverses for future use:

$$\boxed{E = \frac{9\mu K}{3K + \mu}, \quad \nu = \frac{3K - 2\mu}{2(3K + \mu)}; \qquad K = \frac{E}{3(1 - 2\nu)}, \quad \mu = \frac{E}{2(1 + \nu)}.} \tag{11.39}$$

For general queries contact webmaster@press.princeton.edu.

© Copyright Princeton University Press. No part of this book may be distributed, posted, or reproduced in any form by digital or mechanical means without prior written permission of the publisher.

We have already remarked that mechanical stability of a solid requires that $K, \mu > 0$. Using Eq. (11.39), we observe that this imposes a restriction on Poisson's ratio, namely that $-1 < \nu < 1/2$. For metals, Poisson's ratio is typically about 1/3, and the shear modulus is roughly half the bulk modulus. For a substance that is easily sheared but not easily compressed, like rubber (or neutron star crusts; Sec. 11.3.6), the bulk modulus is relatively high and $\nu \simeq 1/2$ (cf. Table 11.1). For some exotic materials, Poisson's ratio can be negative (cf. Yeganeh-Haeri, Weidner, and Parise, 1992).

Although we derived them for a square strut under extension, our expressions for Young's modulus and Poisson's ratio are quite general. To see this, observe that the derivation would be unaffected if we combined many parallel, square fibers together. All that is necessary is that the transverse motion be free, so that the only applied force is uniform and normal to a pair of parallel faces.

11.5 Reducing the Elastostatic Equations to 1 Dimension for a Bent Beam: Cantilever Bridge, Foucault Pendulum, DNA Molecule, Elastica

dimensional reduction

When dealing with bodies that are much thinner in 2 dimensions than the third (e.g., rods, wires, and beams), one can use the *method of moments* to reduce the 3-dimensional elastostatic equations to ordinary differential equations in 1 dimension (a process called *dimensional reduction*). We have already met an almost trivial example of this in our discussion of Hooke's law and Young's modulus (Sec. 11.4 and Fig. 11.1). In this section, we discuss a more complicated example, the bending of a beam through a small displacement angle. In Ex. 11.13, we shall analyze a more complicated example: the bending of a long, elastic wire into a complicated shape called an *elastica*.

Our beam-bending example is motivated by a common method of bridge construction, which uses cantilevers. (A famous historical example is the old bridge over the Firth of Forth in Scotland that was completed in 1890 with a main span of half a kilometer.)

The principle is to attach two independent beams to the two shores as cantilevers, and allow them to meet in the middle. (In practice the beams are usually supported at the shores on piers and strengthened along their lengths with trusses.) Similar cantilevers, with lengths of order a micron or less, are used in atomic force microscopes and other nanotechnology applications, including quantum-information experiments.

Let us make a simple model of a cantilever (Fig. 11.8). Consider a beam clamped rigidly at one end, with length ℓ, horizontal width w, and vertical thickness h. Introduce local Cartesian coordinates with $\mathbf{e}_x$ pointing along the beam and $\mathbf{e}_z$ pointing vertically upward. Imagine the beam extending horizontally in the absence of gravity. Now let it sag under its own weight, so that each element is displaced through a small distance $\boldsymbol{\xi}(\mathbf{x})$. The upper part of the beam is stretched, while the lower part is compressed, so there must be a *neutral surface* where the horizontal strain $\xi_{x,x}$ vanishes.

neutral surface

For general queries contact webmaster@press.princeton.edu.

© Copyright Princeton University Press. No part of this book may be distributed, posted, or reproduced in any form by digital or mechanical means without prior written permission of the publisher.

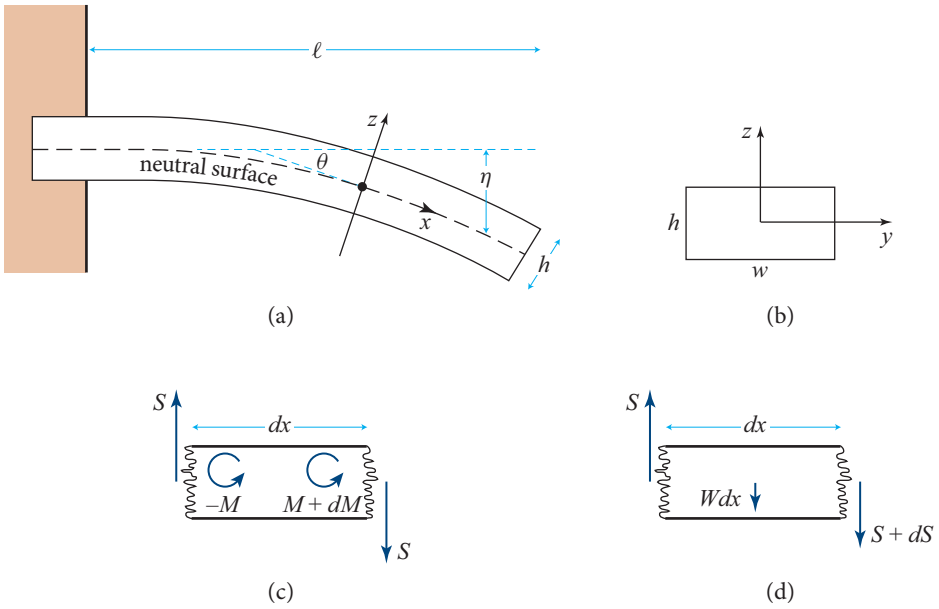

FIGURE 11.8 Bending of a cantilever. (a) A beam is held rigidly at one end and extends horizontally with the other end free. We introduce an orthonormal coordinate system (x, y, z) with $\mathbf{e}_x$ extending along the beam. We only consider small departures from equilibrium. The bottom of the beam will be compressed, the upper portion extended. There is therefore a neutral surface $z = 0$ on which the strain $\xi_{x,x}$ vanishes. (b) The beam has a rectangular cross section with horizontal width w and vertical thickness h; its length is ℓ. (c) The bending torque M must be balanced by the torque exerted by the vertical shear force S. (d) The shear force S must vary along the beam so as to support the beam's weight per unit length, W.

This neutral surface must itself be curved downward. Let its downward displacement from the horizontal plane that it occupied before sagging be $\eta(x)$ (> 0), let a plane tangent to the neutral surface make an angle $\theta(x)$ (also > 0) with the horizontal, and adjust the x and z coordinates so x runs along the slightly curved neutral plane and z is orthogonal to it (Fig. 11.8). The longitudinal strain is then given to first order in small quantities by

$$\xi_{x,x} = \frac{z}{\mathcal{R}} = z\frac{d\theta}{dx} \simeq z\frac{d^2\eta}{dx^2}, \tag{11.40a}$$

longitudinal strain

where $\mathcal{R} = dx/d\theta > 0$ is the radius of curvature of the beam's bend, and we have chosen $z = 0$ at the neutral surface. The 1-dimensional displacement $\eta(x)$ will be the focus for dimensional reduction of the elastostatic equations.

As in our discussion of Hooke's law for a stretched rod (Sec. 11.4), we can regard the beam as composed of a bundle of long, parallel fibers, stretched or squeezed along their length and free to contract transversely. The longitudinal stress is therefore

$$T_{xx} = -E\xi_{x,x} = -Ez\frac{d^2\eta}{dx^2}. \tag{11.40b}$$

For general queries contact webmaster@press.princeton.edu.

© Copyright Princeton University Press. No part of this book may be distributed, posted, or reproduced in any form by digital or mechanical means without prior written permission of the publisher.

We can now compute the horizontal force density, which must vanish in elastostatic equilibrium:[6]

$$f_x = -T_{xx,x} - T_{xz,z} = Ez\frac{d^3\eta}{dx^3} - T_{xz,z} = 0. \tag{11.40c}$$

method of moments

This is a partial differential equation. We convert it into a 1-dimensional ordinary differential equation by the *method of moments*: We multiply it by z and integrate over z (i.e., we compute its "first moment"). Integrating the second term, $\int zT_{xz,z}dz$, by parts and using the boundary condition $T_{xz} = 0$ on the upper and lower surfaces of the beam, we obtain

$$\frac{Eh^3}{12}\frac{d^3\eta}{dx^3} = -\int_{-h/2}^{h/2} T_{xz}\, dz. \tag{11.40d}$$

Using $T_{xz} = T_{zx}$, notice that the integral, when multiplied by the beam's width w in the y direction, is the vertical shear force $S(x)$ in the beam:

shear force, S

$$\boxed{S = \int T_{zx}dydz = w\int_{-h/2}^{h/2} T_{zx}dz = -D\frac{d^3\eta}{dx^3}.} \tag{11.41a}$$

Here

flexural rigidity or bending modulus of an elastic beam, D

$$\boxed{D \equiv E\int z^2 dydz \equiv EA\, r_g^2 = Ewh^3/12} \tag{11.41b}$$

is called the beam's *flexural rigidity,* or its *bending modulus.* Notice that, quite generally, D is the beam's Young's modulus E times the second moment of the beam's cross sectional area A along the direction of bend. Engineers call that second moment $A\, r_g^2$ and call r_g the radius of gyration. For our rectangular beam, this D is $Ewh^3/12$.

As an aside, we can gain some insight into Eq. (11.41a) by examining the torques that act on a segment of the beam with length dx. As shown in Fig. 11.8c, the shear forces on the two ends of the segment exert a clockwise torque $2S(dx/2) = Sdx$. This is balanced by a counterclockwise torque due to the stretching of the upper half of the segment and compression of the lower half (i.e., due to the bending of the beam). This *bending torque* is

bending torque, M

$$\boxed{M \equiv \int T_{xx}zdydz = -D\frac{d^2\eta}{dx^2}} \tag{11.41c}$$

6. Because the coordinates are slightly curvilinear rather than precisely Cartesian, our Cartesian-based analysis makes small errors. Track-Two readers who have studied Sec. 11.8 can evaluate those errors using connection-coefficient terms that were omitted from this equation: $-\Gamma_{xjk}T_{jk} - \Gamma_{jkj}T_{xk}$. Each Γ has magnitude $1/\mathcal{R}$, so these terms are of order $T_{jk}/\mathcal{R}$, whereas the terms kept in Eq. (11.40c) are of order T_{xx}/ℓ and T_{xz}/h. Since the thickness h and length ℓ of the beam are small compared to the beam's radius of curvature $\mathcal{R}$, the connection-coefficient terms are negligible.

For general queries contact webmaster@press.princeton.edu.

© Copyright Princeton University Press. No part of this book may be distributed, posted, or reproduced in any form by digital or mechanical means without prior written permission of the publisher.

on the right end of the segment and minus this on the left, so torque balance says $(dM/dx)dx = Sdx$:

$$\boxed{S = dM/dx;} \tag{11.42}$$

see Fig. 11.8c. This is precisely Eq. (11.41a).

Equation (11.41a) [or equivalently, Eq. (11.42)] embodies half of the elastostatic equations. It is the x component of force balance $f_x = 0$, converted to an ordinary differential equation by evaluating its lowest nonvanishing moment: its first moment, $\int z f_x dy dz = 0$ [Eq. (11.40d)]. The other half is the z component of stress balance, which we can write as

$$T_{zx,x} + T_{zz,z} + \rho g = 0 \tag{11.43}$$

(vertical elastic force balanced by gravitational pull on the beam). We can convert this to a 1-dimensional ordinary differential equation by taking its lowest nonvanishing moment, its zeroth moment (i.e., by integrating over y and z). The result is

$$\boxed{\frac{dS}{dx} = -W,} \tag{11.44}$$

where $W = g\rho wh$ is the beam's weight per unit length (Fig. 11.8d).

weight per unit length, W

Combining our two dimensionally reduced components of force balance, Eqs. (11.41a) and (11.44), we obtain a fourth-order differential equation for our 1-dimensional displacement $\eta(x)$:

$$\boxed{\frac{d^4\eta}{dx^4} = \frac{W}{D}.} \tag{11.45}$$

elastostatic force balance equation for bent beam

(Fourth-order differential equations are characteristic of elasticity.)

Equation (11.45) can be solved subject to four appropriate boundary conditions. However, before we solve it, notice that *for a beam of a fixed length ℓ, the deflection η is inversely proportional to the flexural rigidity*. Let us give a simple example of this scaling. Floors in U.S. homes are conventionally supported by wooden joists of 2" by 6" lumber with the 6" side vertical. Suppose an inept carpenter installed the joists with the 6" side horizontal. The flexural rigidity of the joist would be reduced by a factor 9, and the center of the floor would be expected to sag 9 times as much as if the joists had been properly installed—a potentially catastrophic error.

Also, before solving Eq. (11.45), let us examine the approximations that we have made. First, we have assumed that the sag is small compared with the length of the beam, when making the small-angle approximation in Eq. (11.40a); we have also assumed the beam's radius of curvature is large compared to its length, when treating

For general queries contact webmaster@press.princeton.edu.

© Copyright Princeton University Press. No part of this book may be distributed, posted, or reproduced in any form by digital or mechanical means without prior written permission of the publisher.

our slightly curved coordinates as Cartesian.[7] These assumptions will usually be valid, but are not so for the elastica studied in Ex. 11.13. Second, by using the method of moments rather than solving for the complete local stress tensor field, we have ignored the effects of some components of the stress tensor. In particular, when evaluating the bending torque [Eq. (11.41c)] we have ignored the effect of the T_{zx} component of the stress tensor. This is $O(h/\ell)T_{xx}$, and so our equations can only be accurate for fairly slender beams. Third, the extension above the neutral surface and the compression below the neutral surface lead to changes in the cross sectional shape of the beam. The fractional error here is of order the longitudinal shear, which is small for real materials.

The solution to Eq. (11.45) is a fourth-order polynomial with four unknown constants, to be set by boundary conditions. In this problem, the beam is held horizontal at the fixed end, so that $\eta(0) = \eta'(0) = 0$, where the prime denotes d/dx. At the free end, T_{zx} and T_{xx} must vanish, so the shear force S must vanish, whence $\eta'''(\ell) = 0$ [Eq. (11.41a)]; the bending torque M [Eq. (11.41c)] must also vanish, whence [by Eq. (11.42)] $\int S dx \propto \eta''(\ell) = 0$. By imposing these four boundary conditions $\eta(0) = \eta'(0) = \eta''(\ell) = \eta'''(\ell) = 0$ on the solution of Eq. (11.45), we obtain for the beam shape

displacement of a clamped cantilever

$$\eta(x) = \frac{W}{D}\left(\frac{1}{4}\ell^2 x^2 - \frac{1}{6}\ell x^3 + \frac{1}{24}x^4\right). \tag{11.46a}$$

Therefore, the end of the beam sags by

$$\eta(\ell) = \frac{W\ell^4}{8D}. \tag{11.46b}$$

Problems in which the beam rests on supports rather than being clamped can be solved in a similar manner. The boundary conditions will be altered, but the differential equation (11.45) will be unchanged.

Now suppose that we have a cantilever bridge of constant vertical thickness h and total span $2\ell \sim 100$ m made of material with density $\rho \sim 8 \times 10^3\ \mathrm{kg\,m^{-3}}$ (e.g., steel) and Young's modulus $E \sim 100$ GPa. Suppose further that we want the center of the bridge to sag by no more than $\eta \sim 1$ m. According to Eq. (11.46b), the thickness of the beam must satisfy

$$h \gtrsim \left(\frac{3\rho g \ell^4}{2E\eta}\right)^{1/2} \sim 2.8\ \mathrm{m}. \tag{11.47}$$

This estimate makes no allowance for all the extra strengthening and support present in real structures (e.g., via trusses and cables), and so it is an overestimate.

7. In more technical language, when neglecting the connection-coefficient terms discussed in the previous footnote.

For general queries contact webmaster@press.princeton.edu.

© Copyright Princeton University Press. No part of this book may be distributed, posted, or reproduced in any form by digital or mechanical means without prior written permission of the publisher.

Exercise 11.9 *Derivation: Sag in a Cantilever*

(a) Verify Eqs. (11.46) for the sag in a horizontal beam clamped at one end and allowed to hang freely at the other end.

(b) Now consider a similar beam with constant cross section and loaded with weights, so that the total weight per unit length is $W(x)$. What is the sag of the free end, expressed as an integral over $W(x)$, weighted by an appropriate Green's function?

Exercise 11.10 *Example: Microcantilever*

A microcantilever, fabricated from a single crystal of silicon, is being used to test the inverse square law of gravity on micron scales (Weld et al., 2008). It is clamped horizontally at one end, and its horizontal length is $\ell = 300\ \mu$m, its horizontal width is $w = 12\ \mu$m, and its vertical height is $h = 1\ \mu$m. (The density and Young's modulus for silicon are $\rho = 2{,}000\ \text{kg m}^{-3}$ and $E = 100$ GPa, respectively.) The cantilever is loaded at its free end with a $m = 10\ \mu$g gold mass.

(a) Show that the static deflection of the end of the cantilever is $\eta(\ell) = mg\ell^3/(3D) = 9\ \mu$m, where $g = 10\ \text{m s}^{-2}$ is the acceleration due to gravity. Explain why it is permissible to ignore the weight of the cantilever.

(b) Next suppose the mass is displaced slightly vertically and then released. Show that the natural frequency of oscillation of the cantilever is $f = 1/(2\pi)\sqrt{g/\eta(\ell)} \simeq 170$ Hz.

(c) A second, similar gold mass is placed $100\ \mu$m away from the first. Estimate roughly the Newtonian gravitational attraction between these two masses, and compare with the attraction of Earth. Suggest a method that exploits the natural oscillation of the cantilever to measure the tiny gravitational attraction between the two gold masses.

The motivation for developing this technique was to seek departures from Newton's inverse-square law of gravitation on ∼micron scales, which had been predicted if our universe is a membrane ("brane") in a higher-dimensional space ("bulk") with at least one macroscopic extra dimension. No such departures have been found as of 2016.

Exercise 11.11 *Example: Foucault Pendulum*

In any high-precision Foucault pendulum, it is important that the pendular restoring force be isotropic, since anisotropy will make the swinging period different in different planes and thereby cause precession of the plane of swing.

(a) Consider a pendulum of mass m and length ℓ suspended (as shown in Fig. 11.9) by a rectangular wire with thickness h in the plane of the bend (X-Z plane) and thickness w orthogonal to that plane (Y direction). Explain why the force that the wire exerts on the mass is approximately $-\mathbf{F} = -(mg\cos\theta_o + m\ell\dot{\theta}_o^2)\mathbf{e}_x$, where g is the acceleration of gravity, θ_o is defined in the figure, and $\dot{\theta}_o$ is the time derivative of θ_o due to the swinging of the pendulum. In the second term we have

For general queries contact webmaster@press.princeton.edu.

© Copyright Princeton University Press. No part of this book may be distributed, posted, or reproduced in any form by digital or mechanical means without prior written permission of the publisher.

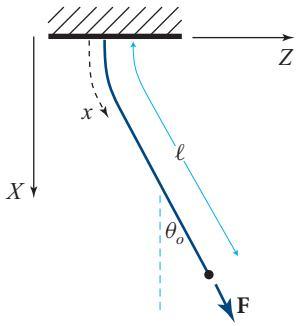

FIGURE 11.9 Foucault pendulum.

assumed that the wire is long compared to its region of bend. Express the second term in terms of the amplitude of swing $\theta_o^{\max}$, and show that for small amplitudes $\theta_o^{\max} \ll 1$, $\mathbf{F} \simeq -mg\mathbf{e}_x$. Use this approximation in the subsequent parts.

(b) Assuming that all along the wire, its angle $\theta(x)$ to the vertical is small, $\theta \ll 1$, show that

$$\theta(x) = \theta_o\big(1 - e^{-x/\lambda}\big), \tag{11.48a}$$

where λ (not to be confused with the second Lamé coefficient) is

$$\lambda = \frac{h}{(12\epsilon)^{1/2}}, \tag{11.48b}$$

$\epsilon = \xi_{x,x}$ is the longitudinal strain in the wire, and h is the wire's thickness in the plane of its bend. [Hint: The solution to Ex. 11.9 might be helpful.] Note that the bending of the wire is concentrated near the support, so this is where dissipation will be most important and where most of the suspension's thermal noise will arise (cf. Sec. 6.8 for discussion of thermal noise).

(c) Hence show that the shape of the wire is given in terms of Cartesian coordinates by

$$Z = [X - \lambda(1 - e^{-X/\lambda})]\,\theta_o \tag{11.48c}$$

to leading order in λ, and that the pendulum period is

$$P = 2\pi \left(\frac{\ell - \lambda}{g}\right)^{1/2}. \tag{11.48d}$$

(d) Finally, show that the pendulum periods when swinging along $\mathbf{e}_x$ and $\mathbf{e}_y$ differ by

$$\frac{\delta P}{P} = \left(\frac{h - w}{\ell}\right)\left(\frac{1}{48\epsilon}\right)^{1/2}. \tag{11.48e}$$

From Eq. (11.48e) one can determine how accurately the two thicknesses h and w must be equal to achieve a desired degree of isotropy in the period. A similar analysis can be carried out for the more realistic case of a slightly elliptical wire.

For general queries contact webmaster@press.princeton.edu.

© Copyright Princeton University Press. No part of this book may be distributed, posted, or reproduced in any form by digital or mechanical means without prior written permission of the publisher.

Exercise 11.12 *Example: DNA Molecule—Bending, Stretching, Young's Modulus, and Yield Point*

A DNA molecule consists of two long strands wound around each other as a helix, forming a cylinder with radius $a \simeq 1\,\text{nm}$. In this exercise, we explore three ways of measuring the molecule's Young's modulus E. For background and further details, see Marko and Cocco (2003) and Nelson (2008, Chap. 9).

(a) Show that if a segment of DNA with length ℓ is bent into a segment of a circle with radius R, its elastic energy is $E_{\text{el}} = D\ell/(2R^2)$, where $D = (\pi/4)a^4E$ is the molecule's flexural rigidity.

(b) Biophysicists define the DNA's *persistence length* ℓ_p as that length which, when bent through an angle of 90°, has elastic energy $E_{\text{el}} = k_BT$, where k_B is Boltzmann's constant and T is the temperature of the molecule's environment. Show that $\ell_p \simeq D/(k_BT)$. Explain why, in a thermalized environment, segments much shorter than ℓ_p will be more or less straight, and segments with length $\sim\ell_p$ will be randomly bent through angles of order 90°.

(c) Explain why a DNA molecule with total length L will usually be found in a random coil with diameter $d \simeq \ell_p\sqrt{L/\ell_p} = \sqrt{L\ell_p}$. Observations at room temperature with $L \simeq 17\ \mu\text{m}$ reveal that $d \simeq 1\,\mu\text{m}$. From this show that the persistence length is $\ell_p \simeq 50\,\text{nm}$ at room temperature, and thence evaluate the molecule's flexural rigidity and from it, show that the molecule's Young's modulus is $E \simeq 0.3\,\text{GPa}$; cf. Table 11.1.

(d) When the ends of a DNA molecule are attached to glass beads and the beads are pulled apart with a gradually increasing force F, the molecule begins to uncoil, just like rubber. To understand this semiquantitatively, think of the molecule as like a chain made of N links, each with length ℓ_p, whose interfaces can bend freely. If the force acts along the z direction, explain why the probability that any chosen link will make an angle θ to the z axis is $dP/d\cos\theta \propto \exp[+F\ell_p\cos\theta/(k_BT)]$. [Hint: This is analogous to the probability $dP/dV \propto \exp[-PV/(k_BT)]$ for the volume V of a system in contact with a bath that has pressure P and temperature T [Eq. (5.49)]; see also the discussion preceding Eq. (11.56).] Infer that when the force is F, the molecule's length along the force's direction is $\bar{L} \simeq L(\coth\alpha - 1/\alpha)$, where $\alpha = F\ell_p/(k_BT)$ and $L = N\ell_p$ is the length of the uncoiled molecule. Infer, further, that for $\alpha \ll 1$ (i.e., $F \ll k_BT/\ell_p \sim 0.1$ pN), our model predicts $\bar{L} \simeq \alpha L/3$, i.e. a linear force-length relation $F = (3k_BT/\ell_p)\bar{L}/L$, with a strongly temperature dependent spring constant, $3k_BT/\ell_p \propto T^2$. The measured value of this spring constant, at room temperature, is about 0.13 pN (Fig. 9.5 of Nelson, 2008). From this infer a value 0.5 GPa for the molecule's Young's modulus. This agrees surprisingly well with the 0.3 GPa deduced in part (c), given the crudeness of the jointed chain model.

(e) Show that when $F \gg k_BT/\ell_p \sim 0.1\,\text{pN}$, our crude model predicts (correctly) that the molecule is stretched to its full length $L = N\ell_p$. At this point, its true

For general queries contact webmaster@press.princeton.edu.

© Copyright Princeton University Press. No part of this book may be distributed, posted, or reproduced in any form by digital or mechanical means without prior written permission of the publisher.

elasticity should take over and allow genuine stretching. That true elasticity turns out to dominate only for forces $\gtrsim 10$ pN. [For details of what happens between 0.1 and 10 pN, see, e.g., Nelson (2008), Secs. 9.1–9.4.] For a force between $\sim$10 and $\sim$80 pN, the molecule is measured to obey Hooke's law, with a Young's modulus $E \simeq 0.3$ GPa that agrees with the value inferred in part (c) from its random-coil diameter. When the applied force reaches $\simeq 65$ pN, the molecule's double helix suddenly stretches greatly with small increases of force, changing its structure, so this is the molecule's yield point. Show that the strain at this yield point is $\Delta\ell/\ell \sim 0.1$; cf. Table 11.1.

Exercise 11.13 ***Example: Elastica*

elastica

Consider a slender wire of rectangular cross section with horizontal thickness h and vertical thickness w that is resting on a horizontal surface, so gravity is unimportant. Let the wire be bent in the horizontal plane as a result of equal and opposite forces F that act at its ends; Fig. 11.10. The various shapes the wire can assume are called *elastica;* they were first computed by Euler in 1744 and are discussed in Love (1927, pp. 401–404). The differential equation that governs the wire's shape is similar to that for the cantilever [Eq. (11.45)], with the simplification that the wire's weight does not enter the problem and the complication that the wire is long enough to deform through large angles.

It is convenient (as in the cantilever problem, Fig. 11.8) to introduce curvilinear coordinates with coordinate x measuring distance along the neutral surface, z measuring distance orthogonal to x in the plane of the bend (horizontal plane), and y measured perpendicular to the bending plane (vertically). The unit vectors along the x, y, and z directions are $\mathbf{e}_x$, $\mathbf{e}_y$, $\mathbf{e}_z$ (Fig. 11.10). Let $\theta(x)$ be the angle between $\mathbf{e}_x$ and the applied force $\mathbf{F}$; $\theta(x)$ is determined, of course, by force and torque balance.

(a) Show that force balance along the x and z directions implies

$$F\cos\theta = \int T_{xx}\,dydz, \qquad F\sin\theta = \int T_{zx}\,dydz \equiv S. \tag{11.49a}$$

(b) Show that torque balance for a short segment of wire implies

$$S = \frac{dM}{dx}, \tag{11.49b}$$

where $M(x) \equiv \int zT_{xx}\,dydz$ is the bending torque.

(c) Show that the stress-strain relation in the wire implies

$$M = -D\frac{d\theta}{dx}, \tag{11.49c}$$

where $D = Ewh^3/12$ is the flexural rigidity [Eq. (11.41b)].

For general queries contact webmaster@press.princeton.edu.

© Copyright Princeton University Press. No part of this book may be distributed, posted, or reproduced in any form by digital or mechanical means without prior written permission of the publisher.

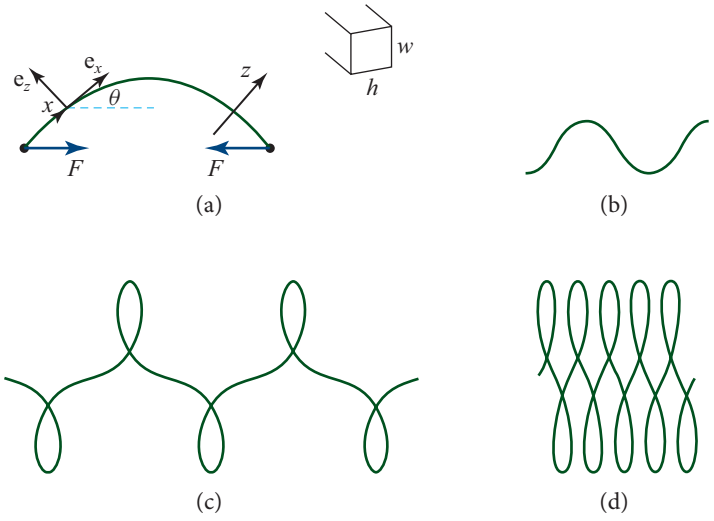

FIGURE 11.10 Elastica. (a) A bent wire is in elastostatic equilibrium under the action of equal and opposite forces applied at its two ends. x measures distance along the neutral surface; z measures distance orthogonal to the wire in the plane of the bend. (b)–(d) Examples of the resulting shapes.

(d) From the relations in parts (a)–(c), derive the following differential equation for the shape of the wire:

$$\boxed{\frac{d^2\theta}{dx^2} = -\frac{F\sin\theta}{D}.} \tag{11.49d}$$

This is the same equation as describes the motion of a simple pendulum!

(e) For Track-Two readers who have studied Sec. 11.8: Go back through your analysis and identify any place that connection coefficients would enter into a more careful computation, and explain why the connection-coefficient terms are negligible.

(f) Find one nontrivial solution of the elastica equation (11.49d) either analytically using elliptic integrals or numerically. (The general solution can be expressed in terms of elliptic integrals.)

(g) Solve analytically or numerically for the shape adopted by the wire corresponding to your solution in part (f), in terms of precisely Cartesian coordinates (X, Z) in the bending (horizontal) plane. Hint: Express the curvature of the wire, $1/\mathcal{R} = d\theta/dx$, as

$$\frac{d\theta}{dx} = -\frac{d^2X}{dZ^2}\left[1+\left(\frac{dX}{dZ}\right)^2\right]^{-3/2}. \tag{11.49e}$$

(h) Obtain a uniform piece of wire and adjust the force **F** to compare your answer with experiment.

For general queries contact webmaster@press.princeton.edu.

© Copyright Princeton University Press. No part of this book may be distributed, posted, or reproduced in any form by digital or mechanical means without prior written permission of the publisher.

11.6 Buckling and Bifurcation of Equilibria

So far, we have considered stable elastostatic equilibria and have implicitly assumed that the only reason for failure of a material is exceeding the yield limit. However, anyone who has built a house of cards knows that mechanical equilibria can be unstable, with startling consequences. In this section, we explore a specific, important example of a mechanical instability: *buckling*—the theory of which was developed long ago, in 1744 by Leonard Euler.

A tragic example of buckling was the collapse of the World Trade Center's Twin Towers on September 11, 2001. We discuss it near the end of this section, after first developing the theory in the context of a much simpler and cleaner example.

11.6.1 Elementary Theory of Buckling and Bifurcation

buckling

Take a new playing card and squeeze it between your finger and thumb (Fig. 11.11). When you squeeze gently, the card remains flat. But when you gradually increase the compressive force F past a critical value $F_{\rm crit}$, the card suddenly buckles (i.e., bends), and the curvature of the bend then increases rather rapidly with increasing applied force.

To understand quantitatively the sudden onset of buckling, we derive an eigenequation for the transverse displacement η as a function of distance x from one end of the card. (Although the card is effectively 2-dimensional, it has translation symmetry along its transverse dimension, so we can use the 1-dimensional equations of Sec. 11.5.) We suppose that the ends are free to pivot but not move transversely, so

$$\eta(0) = \eta(\ell) = 0. \tag{11.50}$$

For small displacements, the bending torque of our dimensionally reduced 1-dimensional theory is [Eq. (11.41c)]

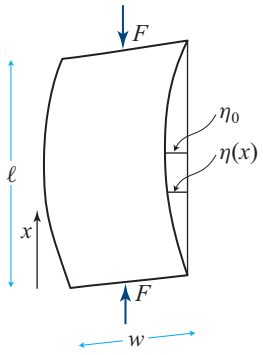

FIGURE 11.11 A playing card of length ℓ, width w, and thickness h is subjected to a compressive force F applied at both ends. The ends of the card are free to pivot.

For general queries contact webmaster@press.princeton.edu.

© Copyright Princeton University Press. No part of this book may be distributed, posted, or reproduced in any form by digital or mechanical means without prior written permission of the publisher.

$$M(x) = -D\frac{d^2\eta}{dx^2}, \tag{11.51}$$

where $D = wh^3E/12$ is the flexural rigidity [Eq. (11.41b)]. As the card is very light (negligible gravity), the total torque around location x, acting on a section of the card from x to one end, is the bending torque $M(x)$ acting at x plus the torque $-F\eta(x)$ associated with the applied force. This sum must vanish:

$$D\frac{d^2\eta}{dx^2} + F\eta = 0. \tag{11.52}$$

The eigensolutions of Eq. (11.52) satisfying boundary conditions (11.50) are

$$\eta = \eta_0 \sin kx, \tag{11.53a}$$

with eigenvalues

$$k = \left(\frac{F}{D}\right)^{1/2} = \frac{n\pi}{\ell} \quad \text{for nonnegative integers } n. \tag{11.53b}$$

Therefore, there is a critical force (first derived by Leonhard Euler in 1744), given by

$$F_{\text{crit}} = \frac{\pi^2 D}{\ell^2} = \frac{\pi^2 wh^3 E}{12\ell^2}. \tag{11.54}$$

critical force for buckling

When $F < F_{\text{crit}}$, there is no solution except $\eta = 0$ (an unbent card). When $F = F_{\text{crit}}$, the unbent card is still a solution, and there suddenly is the additional, arched solution (11.53) with $n = 1$, depicted in Fig. 11.11.

The linear approximation we have used cannot tell us the height η_0 of the arch as a function of F for $F \geq F_{\text{crit}}$; it reports, incorrectly, that for $F = F_{\text{crit}}$ all arch heights are allowed, and that for $F > F_{\text{crit}}$ there is no solution with $n = 1$. However, when nonlinearities are taken into account (Ex. 11.14), the $n = 1$ solution continues to exist for $F > F_{\text{crit}}$, and the arch height η_0 is related to F by

$$F = F_{\text{crit}}\left\{1 + \frac{1}{2}\left(\frac{\pi\eta_0}{2\ell}\right)^2 + O\left[\left(\frac{\pi\eta_0}{2\ell}\right)^4\right]\right\}. \tag{11.55}$$

The sudden appearance of the arched equilibrium state as F is increased through F_{crit} is called a *bifurcation of equilibria*. This bifurcation also shows up in the elastodynamics of the playing card, as we deduce in Sec. 12.3.5. When $F < F_{\text{crit}}$, small perturbations of the card's unbent shape oscillate stably. When $F = F_{\text{crit}}$, the unbent card is neutrally stable, and its zero-frequency motion leads the card from its unbent equilibrium state to its $n = 1$, arched equilibrium. When $F > F_{\text{crit}}$, the straight card is an unstable equilibrium: its $n = 1$ perturbations grow in time, driving the card toward the $n = 1$ arched equilibrium state.

A nice way of looking at this bifurcation is in terms of free energy. Consider candidate equilibrium states labeled by the height η_0 of their arch. For each value of η_0, give the card (for concreteness) the $n = 1$ sine-wave shape $\eta = \eta_0 \sin(\pi x/\ell)$. Compute the total elastic energy $E(\eta_0)$ associated with the card's bending, and subtract off the

For general queries contact webmaster@press.princeton.edu.

© Copyright Princeton University Press. No part of this book may be distributed, posted, or reproduced in any form by digital or mechanical means without prior written permission of the publisher.

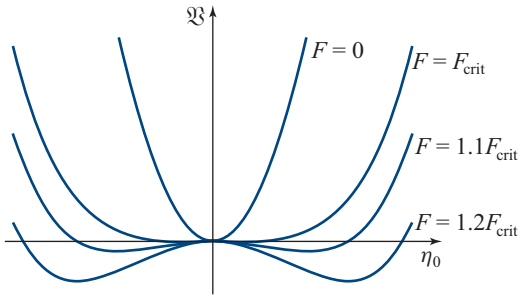

FIGURE 11.12 Representation of bifurcation by a potential energy function $\mathfrak{V}(\eta_0)$. When the applied force is small ($F \le F_{\text{crit}}$), there is only one stable equilibrium. As the applied force F is increased, the bottom of the potential well flattens, and eventually (for $F > F_{\text{crit}}$) the number of equilibria increases from one to three, of which only two are stable.

work $F\delta X$ done on the card by the applied force F when the card arches from $\eta_0 = 0$ to height η_0. [Here $\delta X(\eta_0)$ is the arch-induced decrease in straight-line separation between the card's ends.] The resulting quantity, $\mathfrak{V}(\eta_0) = E - F\delta X$, is the card's *free energy*—analogous to the physical free energy $F = E - TS$ for a system in contact with a heat bath (Secs. 5.4.1 and 11.3.5), the enthalpic free energy when in contact with a pressure bath (Ex. 5.5h), and the Gibbs (chemical) free energy $G = E - TS + PV$ when in contact with a heat and pressure bath (Sec. 5.5). It is the relevant energy for analyzing the card's equilibrium and dynamics when the force F is continually being applied at the two ends. In Ex. 11.15 we deduce that this free energy is

free energy of a bent card or beam

$$\mathfrak{V} = \left(\frac{\pi\eta_0}{2\ell}\right)^2 \ell \left[(F_{\text{crit}} - F) + \frac{1}{4}F_{\text{crit}}\left(\frac{\pi\eta_0}{2\ell}\right)^2\right] + O\left[F_{\text{crit}}\ell\left(\frac{\pi\eta_0}{2\ell}\right)^6\right], \quad (11.56)$$

which we depict in Fig. 11.12.

At small values of the compressive force $F < F_{\text{crit}}$, the free energy has only one minimum $\eta_0 = 0$ corresponding to a single stable equilibrium, the straight card. However, as the force is increased through F_{crit}, the potential minimum flattens out and then becomes a maximum flanked by two new minima (e.g., the curve $F = 1.2F_{\text{crit}}$). The maximum for $F > F_{\text{crit}}$ is the unstable, zero-displacement (straight-card) equilibrium, and the two minima are the stable, finite-amplitude equilibria with positive and negative η_0 given by Eq. (11.55).

This procedure of representing a continuous system with an infinite number of degrees of freedom by just one or a few coordinates and finding the equilibrium by minimizing a free energy is quite common and powerful.

Thus far, we have discussed only two of the card's equilibrium shapes (11.53): the straight shape $n = 0$ and the single-arch shape $n = 1$. If the card were constrained, by gentle, lateral stabilizing forces, to remain straight beyond $F = F_{\text{crit}}$, then at $F = n^2 F_{\text{crit}}$ for each $n = 2, 3, 4, \ldots$, the nth-order perturbative mode, with

higher order equilibria

For general queries contact webmaster@press.princeton.edu.

© Copyright Princeton University Press. No part of this book may be distributed, posted, or reproduced in any form by digital or mechanical means without prior written permission of the publisher.

$\eta = \eta_0 \sin(n\pi x/\ell)$, would become unstable, and a new, stable equilibrium with this shape would bifurcate from the straight equilibrium. You can easily explore this for $n = 2$ using a new playing card.

These higher-order modes are rarely of practical importance. In the case of a beam with no lateral constraints, as F increases above $F_{\rm crit}$, it will buckle into its single-arched shape. For beam dimensions commonly used in construction, a fairly modest further increase of F will bend it enough that its yield point and then rupture point are reached. To experience this yourself, take a thin meter stick, compress its ends between your two hands, and see what happens.

11.6.2 Collapse of the World Trade Center Buildings

11.6.2

Now we return to the example with which we began this section. On September 11, 2001, al-Qaeda operatives hijacked two Boeing 767 passenger airplanes and crashed them into the 110-story Twin Towers of the World Trade Center in New York City, triggering the towers' collapse a few hours later, with horrendous loss of life.

The weight of a tall building such as the towers is supported by vertical steel beams, called "columns." The longer the column is, the lower the weight it can support without buckling, since $F_{\rm crit} = \pi^2 D/\ell^2 = \pi^2 E A (r_g/\ell)^2$, with A the beam's cross sectional area, r_g its radius of gyration along its bending direction, and ℓ its length [Eqs. (11.54) and (11.41b)].[8] The column lengths are typically chosen such that the critical stress for buckling, $F_{\rm crit}/A = E(\pi r_g/\ell)^2$, is roughly the same as the yield stress, $F_{\rm yield} \simeq 0.003E$ (cf. Table 11.1), which means that the columns' *slenderness ratio* is $\ell/r_g \sim 50$. The columns are physically far longer than $50r_g$, but they are anchored to each other laterally every $\sim 50r_g$ by beams and girders in the floors, so their effective length for buckling is $\ell \sim 50r_g$. The columns' radii of gyration r_g are generally made large, without using more steel than needed to support the overhead weight, by making the columns hollow, or giving them H-shaped cross sections. In the Twin Towers, the thinnest beams had $r_g \sim 13$ cm, and they were anchored in every floor, with floor separations $\ell \simeq 3.8$ m, so their slenderness ratio was actually $\ell/r_g \simeq 30$.

description of failure modes

According to a detailed investigation (NIST, 2005, especially Secs. 6.14.2 and 6.14.3), the crashing airplanes ignited fires in and near floors 93–99 of the North Tower and 78–83 of the South Tower, where the airplanes hit. The fires were most intense in the floors and around uninsulated central steel columns. The heated central columns lost their rigidity and began to sag, and trusses then transferred some of the weight above to the outer columns. In parallel, the heated floor structures began

8. As noted in the discussion, after Eq. (11.41b), Ar_g^2 is really the second moment of the column's cross sectional area, along its direction of bend. If the column is supported at its ends against movement in both transverse directions, then the relevant second moment is the transverse tensor $\int x^i x^j dx dy$, and the direction of buckling (if it occurs) will be the eigendirection of this tensor that has the smallest eigenvalue (the column's narrowest direction).

For general queries contact webmaster@press.princeton.edu.

© Copyright Princeton University Press. No part of this book may be distributed, posted, or reproduced in any form by digital or mechanical means without prior written permission of the publisher.

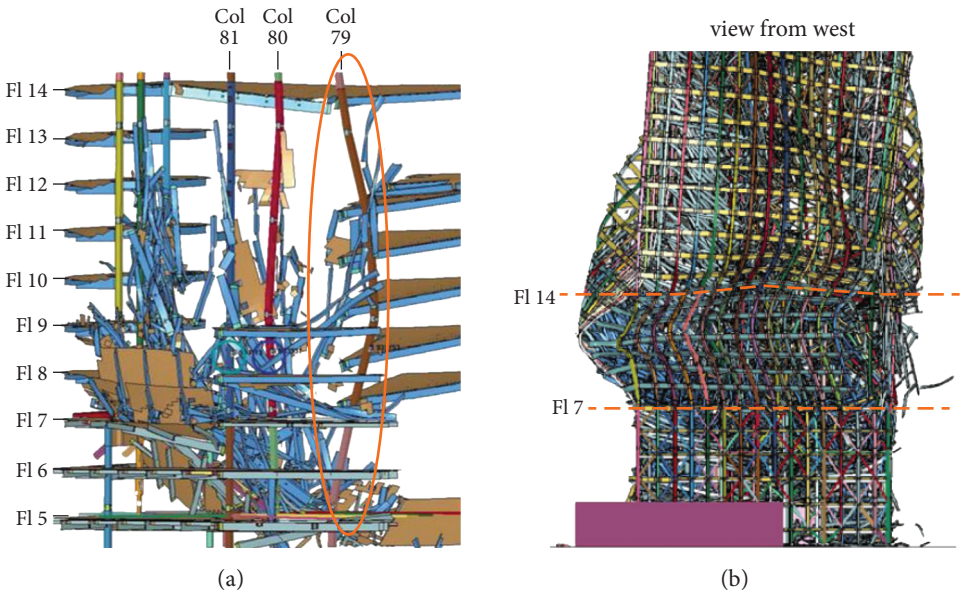

FIGURE 11.13 (a) The buckling of column 79 in building WTC7 at the World Trade Center, based on a finite-element simulation informed by all available observational data. (b) The subsequent buckling of the building's core. From NIST (2008).

to sag, pulling inward on the buildings' exterior steel columns, which bowed inward and then buckled, initiating the buildings' collapse. [This is a somewhat oversimplified description of a complex situation; for full complexities, see the report, NIST (2005).]

This column buckling was somewhat different from the buckling of a playing card because of the inward pull of the sagging floors. Much more like our playing-card buckle was the fate of an adjacent, 47-story building called WTC7. When the towers collapsed, they injected burning debris onto and into WTC7. About 7 hours later, fire-induced thermal expansion triggered a cascade of failures in floors 13–16, which left column 79 with little stabilizing lateral support, so its effective length ℓ was increased far beyond $50r_g$. It then quickly buckled (Fig. 11.13a) in much the same manner as our playing card, followed by column 80, then 81, and subsequently columns 77, 78, and 76 (NIST, 2008, especially Sec. 2.4). Within seconds, the building's entire core was buckling (Fig. 11.13b).

11.6.3

11.6.3 Buckling with Lateral Force; Connection to Catastrophe Theory

Returning to the taller Twin Towers, we can crudely augment the inward pull of the sagging floors into our free-energy description of buckling, by adding a term $-F_{\rm lat}\eta_0$, which represents the energy inserted into a bent column by a lateral force $F_{\rm lat}$ when its center has been displaced laterally through the distance η_0. Then the free energy

For general queries contact webmaster@press.princeton.edu.

© Copyright Princeton University Press. No part of this book may be distributed, posted, or reproduced in any form by digital or mechanical means without prior written permission of the publisher.

(11.56), made dimensionless and with its terms rearranged, takes the form

$$\varphi \equiv \frac{\mathfrak{V}}{F_{\rm crit}\ell} = \frac{1}{4}\left(\frac{\pi\eta_0}{2\ell}\right)^4 - \frac{1}{2}\left(\frac{2(F-F_{\rm crit})}{F_{\rm crit}}\right)\left(\frac{\pi\eta_0}{2\ell}\right)^2 - \left(\frac{2F_{\rm lat}}{\pi F_{\rm crit}}\right)\left(\frac{\pi\eta_0}{2\ell}\right). \tag{11.57}$$

Notice that this equation has the canonical form $\varphi = \frac{1}{4}a^4 - \frac{1}{2}za^2 - xa$ for the potential that governs a cusp catastrophe, whose state variable is $a = \pi\eta_0/(2\ell)$ and control variables are $z = 2(F - F_{\rm crit})/F_{\rm crit}$ and $x = (2/\pi)F_{\rm lat}/F_{\rm crit}$; see Eq. (7.72).[9] From the elementary mathematics of this catastrophe, as worked out in Sec. 7.5.1, we learn that although the lateral force $F_{\rm lat}$ will make the column bend, it will not induce a bifurcation of equilibria until the control-space cusp $x = \pm 2(z/3)^{3/2}$ is reached:

interpretation in terms of catastrophe theory

$$\frac{F_{\rm lat}}{F_{\rm crit}} = \pm\pi\left(\frac{2(F-F_{\rm crit})}{3F_{\rm crit}}\right)^{3/2}. \tag{11.58}$$

Notice that the lateral force $F_{\rm lat}$ actually delays the bifurcation to a higher vertical force, $F > F_{\rm crit}$. However, this is not significant for the physical buckling, since the column in this case is bent from the outset, and as $F_{\rm lat}$ increases, it stops carrying its share of the building's weight and moves smoothly toward its yield point and rupture; Ex. 11.16.

11.6.4 Other Bifurcations: Venus Fly Trap, Whirling Shaft, Triaxial Stars, and Onset of Turbulence

11.6.4

This bifurcation of equilibria, associated with the buckling of a column, is just one of many bifurcations that occur in physical systems. Another is a buckling type bifurcation that occurs in the 2-dimensional leaves of the Venus fly trap plant; the plant uses the associated instability to snap together a pair of leaves in a small fraction of a second, thereby capturing insects for it to devour; see Fortere et al. (2005). Yet another is the onset of a lateral bend in a shaft (rod) that spins around its longitudinal axis (see Love, 1927, Sec. 286). This is called *whirling;* it is an issue in drive shafts for automobiles and propellers, and a variant of it occurs in spinning DNA molecules during replication—see Wolgemuth, Powers, and Goldstein (2000). One more example is the development of triaxiality in self-gravitating fluid masses (i.e., stars) when their rotational kinetic energy reaches a critical value, about 1/4 of their gravitational energy; see Chandrasekhar (1962). Bifurcations also play a major role in the onset of turbulence in fluids and in the route to chaos in other dynamical systems; we study turbulence and chaos in Sec. 15.6.

whirling shaft

9. The lateral force $F_{\rm lat}$ makes the bifurcation *structurally stable*, in the language of catastrophe theory (discussed near the end of Sec. 7.5) and thereby makes it describable by one of the generic catastrophes. Without $F_{\rm lat}$, the bifurcation is not structurally stable.

For general queries contact webmaster@press.princeton.edu.

© Copyright Princeton University Press. No part of this book may be distributed, posted, or reproduced in any form by digital or mechanical means without prior written permission of the publisher.

For further details on the mathematics of bifurcations with emphasis on elastostatics and elastodynamics, see, for example, Marsden and Hughes (1986, Chap. 7). For details on buckling from an engineering viewpoint, see Ugural and Fenster (2012, Chap. 11).

EXERCISES

Exercise 11.14 *Derivation and Example: Bend as a Function of Applied Force*
Derive Eq. (11.55) relating the angle $\theta_o = (d\eta/dx)_{x=0} = k\eta_o = \pi\eta_o/\ell$ to the applied force F when the card has an $n = 1$, arched shape. [Hint: Consider the card as comprising many thin parallel wires and use the elastica differential equation $d^2\theta/dx^2 = -(F/D)\sin\theta$ [Eq. (11.49d)] for the angle between the card and the applied force at distance x from the card's end. The $\sin\theta$ becomes θ in the linear approximation used in the text; the nonlinearities embodied in the sine give rise to the desired relation. The following steps along the way toward a solution are mathematically the same as used when computing the period of a pendulum as a function of its amplitude of swing.]

(a) Derive the first integral of the elastica equation

$$(d\theta/dx)^2 = 2(F/D)(\cos\theta - \cos\theta_o), \tag{11.59}$$

where θ_o is an integration constant. Show that the boundary condition of no bending torque (no inflection of the card's shape) at the card ends implies $\theta = \theta_o$ at $x = 0$ and $x = \ell$; whence $\theta = 0$ at the card's center, $x = \ell/2$.

(b) Integrate the differential equation (11.59) to obtain

$$\frac{\ell}{2} = \sqrt{\frac{D}{2F}}\int_0^{\theta_o}\frac{d\theta}{\sqrt{\cos\theta - \cos\theta_o}}. \tag{11.60}$$

(c) Perform the change of variable $\sin(\theta/2) = \sin(\theta_o/2)\sin\phi$ and thereby bring Eq. (11.60) into the form

$$\ell = 2\sqrt{\frac{D}{F}}\int_0^{\pi/2}\frac{d\phi}{\sqrt{1 - \sin^2(\theta_o/2)\sin^2\phi}} = 2\sqrt{\frac{D}{F}}\,K[\sin^2(\theta_o/2)]. \tag{11.61}$$

Here $K(y)$ is the complete elliptic integral of the first type, with the parameterization used by Mathematica (which differs from that of many books).

(d) Expand Eq. (11.61) in powers of $\theta_o/2$ to obtain

$$F = F_{\rm crit}\frac{4}{\pi^2}K^2[\sin^2(\theta_o/2)] = F_{\rm crit}\left[1 + \frac{1}{2}\left(\frac{\theta_o/2}{2}\right)^2 + \ldots\right], \tag{11.62}$$

from which deduce our desired result, Eq. (11.55).

Exercise 11.15 *Problem: Free Energy of a Bent, Compressed Beam*
Derive Eq. (11.56) for the free energy $\mathfrak{V}$ of a beam that is compressed with a force F and has a critical compression $F_{\rm crit} = \pi^2 D/\ell^2$, where D is its flexural rigidity. [Hint: It

For general queries contact webmaster@press.princeton.edu.

© Copyright Princeton University Press. No part of this book may be distributed, posted, or reproduced in any form by digital or mechanical means without prior written permission of the publisher.

must be that $\partial V/\partial \eta_0 = 0$ gives Eq. (11.55) for the beam's equilibrium bend amplitude η_0 as a function of $F - F_{\rm crit}$. Use this to reduce the number of terms in $\mathfrak{V}(\eta_0)$ in Eq. (11.56) that you need to derive.]

Exercise 11.16 *Problem: Bent Beam with Lateral Force*

Explore numerically the free energy (11.57) of a bent beam with a compressive force F and lateral force $F_{\rm lat}$. Examine how the extrema (equilibrium states) evolve as F and $F_{\rm lat}$ change, and deduce the physical consequences.

Exercise 11.17 ***Problem: Applications of Buckling—Mountains and Pipes*

Buckling plays a role in many natural and human-caused phenomena. Explore the following examples.

(a) *Mountain building.* When two continental plates are in (very slow) collision, the compressional force near their interface drives their crustal rock to buckle upward, producing mountains. Estimate how high such mountains can be on Earth and on Mars, and compare your estimates with their actual heights. Read about such mountain building in books or on the web.

(b) *Thermal expansion of pipes.* When a segment of pipe is heated (e.g., by the rising sun in the morning), it will expand. If its ends are held fixed, this can easily produce a longitudinal stress large enough to buckle the pipe. How would you deal with this in an oil pipeline on Earth's surface? In a long vacuum tube? Compare your answers with standard engineering solutions, which you can find in books or on the web.

Exercise 11.18 *Example: Allometry*

Allometry is the study of biological scaling laws that relate various features of an animal to its size or mass. One example concerns the ratio of the width to the length of leg bones. Explain why the width to the length of a thigh bone in a quadruped might scale as the square root of the stress that it has to support. Compare elephants with cats in this regard. (The density of bone is roughly 1.5 times that of water, and its Young's modulus is ∼20 GPa.)

11.7 Reducing the Elastostatic Equations to 2 Dimensions for a Deformed Thin Plate: Stress Polishing a Telescope Mirror

The world's largest optical telescopes (as of 2016) are the Gran Telescopio Canarias in the Canary Islands and the two Keck telescopes on Mauna Kea in Hawaii, which are all about 10 m in diameter. It is very difficult to support traditional, monolithic mirrors so that the mirror surfaces maintain their shape (their "figure") as the telescope slews, because they are so heavy, so for Keck a new method of fabrication was sought. The solution devised by Jerry Nelson and his colleagues was to construct the telescope out

For general queries contact webmaster@press.princeton.edu.

© Copyright Princeton University Press. No part of this book may be distributed, posted, or reproduced in any form by digital or mechanical means without prior written permission of the publisher.

of 36 separate hexagons, each 0.9 m on a side. However, this posed a second problem: how to grind each hexagon's reflecting surface to the required hyperboloidal shape. For this, a novel technique called *stressed mirror polishing* was developed. This technique relies on the fact that it is relatively easy to grind a surface to a spherical shape, but technically highly challenging to create a nonaxisymmetric shape. So during the grinding, stresses are applied around the boundary of the mirror to deform it, and a spherical surface is produced. The stresses are then removed, and the mirror springs into the desired nonspherical shape. Computing the necessary stresses is a problem in classical elasticity theory and, in fact, is a good example of a large number of applications where the elastic body can be approximated as a thin plate and its shape analyzed using elasticity equations that are reduced from 3 dimensions to 2 by the method of moments.

stressed mirror polishing

For stress polishing of mirrors, the applied stresses are so large that we can ignore gravitational forces (at least in our simplified treatment). We suppose that the hexagonal mirror has a uniform thickness h and idealize it as a circle of radius R, and we introduce Cartesian coordinates with (x, y) in the horizontal plane (the plane of the mirror before deformation and polishing begin), and z vertical. The mirror is deformed as a result of a net vertical force per unit area (pressure) $P(x, y)$. This pressure is applied at the lower surface when upward (positive) and the upper surface when downward (negative). In addition, there are shear forces and bending torques applied around the rim of the mirror.

As in our analysis of a cantilever in Sec. 11.5, we assume the existence of a neutral surface in the deformed mirror, where the horizontal strain vanishes, $T_{ab} = 0$. (Here and below we use letters from the early part of the Latin alphabet for horizontal components $x = x^1$ and $y = x^2$.) We denote the vertical displacement of the neutral surface by $\eta(x, y)$. By applying the method of moments to the 3-dimensional stress-balance equation $T_{jk,k} = 0$ in a manner similar to our cantilever analysis, we obtain the following 2-dimensional equation for the mirror's shape (Ex. 11.19):

elastostatic force balance for a bent plate on which a pressure P acts: shape equation

$$\boxed{\nabla^2(\nabla^2\eta) = P(x, y)/D.} \tag{11.63a}$$

Here ∇^2 is the horizontal Laplacian: $\nabla^2\eta \equiv \eta_{,aa} = \eta_{,xx} + \eta_{,yy}$. Equation (11.63a) is the 2-dimensional analog of the equation $d^4\eta/dx^4 = W(x)/D$ for the shape of a cantilever on which a downward force per unit length $W(x)$ acts [Eq. (11.45)]. The 2-dimensional flexural rigidity that appears in Eq. (11.63a) is

2-dimensional flexural rigidity

$$\boxed{D = \frac{Eh^3}{12(1-\nu^2)},} \tag{11.63b}$$

where E is the mirror's Young's modulus, h is its thickness, and ν is its Poisson's ratio. The operator $\nabla^2\nabla^2$ acting on η in the shape equation (11.63a) is called the *biharmonic operator;* it also appears in 3-dimensional form in the biharmonic equation (11.34a)

biharmonic operator

For general queries contact webmaster@press.princeton.edu.

© Copyright Princeton University Press. No part of this book may be distributed, posted, or reproduced in any form by digital or mechanical means without prior written permission of the publisher.

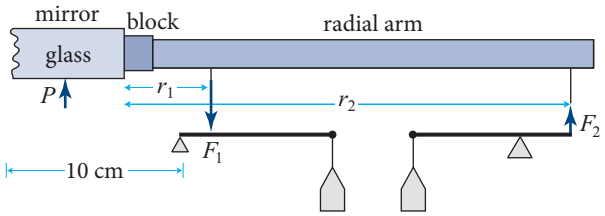

FIGURE 11.14 Schematic showing the mirror rim, a radial arm attached to it via a block, and a lever assembly used to apply shear forces and bending torques to the rim during stress polishing. (F_1 need not equal F_2, as there is a pressure P applied to the back surface of the mirror and forces applied at 23 other points around its rim.) The shear force on the mirror rim is $S = F_2 - F_1$, and the bending torque is $M = r_2F_2 - r_1F_1$.

for the displacement inside a homogeneous, isotropic body to which surface stresses are applied.

The shape equation (11.63a) must be solved subject to boundary conditions around the mirror's rim: the applied shear forces and bending torques.

The individual Keck mirror segments were constructed out of a ceramic material with Young's modulus $E = 89$ GPa and Poisson's ratio $\nu = 0.24$ (similar to glass; cf. Table 11.1). A mechanical jig was constructed to apply the shear forces and bending torques at 24 uniformly spaced points around the rim of the mirror (Fig. 11.14). The maximum stress was applied for the six outermost mirrors and was 2.4×10^6 N m^{-2}, 12% of the material's breaking tensile strength (2×10^7 N m^{-2}).

This stress polishing worked beautifully, and the Keck telescopes have become highly successful tools for astronomical research.

EXERCISES

Exercise 11.19 ***Derivation and Example: Dimensionally Reduced Shape Equation for a Stressed Plate*

Use the method of moments (Sec. 11.5) to derive the 2-dimensional shape equation (11.63a) for the stress-induced deformation of a thin plate, and expression (11.63b) for the 2-dimensional flexural rigidity. Here is a step-by-step guide, in case you want or need it.

(a) Show on geometrical grounds that the in-plane strain is related to the vertical displacement by [cf. Eq. (11.40a)]

$$\xi_{a,b} = -z\eta_{,ab}. \tag{11.64a}$$

(b) Derive an expression for the horizontal components of the stress, T_{ab}, in terms of double derivatives of the displacement function $\eta(x, y)$ [analog of $T_{xx} = -Ezd^2\eta/dx^2$, Eq. (11.40b), for a stressed rod]. This can be done (i) by arguing on physical grounds that the vertical component of stress, T_{zz}, is much smaller than the horizontal components and therefore can be approximated as zero [an

For general queries contact webmaster@press.princeton.edu.

© Copyright Princeton University Press. No part of this book may be distributed, posted, or reproduced in any form by digital or mechanical means without prior written permission of the publisher.

approximation to be checked in part (f)]; (ii) by expressing $T_{zz} = 0$ in terms of the strain and thence displacement and using Eqs. (11.39) to obtain

$$\Theta = -\left(\frac{1-2\nu}{1-\nu}\right) z\nabla^2\eta, \tag{11.64b}$$

where ∇^2 is the horizontal Laplacian; and (iii) by then writing T_{ab} in terms of Θ and $\xi_{a,b}$ and combining with Eqs. (11.64a) and (11.64b) to get the desired equation:

$$T_{ab} = Ez\left[\frac{\nu}{(1-\nu^2)}\nabla^2\eta\,\delta_{ab} + \frac{\eta_{,ab}}{(1+\nu)}\right]. \tag{11.64c}$$

(c) With the aid of Eq. (11.64c), write the horizontal force density in the form

$$f_a = -T_{ab,b} - T_{az,z} = -\frac{Ez}{1-\nu^2}\nabla^2\eta_{,a} - T_{az,z} = 0. \tag{11.64d}$$

Then, as in the cantilever analysis [Eq. (11.40d)], reduce the dimensionality of this force equation by the method of moments. The zeroth moment (integral over z) vanishes. Why? Therefore, the lowest nonvanishing moment is the first (multiply f_a by z and integrate). Show that this gives

$$S_a \equiv \int T_{za}dz = D\nabla^2\eta_{,a}, \tag{11.64e}$$

where D is the 2-dimensional flexural rigidity (11.63b). The quantity S_a is the vertical shear force per unit length acting perpendicular to a line in the mirror whose normal is in the direction a; it is the 2-dimensional analog of a stressed rod's shear force S [Eq. (11.41a)].

(d) For physical insight into Eq. (11.64e), define the bending torque per unit length (bending torque density) as

$$M_{ab} \equiv \int zT_{ab}dz, \tag{11.64f}$$

and show with the aid of Eq. (11.64c) that (11.64e) is the *law of torque balance* $S_a = M_{ab,b}$—the 2-dimensional analog of a stressed rod's $S = dM/dx$ [Eq. (11.42)].

(e) Compute the total vertical shear force acting on a small area of the plate as the line integral of S_a around its boundary, and by applying Gauss's theorem, deduce that the vertical shear force per unit area is $S_{a,a}$. Argue that this must be balanced by the net pressure P applied to the face of the plate, and thereby deduce the *law of vertical force balance:*

$$S_{a,a} = P. \tag{11.64g}$$

By combining this equation with the law of torque balance (11.64e), obtain the plate's bending equation $\nabla^2(\nabla^2\eta) = P/D$ [Eq. (11.63a)—the final result we were seeking].

For general queries contact webmaster@press.princeton.edu.

© Copyright Princeton University Press. No part of this book may be distributed, posted, or reproduced in any form by digital or mechanical means without prior written permission of the publisher.

(f) Use this bending equation to verify the approximation made in part (b) that T_{zz} is small compared to the horizontal stresses. Specifically, show that $T_{zz} \simeq P$ is $O(h/R)^2 T_{ab}$, where h is the plate thickness, and R is the plate radius.

Exercise 11.20 *Example: Paraboloidal Mirror*

Show how to construct a paraboloidal mirror of radius R and focal length f by stress polishing.

(a) Adopt a strategy of polishing the stressed mirror into a segment of a sphere with radius of curvature equal to that of the desired paraboloid at its center, $r = 0$. By comparing the shape of the desired paraboloid to that of the sphere, show that the required vertical displacement of the stressed mirror during polishing is

$$\eta(r) = \frac{r^4}{64 f^3}, \tag{11.64h}$$

where r is the radial coordinate, and we only retain terms of leading order.

(b) Hence use Eq. (11.63a) to show that a uniform force per unit area

$$P = \frac{D}{f^3}, \tag{11.64i}$$

where D is the flexural rigidity, must be applied to the bottom of the mirror. (Ignore the weight of the mirror.)

(c) Based on the results of part (b), show that if there are N equally spaced levers attached at the rim, the vertical force applied at each of them must be

$$F_z = \frac{\pi D R^2}{N f^3}. \tag{11.64j}$$

(d) Show that the radial displacement inside the mirror is

$$\xi_r = -\frac{r^3 z}{16 f^3}, \tag{11.64k}$$

where z is the vertical distance from the neutral surface, halfway through the mirror.

(e) Hence show that the maximum stress in the mirror is

$$T_{\max} = \frac{(3+\nu) R^2 h E}{32(1-\nu^2) f^3}, \tag{11.64l}$$

where h is the mirror thickness.

(f) Calculate the bending torque M that must be applied at each lever (Fig. 11.14). Comment on the limitations of this technique for making a thick, "fast" (i.e., $2R/f$ large) mirror.

For general queries contact webmaster@press.princeton.edu.

© Copyright Princeton University Press. No part of this book may be distributed, posted, or reproduced in any form by digital or mechanical means without prior written permission of the publisher.

11.8 Cylindrical and Spherical Coordinates: Connection Coefficients and Components of the Gradient of the Displacement Vector T2

Thus far in our discussion of elasticity, we have restricted ourselves to Cartesian coordinates. However, many problems in elasticity are most efficiently solved using cylindrical or spherical coordinates, so in this section, we develop some mathematical tools for those coordinate systems. In doing so, we follow the vectorial conventions of standard texts on electrodynamics and quantum mechanics (e.g., Jackson, 1999; Cohen-Tannoudji, Diu, and Laloë, 1977). We introduce an *orthonormal* set of basis vectors associated with each of our curvilinear coordinate systems; the coordinate lines are orthogonal to one another, and the basis vectors have unit lengths and point along the coordinate lines. In our study of continuum mechanics (Part IV, Elasticity; Part V, Fluid Dynamics; and Part VI, Plasma Physics), we follow this practice. When studying General Relativity (Part VII), we introduce and use basis vectors that are *not* orthonormal.

orthonormal basis vectors of cylindrical or spherical coordinates

cylindrical coordinates

Our notation for cylindrical coordinates is (ϖ, ϕ, z); ϖ (pronounced "pomega") is distance from the z-axis, and ϕ is the angle around the z-axis:

$$\varpi = \sqrt{x^2 + y^2}, \qquad \phi = \arctan(y/x). \tag{11.65a}$$

The unit basis vectors that point along the coordinate axes are denoted $\mathbf{e}_\varpi$, $\mathbf{e}_\phi$, and $\mathbf{e}_z$, and are related to the Cartesian basis vectors by

$$\mathbf{e}_\varpi = (x/\varpi)\mathbf{e}_x + (y/\varpi)\mathbf{e}_y, \quad \mathbf{e}_\phi = -(y/\varpi)\mathbf{e}_x + (x/\varpi)\mathbf{e}_y,$$
$$\mathbf{e}_z = \text{Cartesian } \mathbf{e}_z. \tag{11.65b}$$

spherical coordinates

Our notation for spherical coordinates is (r, θ, ϕ), with (as should be very familiar)

$$r = \sqrt{x^2 + y^2 + z^2}, \qquad \theta = \arccos(z/r), \qquad \phi = \arctan(y/x). \tag{11.66a}$$

The unit basis vectors associated with these coordinates are

$$\mathbf{e}_r = \frac{x}{r}\mathbf{e}_x + \frac{y}{r}\mathbf{e}_y + \frac{z}{r}\mathbf{e}_z, \quad \mathbf{e}_\theta = \frac{z}{r}\mathbf{e}_\varpi - \frac{\varpi}{r}\mathbf{e}_z, \quad \mathbf{e}_\phi = -\frac{y}{\varpi}\mathbf{e}_x + \frac{x}{\varpi}\mathbf{e}_y. \tag{11.66b}$$

Because our bases are orthonormal, the components of the metric of 3-dimensional space retain the Kronecker-delta values

$$\boxed{g_{jk} \equiv \mathbf{e}_j \cdot \mathbf{e}_k = \delta_{jk},} \tag{11.67}$$

which permits us to keep all vector and tensor indices down, by contrast with space-time, where we must distinguish between up and down; cf. Sec. 2.5.[10]

10. Occasionally—e.g., in the useful equation $\epsilon_{ijm}\epsilon_{klm} = \delta^{ij}_{kl} \equiv \delta^i_k\delta^j_l - \delta^i_l\delta^j_k$ [Eq. (1.23)]—it is convenient to put some indices up. In our orthonormal basis, any component with an index up is equal to that same component with an index down: e.g., $\delta^i_k \equiv \delta_{ik}$.

For general queries contact webmaster@press.princeton.edu.

© Copyright Princeton University Press. No part of this book may be distributed, posted, or reproduced in any form by digital or mechanical means without prior written permission of the publisher.

In Jackson (1999), Cohen-Tannoudji, Diu, and Laloë (1977), and other standard texts, formulas are written down for the gradient and Laplacian of a scalar field, and the divergence and curl of a vector field, in cylindrical and spherical coordinates; one uses these formulas over and over again. In elasticity theory, we deal largely with second-rank tensors and will need formulas for their various derivatives in cylindrical and spherical coordinates. In this book we introduce a mathematical tool, *connection coefficients* Γ_{ijk}, by which those formulas can be derived when needed.

connection coefficients

The connection coefficients quantify the turning of the orthonormal basis vectors as one moves from point to point in Euclidean 3-space: they tell us how the basis vectors at one point in space are *connected to* (related to) those at another point. More specifically, we define Γ_{ijk} by the two equivalent relations

$$\boxed{\nabla_k \mathbf{e}_j = \Gamma_{ijk}\mathbf{e}_i; \qquad \Gamma_{ijk} = \mathbf{e}_i \cdot (\nabla_k \mathbf{e}_j).} \tag{11.68}$$

Here $\nabla_k \equiv \nabla_{\mathbf{e}_k}$ is the directional derivative along the orthonormal basis vector $\mathbf{e}_k$; cf. Eq. (1.15a). Notice that (as is true quite generally; cf. Sec. 1.7) the differentiation index comes *last* on Γ; and notice that the middle index of Γ names the basis vector that is differentiated. Because our basis is orthonormal, it must be that $\nabla_k(\mathbf{e}_i \cdot \mathbf{e}_j) = 0$. Expanding this expression out using the standard rule for differentiating products, we obtain $\mathbf{e}_j \cdot (\nabla_k \mathbf{e}_i) + \mathbf{e}_i \cdot (\nabla_k \mathbf{e}_j) = 0$. Then invoking the definition (11.68) of the connection coefficients, we see that Γ_{ijk} is antisymmetric on its first two indices:

$$\boxed{\Gamma_{ijk} = -\Gamma_{jik}.} \tag{11.69}$$

In Part VII, when we use nonorthonormal bases, this antisymmetry will break down.

It is straightforward to compute the connection coefficients for cylindrical and spherical coordinates from (i) the definition (11.68); (ii) expressions (11.65b) and (11.66b) for the cylindrical and spherical basis vectors in terms of the Cartesian basis vectors; and (iii) the fact that *in Cartesian coordinates the connection coefficients vanish* ($\mathbf{e}_x$, $\mathbf{e}_y$, and $\mathbf{e}_z$ do not rotate as one moves through Euclidean 3-space). One can also deduce the cylindrical and spherical connection coefficients by drawing pictures of the basis vectors and observing how they change from point to point. As an example, for cylindrical coordinates we see from Fig. 11.15 that $\nabla_\phi \mathbf{e}_\varpi = \mathbf{e}_\phi/\varpi$. A similar pictorial calculation (which the reader is encouraged to do) reveals that $\nabla_\phi \mathbf{e}_\phi = -\mathbf{e}_\varpi/\varpi$. All other derivatives vanish. By comparing with Eq. (11.68), we see that *the only nonzero connection coefficients in cylindrical coordinates are*

connection coefficients for orthonormal bases of cylindrical and spherical coordinates

$$\boxed{\Gamma_{\varpi\phi\phi} = -\frac{1}{\varpi}, \quad \Gamma_{\phi\varpi\phi} = \frac{1}{\varpi},} \tag{11.70}$$

For general queries contact webmaster@press.princeton.edu.

© Copyright Princeton University Press. No part of this book may be distributed, posted, or reproduced in any form by digital or mechanical means without prior written permission of the publisher.

T2

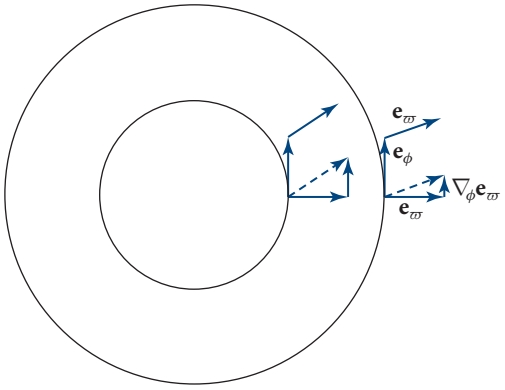

FIGURE 11.15 Pictorial evaluation of $\Gamma_{\phi\varpi\phi}$. In the rightmost assemblage of vectors we compute $\nabla_\phi \mathbf{e}_\varpi$ as follows. We draw the vector to be differentiated, $\mathbf{e}_\varpi$, at the tail of $\mathbf{e}_\phi$ (the vector along which we differentiate) and also at its head. We then subtract $\mathbf{e}_\varpi$ at the head from that at the tail; this difference is $\nabla_\phi \mathbf{e}_\varpi$. It obviously points in the $\mathbf{e}_\phi$ direction. When we perform the same calculation at a radius ϖ that is smaller by a factor 2 (left assemblage of vectors), we obtain a result, $\nabla_\phi \mathbf{e}_\varpi$, that is twice as large. Therefore, the length of this vector must scale as $1/\varpi$. By looking quantitatively at the length at some chosen radius ϖ, one can see that the multiplicative coefficient is unity: $\nabla_\phi \mathbf{e}_\varpi = \mathbf{e}_\phi/\varpi$. Comparing with Eq. (11.68), we deduce that $\Gamma_{\phi\varpi\phi} = 1/\varpi$.

which have the required antisymmetry [Eq. (11.69)]. Likewise, for spherical coordinates (Ex. 11.22), we have

$$\boxed{\Gamma_{\theta r\theta} = \Gamma_{\phi r\phi} = -\Gamma_{r\theta\theta} = -\Gamma_{r\phi\phi} = \frac{1}{r}, \quad \Gamma_{\phi\theta\phi} = -\Gamma_{\theta\phi\phi} = \frac{\cot\theta}{r}.} \tag{11.71}$$

These connection coefficients are the keys to differentiating vectors and tensors. Consider the gradient of the displacement, $\mathbf{W} = \boldsymbol{\nabla}\boldsymbol{\xi}$. Applying the product rule for differentiation, we obtain

$$\nabla_k(\xi_j \mathbf{e}_j) = (\nabla_k \xi_j)\mathbf{e}_j + \xi_j(\nabla_k \mathbf{e}_j) = \xi_{j,k}\mathbf{e}_j + \xi_j \Gamma_{ljk}\mathbf{e}_l. \tag{11.72}$$

directional derivative along basis vector

Here the comma denotes the directional derivative, along a basis vector, of the components treated as scalar fields. For example, in cylindrical coordinates we have

$$\xi_{i,\varpi} = \frac{\partial \xi_i}{\partial \varpi}, \quad \xi_{i,\phi} = \frac{1}{\varpi}\frac{\partial \xi_i}{\partial \phi}, \quad \xi_{i,z} = \frac{\partial \xi_i}{\partial z}; \tag{11.73}$$

and in spherical coordinates we have

$$\xi_{i,r} = \frac{\partial \xi_i}{\partial r}, \quad \xi_{i,\theta} = \frac{1}{r}\frac{\partial \xi_i}{\partial \theta}, \quad \xi_{i,\phi} = \frac{1}{r\sin\theta}\frac{\partial \xi_i}{\partial \phi}. \tag{11.74}$$

For general queries contact webmaster@press.princeton.edu.

© Copyright Princeton University Press. No part of this book may be distributed, posted, or reproduced in any form by digital or mechanical means without prior written permission of the publisher.

Taking the ith component of Eq. (11.72) we obtain

$$\boxed{W_{ik} = \xi_{i;k} = \xi_{i,k} + \Gamma_{ijk}\xi_j.} \tag{11.75}$$

Here $\xi_{i;k}$ are the nine components of the gradient of the vector field $\boldsymbol{\xi}(\mathbf{x})$.

We can use Eq. (11.75) to evaluate the expansion $\Theta = \mathrm{Tr}\,\mathbf{W} = \boldsymbol{\nabla}\cdot\boldsymbol{\xi}$. Using Eqs. (11.70) and (11.71), we obtain

$$\begin{aligned}\Theta = \boldsymbol{\nabla}\cdot\boldsymbol{\xi} &= \frac{\partial\xi_\varpi}{\partial\varpi} + \frac{1}{\varpi}\frac{\partial\xi_\phi}{\partial\phi} + \frac{\partial\xi_z}{\partial z} + \frac{\xi_\varpi}{\varpi} \\ &= \frac{1}{\varpi}\frac{\partial}{\partial\varpi}\left(\varpi\xi_\varpi\right) + \frac{1}{\varpi}\frac{\partial\xi_\phi}{\partial\phi} + \frac{\partial\xi_z}{\partial z}\end{aligned} \tag{11.76}$$

in cylindrical coordinates and

$$\begin{aligned}\Theta = \boldsymbol{\nabla}\cdot\boldsymbol{\xi} &= \frac{\partial\xi_r}{\partial r} + \frac{1}{r}\frac{\partial\xi_\theta}{\partial\theta} + \frac{1}{r\sin\theta}\frac{\partial\xi_\phi}{\partial\phi} + \frac{2\xi_r}{r} + \frac{\cot\theta\,\xi_\theta}{r} \\ &= \frac{1}{r^2}\frac{\partial}{\partial r}(r^2\xi_r) + \frac{1}{r\sin\theta}\frac{\partial}{\partial\theta}(\sin\theta\,\xi_\theta) + \frac{1}{r\sin\theta}\frac{\partial\xi_\phi}{\partial\phi}\end{aligned} \tag{11.77}$$

in spherical coordinates, in agreement with formulas in standard textbooks, such as the flyleaf of Jackson (1999).

The components of the rotation are most easily deduced using $R_{ij} = -\epsilon_{ijk}\phi_k$ with $\boldsymbol{\phi} = \frac{1}{2}\boldsymbol{\nabla}\times\boldsymbol{\xi}$, and the standard expressions for the curl in cylindrical and spherical coordinates (Jackson, 1999). Since the rotation does not enter into elasticity theory in a significant way, we refrain from writing down the results. The components of the shear are computed in Box 11.4.

By a computation analogous to Eq. (11.72), we can construct an expression for the gradient of a tensor of any rank. For a second-rank tensor $\mathbf{T} = T_{ij}\mathbf{e}_i\otimes\mathbf{e}_j$ we obtain (Ex. 11.21)

components of gradient of a tensor

$$\boxed{T_{ij;k} = T_{ij,k} + \Gamma_{ilk}T_{lj} + \Gamma_{jlk}T_{il}.} \tag{11.78}$$

Equation (11.78) for the components of the gradient can be understood as follows. In cylindrical or spherical coordinates, the components T_{ij} can change from point to point as a result of two things: a change of the tensor $\mathbf{T}$ or the turning of the basis vectors. The two connection coefficient terms in Eq. (11.78) remove the effects of the basis turning, leaving in $T_{ij;k}$ only the influence of the change of $\mathbf{T}$ itself. There are two correction terms corresponding to the two slots (indices) of $\mathbf{T}$; the effects of basis turning on each slot get corrected one after another. If $\mathbf{T}$ had had n slots, then there would have been n correction terms, each with the form of the two in Eq. (11.78).

These expressions for derivatives of tensors are not required for dealing with the vector fields of introductory electromagnetic theory or quantum theory, but they are essential for manipulating the tensor fields encountered in elasticity. As we shall see in Sec. 24.3, with one further generalization, we can go on to differentiate tensors in

For general queries contact webmaster@press.princeton.edu.

© Copyright Princeton University Press. No part of this book may be distributed, posted, or reproduced in any form by digital or mechanical means without prior written permission of the publisher.

T2

BOX 11.4. SHEAR TENSOR IN SPHERICAL AND CYLINDRICAL COORDINATES T2

Using our rules (11.75) for forming the gradient of a vector, we can derive a general expression for the shear tensor:

$$\begin{aligned}\Sigma_{ij} &= \frac{1}{2}(\xi_{i;j} + \xi_{j;i}) - \frac{1}{3}\delta_{ij}\xi_{k;k} \\ &= \frac{1}{2}(\xi_{i,j} + \xi_{j,i} + \Gamma_{ilj}\xi_l + \Gamma_{jli}\xi_l) - \frac{1}{3}\delta_{ij}(\xi_{k,k} + \Gamma_{klk}\xi_l). \qquad (1)\end{aligned}$$

Evaluating this in cylindrical coordinates using the connection coefficients (11.70), we obtain

$$\begin{aligned}\Sigma_{\varpi\varpi} &= \frac{2}{3}\frac{\partial\xi_\varpi}{\partial\varpi} - \frac{1}{3}\frac{\xi_\varpi}{\varpi} - \frac{1}{3\varpi}\frac{\partial\xi_\phi}{\partial\phi} - \frac{1}{3}\frac{\partial\xi_z}{\partial z}, \\ \Sigma_{\phi\phi} &= \frac{2}{3\varpi}\frac{\partial\xi_\phi}{\partial\phi} + \frac{2}{3}\frac{\xi_\varpi}{\varpi} - \frac{1}{3}\frac{\partial\xi_\varpi}{\partial\varpi} - \frac{1}{3}\frac{\partial\xi_z}{\partial z}, \\ \Sigma_{zz} &= \frac{2}{3}\frac{\partial\xi_z}{\partial z} - \frac{1}{3}\frac{\partial\xi_\varpi}{\partial\varpi} - \frac{1}{3}\frac{\xi_\varpi}{\varpi} - \frac{1}{3\varpi}\frac{\partial\xi_\phi}{\partial\phi}, \\ \Sigma_{\phi z} &= \Sigma_{z\phi} = \frac{1}{2\varpi}\frac{\partial\xi_z}{\partial\phi} + \frac{1}{2}\frac{\partial\xi_\phi}{\partial z}, \\ \Sigma_{z\varpi} &= \Sigma_{\varpi z} = \frac{1}{2}\frac{\partial\xi_\varpi}{\partial z} + \frac{1}{2}\frac{\partial\xi_z}{\partial\varpi}, \\ \Sigma_{\varpi\phi} &= \Sigma_{\phi\varpi} = \frac{1}{2}\frac{\partial\xi_\phi}{\partial\varpi} - \frac{\xi_\phi}{2\varpi} + \frac{1}{2\varpi}\frac{\partial\xi_\varpi}{\partial\phi}. \qquad (2)\end{aligned}$$

Likewise, in spherical coordinates using the connection coefficients (11.71), we obtain

$$\begin{aligned}\Sigma_{rr} &= \frac{2}{3}\frac{\partial\xi_r}{\partial r} - \frac{2}{3r}\xi_r - \frac{\cot\theta}{3r}\xi_\theta - \frac{1}{3r}\frac{\partial\xi_\theta}{\partial\theta} - \frac{1}{3r\sin\theta}\frac{\partial\xi\phi}{\partial\phi}, \\ \Sigma_{\theta\theta} &= \frac{2}{3r}\frac{\partial\xi_\theta}{\partial\theta} + \frac{\xi_r}{3r} - \frac{1}{3}\frac{\partial\xi_r}{\partial r} - \frac{\cot\theta\xi_\theta}{3r} - \frac{1}{3r\sin\theta}\frac{\partial\xi_\phi}{\partial\phi}, \\ \Sigma_{\phi\phi} &= \frac{2}{3r\sin\theta}\frac{\partial\xi_\phi}{\partial\phi} + \frac{2\cot\theta\xi_\theta}{3r} + \frac{\xi_r}{3r} - \frac{1}{3}\frac{\partial\xi_r}{\partial r} - \frac{1}{3r}\frac{\partial\xi_\theta}{\partial\theta}, \\ \Sigma_{\theta\phi} &= \Sigma_{\phi\theta} = \frac{1}{2r}\frac{\partial\xi_\phi}{\partial\theta} - \frac{\cot\theta\xi_\phi}{2r} + \frac{1}{2r\sin\theta}\frac{\partial\xi_\theta}{\partial\phi}, \\ \Sigma_{\phi r} &= \Sigma_{r\phi} = \frac{1}{2r\sin\theta}\frac{\partial\xi_r}{\partial\phi} + \frac{1}{2}\frac{\partial\xi_\phi}{\partial r} - \frac{\xi_\phi}{2r}, \\ \Sigma_{r\theta} &= \Sigma_{\theta r} = \frac{1}{2}\frac{\partial\xi_\theta}{\partial r} - \frac{\xi_\theta}{2r} + \frac{1}{2r}\frac{\partial\xi_r}{\partial\theta}. \qquad (3)\end{aligned}$$

For general queries contact webmaster@press.princeton.edu.

© Copyright Princeton University Press. No part of this book may be distributed, posted, or reproduced in any form by digital or mechanical means without prior written permission of the publisher.

any basis (orthonormal or nonorthonormal) in a curved spacetime, as is needed to perform calculations in general relativity. T2

Although the algebra of evaluating the components of derivatives such as in Eq. (11.78) in explicit form (e.g., in terms of $\{r, \theta, \phi\}$) can be long and tedious when done by hand, in the modern era of symbolic manipulation using computers (e.g., Mathematica, Matlab, or Maple), the algebra can be done quickly and accurately to obtain expressions such as Eqs. (3) of Box 11.4.

EXERCISES

Exercise 11.21 *Derivation and Practice: Gradient of a Second-Rank Tensor* T2
By a computation analogous to Eq. (11.72), derive Eq. (11.78) for the components of the gradient of a second-rank tensor in any orthonormal basis.

Exercise 11.22 *Derivation and Practice: Connection in Spherical Coordinates* T2
(a) By drawing pictures analogous to Fig. 11.15, show that

$$\nabla_\phi \mathbf{e}_r = \frac{1}{r}\mathbf{e}_\phi, \qquad \nabla_\theta \mathbf{e}_r = \frac{1}{r}\mathbf{e}_\theta, \qquad \nabla_\phi \mathbf{e}_\theta = \frac{\cot\theta}{r}\mathbf{e}_\phi. \tag{11.79}$$

(b) From these relations and antisymmetry on the first two indices [Eq. (11.69)], deduce the connection coefficients (11.71).

Exercise 11.23 *Derivation and Practice: Expansion in Cylindrical and Spherical Coordinates* T2
Derive Eqs. (11.76) and (11.77) for the divergence of the vector field $\boldsymbol{\xi}$ in cylindrical and spherical coordinates using the connection coefficients (11.70) and (11.71).

11.9 Solving the 3-Dimensional Navier-Cauchy Equation in Cylindrical Coordinates T2 11.9

11.9.1 Simple Methods: Pipe Fracture and Torsion Pendulum T2 11.9.1

As an example of an elastostatic problem with cylindrical symmetry, consider a cylindrical pipe that carries a high-pressure fluid (e.g., water, oil, natural gas); Fig. 11.16. How thick must the pipe's wall be to ensure that it will not burst due to the fluid's pressure? We sketch the solution, leaving the details to Ex. 11.24.

We suppose, for simplicity, that the pipe's length is held fixed by its support system: it does not lengthen or shorten when the fluid pressure is changed. Then by symmetry, the displacement field in the pipe wall is purely radial and depends only on radius: its only nonzero component is $\xi_\varpi(\varpi)$. The radial dependence is governed by radial force balance,

$$f_\varpi = K\Theta_{;\varpi} + 2\mu\Sigma_{\varpi j;j} = 0 \tag{11.80}$$

[Eq. (11.30)].

For general queries contact webmaster@press.princeton.edu.

© Copyright Princeton University Press. No part of this book may be distributed, posted, or reproduced in any form by digital or mechanical means without prior written permission of the publisher.

T2

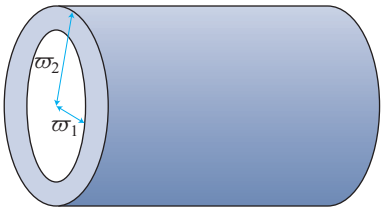

FIGURE 11.16 A pipe whose wall has inner and outer radii ϖ_1 and ϖ_2.

Because ξ_ϖ is independent of ϕ and z, the expansion [Eq. (11.76)] is given by

$$\Theta = \frac{d\xi_\varpi}{d\varpi} + \frac{\xi_\varpi}{\varpi}. \tag{11.81}$$

The second term in the radial force balance equation (11.80) is proportional to $\Sigma_{\varpi j;j}$ which—using Eq. (11.78) and noting that the only nonzero connection coefficients are $\Gamma_{\varpi\phi\phi} = -\Gamma_{\phi\varpi\phi} = -1/\varpi$ [Eq. (11.70)] and that symmetry requires the shear tensor to be diagonal—becomes

$$\Sigma_{\varpi j;j} = \Sigma_{\varpi\varpi,\varpi} + \Gamma_{\varpi\phi\phi}\Sigma_{\phi\phi} + \Gamma_{\phi\varpi\phi}\Sigma_{\varpi\varpi}. \tag{11.82}$$

Inserting the components of the shear tensor from Eqs. (2) of Box 11.4 and the values of the connection coefficients and comparing the result with expression (11.81) for the expansion, we obtain the remarkable result that $\Sigma_{\varpi j;j} = \frac{2}{3}\partial\Theta/\partial\varpi$. Inserting this into the radial force balance equation (11.80), we obtain

$$f_\varpi = \left(K + \frac{4\mu}{3}\right)\frac{d\Theta}{d\varpi} = 0. \tag{11.83}$$

Thus, inside the pipe wall, the expansion is independent of radius ϖ, and correspondingly, the radial displacement must have the form [cf. Eq. (11.81)]

$$\xi_\varpi = A\varpi + \frac{B}{\varpi} \tag{11.84}$$

for some constants A and B, whence $\Theta = 2A$ and $\Sigma_{\varpi\varpi} = \frac{1}{3}A - B/\varpi^2$. The values of A and B are fixed by the boundary conditions at the inner and outer faces of the pipe wall: $T_{\varpi\varpi} = P$ at $\varpi = \varpi_1$ (inner wall) and $T_{\varpi\varpi} = 0$ at $\varpi = \varpi_2$ (outer wall). Here P is the pressure of the fluid that the pipe carries, and we have neglected the atmosphere's pressure on the outer face by comparison. Evaluating $T_{\varpi\varpi} = -K\Theta - 2\mu\Sigma_{\varpi\varpi}$ and then imposing these boundary conditions, we obtain

$$A = \frac{P}{2(K + \mu/3)}\frac{\varpi_1^2}{(\varpi_2^2 - \varpi_1^2)}, \qquad B = \frac{P}{2\mu}\frac{\varpi_1^2\varpi_2^2}{(\varpi_2^2 - \varpi_1^2)}. \tag{11.85}$$

For general queries contact webmaster@press.princeton.edu.

© Copyright Princeton University Press. No part of this book may be distributed, posted, or reproduced in any form by digital or mechanical means without prior written permission of the publisher.

The only nonvanishing components of the strain then work out to be T2

$$S_{\varpi\varpi} = \frac{\partial \xi_\varpi}{\partial \varpi} = A - \frac{B}{\varpi^2}, \quad S_{\phi\phi} = \frac{\xi_\varpi}{\varpi} = A + \frac{B}{\varpi^2}. \tag{11.86}$$

This strain is maximal at the inner wall of the pipe; expressing it in terms of the ratio $\zeta \equiv \varpi_2/\varpi_1$ of the outer to the inner pipe radius and using the values of $K = 180\,\text{GPa}$ and $\mu = 81\,\text{GPa}$ for steel, we bring this maximum strain into the form

$$S_{\varpi\varpi} \simeq -\frac{P}{\mu}\frac{5\zeta^2 - 2}{10(\zeta^2 - 1)}, \quad S_{\phi\phi} \simeq \frac{P}{\mu}\frac{5\zeta^2 + 2}{10(\zeta^2 - 1)}. \tag{11.87}$$

Note that $|S_{\phi\phi}| > |S_{\varpi\varpi}|$.

criterion for safety against fracture

The pipe will fracture at a strain $\sim 10^{-3}$; for safety it is best to keep the actual strain smaller than this by an order of magnitude, $|S_{ij}| \lesssim 10^{-4}$. A typical pressure for an oil pipeline is $P \simeq 10$ atmospheres ($\simeq 10^6$ Pa), compared to the shear modulus of steel $\mu = 81\,\text{GPa}$, so $P/\mu \simeq 1.2 \times 10^{-5}$. Inserting this number into Eq. (11.87) with $|S_{\phi\phi}| \lesssim 10^{-4}$, we deduce that the ratio of the pipe's outer radius to its inner radius must be $\zeta = \varpi_2/\varpi_1 \gtrsim 1.04$. If the pipe has a diameter of a half meter, then its wall thickness should be about 1 cm or more. This is typical of oil pipelines.

Exercise 11.25 presents a second fairly simple example of elastostatics in cylindrical coordinates: a computation of the period of a torsion pendulum.

EXERCISES

Exercise 11.24 *Derivation and Practice: Fracture of a Pipe* T2

Fill in the details of the text's analysis of the deformation of a pipe carrying a high-pressure fluid, and the wall thickness required to protect the pipe against fracture. (See Fig. 11.16.)

Exercise 11.25 *Practice: Torsion Pendulum* T2

A torsion pendulum is a very useful tool for testing the equivalence principle (Sec. 25.2), for seeking evidence for hypothetical fifth (not to mention sixth!) forces, and for searching for deviations from gravity's inverse-square law on submillimeter scales, which could arise from gravity being influenced by macroscopic higher spatial dimensions. (See, e.g., Kapner et al., 2008; Wagner et al., 2012.) It would be advantageous to design a torsion pendulum with a 1-day period (Fig. 11.17). Here we estimate whether this is possible. The pendulum consists of a thin cylindrical wire of length ℓ and radius a. At the bottom of the wire are suspended three masses at the corners of an equilateral triangle at a distance b from the wire.

(a) Show that the longitudinal strain is

$$\xi_{z;z} = \frac{3mg}{\pi a^2 E}. \tag{11.88a}$$

For general queries contact webmaster@press.princeton.edu.

© Copyright Princeton University Press. No part of this book may be distributed, posted, or reproduced in any form by digital or mechanical means without prior written permission of the publisher.

T2

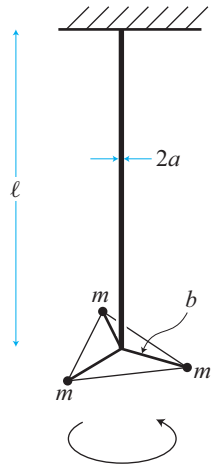

FIGURE 11.17 Torsion pendulum.

(b) What component of shear is responsible for the restoring force in the wire, which causes the torsion pendulum to oscillate?

(c) Show that the pendulum undergoes torsional oscillations with period

$$P = 2\pi \left(\frac{\ell}{g}\right)^{1/2} \left(\frac{2b^2 E \xi_{z;z}}{a^2 \mu}\right)^{1/2} . \tag{11.88b}$$

(d) Do you think you could design a pendulum that attains the goal of a 1-day period?

11.9.2

11.9.2 Separation of Variables and Green's Functions: Thermoelastic Noise in Mirrors T2

In complicated situations that have moderate amounts of symmetry, the elastostatic equations can be solved by the same kinds of sophisticated mathematical techniques as one uses in electrostatics: separation of variables, Green's functions, complex potentials, or integral transform methods (see, e.g., Gladwell, 1980). We provide an example in this section, focusing on separation of variables and Green's functions.

MOTIVATION

Our example is motivated by an important issue in high-precision measurements with light, including, among others, gravitational-wave detectors and quantum-optics experiments in which photons and atoms are put into entangled nonclassical states by coupling them to one another inside Fabry-Perot cavities.

In these situations, noise due to thermal motions of the mirror is a serious issue. It can hide a gravitational wave, and it can cause decoherence of the atom/photon quantum states. In Sec. 6.8.2, we formulated a generalized fluctuation-dissipation theorem by which this mirror thermal noise can be computed (Levin, 1998).

For general queries contact webmaster@press.princeton.edu.

© Copyright Princeton University Press. No part of this book may be distributed, posted, or reproduced in any form by digital or mechanical means without prior written permission of the publisher.

Specifically, in a thought experiment one applies to the mirror face a force F_o that oscillates at some frequency f at which one wants to evaluate the thermal noise. This force has the same transverse pressure distribution as the light beam—say, for concreteness, a Gaussian distribution:

$$T_{zz}^{\text{applied}} = \frac{e^{-\varpi^2/\varpi_o^2}}{\pi\varpi_o^2} F_o \cos(2\pi f t). \tag{11.89}$$

This applied pressure induces a strain distribution $\mathbf{S}$ inside the mirror, and that oscillating strain interacts with imperfections to dissipate energy at some rate $W_{\text{diss}}(f)$. The fluctuation-dissipation theorem states that in the real experiment, where the light beam bounces off the mirror, the reflected light will encode a noisy transverse-averaged position q for the mirror face, and the noise spectral density for q will be

$$S_q(f) = \frac{8W_{\text{diss}}(f)k_B T}{(2\pi f)^2 F_o^2} \tag{11.90}$$

[Eq. (6.88b)].

Even if one could make the mirror perfect (no dislocations or impurities), so there is no dissipation due to imperfections, there will remain one other source of dissipation in this thought experiment: the applied pressure (11.89) will produce a spatially inhomogeneous expansion $\Theta(\mathbf{x}, t)$ inside the mirror, which in turn will produce the thermoelastic temperature change $\Delta T/T = -[3\alpha K/(\rho c_V)]\Theta$ [Eq. (11.29)]. The gradient of this temperature will induce heat flow, with a thermal energy flux $\mathbf{F}_{\text{th}} = -\kappa\nabla\Delta T$, where κ is the thermal conductivity. When an amount Q of this thermal energy flows from a region with temperature T to a region of lower temperature $T - dT$, it produces an entropy increase $dS = Q/(T - dT) - Q/T = QdT/T^2$; and correspondingly, there is a rate of entropy increase per unit volume given by $d^2S/dVdt = -\mathbf{F}_{\text{th}} \cdot \nabla\Delta T/T^2 = \kappa(\nabla\Delta T)^2/T^2$. This entropy increase has an accompanying energy dissipation rate $W_{\text{diss}} = \int T(d^2S/dtdV)dV = \int(\kappa/T)(\nabla\Delta T)^2 dV$. Expressing ΔT in terms of the expansion that drives it via $\Delta T/T = -[3\alpha K/(\rho c_V)]\Theta$ and inserting that into Eq. (11.90) and using the third of Eqs. (11.39), we obtain the thermal noise spectral density that the experimenters must contend with:

$$S_q(f) = \frac{8\kappa E^2\alpha^2 k_B T^2}{(1-2\nu)^2 c_V^2 \rho^2 F_o^2 (2\pi f)^2} \left\langle \int (\nabla\Theta)^2 \varpi\, d\phi\, d\varpi\, dz \right\rangle. \tag{11.91}$$

Here $\langle\cdot\rangle$ means average over time as Θ oscillates due to the oscillation of the driving force $F_o \cos(2\pi f t)$. Because the dissipation producing this noise is due to heat flowing down a thermoelastic temperature gradient, it is called *thermoelastic noise*.

This is the motivation for an elasticity problem that we shall solve to illustrate separation of variables: to evaluate this thermoelastic noise, we must compute the expansion $\Theta(\mathbf{x}, t)$ inside a mirror, produced by the oscillating pressure (11.89) on the mirror face; and we must then perform the integral (11.91).

For general queries contact webmaster@press.princeton.edu.

© Copyright Princeton University Press. No part of this book may be distributed, posted, or reproduced in any form by digital or mechanical means without prior written permission of the publisher.

T2

SOLUTION FOR Θ VIA SEPARATION OF VARIABLES

The frequencies f at which we wish to evaluate the thermal noise are low compared to the inverse sound travel time across the mirror, so when computing Θ we can regard the force as oscillating very slowly (i.e., we can use our elastostatic equations rather than dynamical equations of the next chapter). Also, the size of the light spot on the mirror is usually small compared to the mirror's transverse size and thickness, so we can idealize the mirror as being infinitely large and thick—a homogeneous half-space of isotropic, elastic material.

Because the applied stress is axially symmetric, the induced strain and expansion will also be axially symmetric and are thus computed most easily using cylindrical coordinates. Our challenge, then, is to solve the Navier-Cauchy equation $\mathbf{f} = (K + \frac{1}{3}\mu)\boldsymbol{\nabla}(\boldsymbol{\nabla}\cdot\boldsymbol{\xi}) + \mu\nabla^2\boldsymbol{\xi} = 0$ for the cylindrical components $\xi_\varpi(z, \varpi)$ and $\xi_z(z, \varpi)$ of the displacement, and then evaluate the expansion $\Theta = \boldsymbol{\nabla}\cdot\boldsymbol{\xi}$. (The component ξ_ϕ vanishes by symmetry.)

Equations of elasticity in cylindrical coordinates, and their homogeneous solution

It is straightforward, using the techniques of Sec. 11.8, to compute the cylindrical components of $\mathbf{f}$. Reexpressing the bulk K and shear μ moduli in terms of Young's modulus E and Poisson's ratio ν [Eqs. (11.39)] and setting the internal forces to zero, we obtain

elastostatic force balance in cylindrical coordinates

$$f_\varpi = \frac{E}{2(1+\nu)(1-2\nu)}\left[2(1-\nu)\left(\frac{\partial^2\xi_\varpi}{\partial\varpi^2} + \frac{1}{\varpi}\frac{\partial\xi_\varpi}{\partial\varpi} - \frac{\xi_\varpi}{\varpi^2}\right) + (1-2\nu)\frac{\partial^2\xi_\varpi}{\partial z^2} + \frac{\partial^2\xi_z}{\partial z\partial\varpi}\right] = 0, \tag{11.92a}$$

$$f_z = \frac{E}{2(1+\nu)(1-2\nu)}\left[(1-2\nu)\left(\frac{\partial^2\xi_z}{\partial\varpi^2} + \frac{1}{\varpi}\frac{\partial\xi_z}{\partial\varpi}\right) + 2(1-\nu)\frac{\partial^2\xi_z}{\partial z^2} + \frac{\partial^2\xi_\varpi}{\partial z\partial\varpi} + \frac{1}{\varpi}\frac{\partial\xi_\varpi}{\partial z}\right] = 0. \tag{11.92b}$$

These are two coupled, linear, second-order differential equations for the two unknown components of the displacement vector. As with the analogous equations of electrostatics and magnetostatics, these can be solved by separation of variables, that is, by setting $\xi_\varpi = R_\varpi(\varpi)Z_\varpi(z)$ and $\xi_z = R_z(\varpi)Z_z(z)$, and inserting into Eq. (11.92a). We seek the general solution that dies out at large ϖ and z. The general solution of this sort, to the complicated-looking Eqs. (11.92), turns out to be (really!!)

separation-of-variables solution of force-balance equation $f_j = 0$

$$\xi_\varpi = \int_0^\infty [\alpha(k) - (2 - 2\nu - kz)\beta(k)]\, e^{-kz} J_1(k\varpi)\, dk,$$
$$\xi_z = \int_0^\infty [\alpha(k) + (1 - 2\nu + kz)\beta(k)]\, e^{-kz} J_0(k\varpi)\, dk. \tag{11.93}$$

For general queries contact webmaster@press.princeton.edu.

© Copyright Princeton University Press. No part of this book may be distributed, posted, or reproduced in any form by digital or mechanical means without prior written permission of the publisher.

Here J_0 and J_1 are Bessel functions of order 0 and 1, and $\alpha(k)$ and $\beta(k)$ are arbitrary functions.

Boundary conditions

The functions $\alpha(k)$ and $\beta(k)$ are determined by boundary conditions on the face of the test mass. The force per unit area exerted across the face by the strained test-mass material, T_{zj} at $z=0$ with $j=\{\varpi,\phi,z\}$, must be balanced by the applied force per unit area, $T_{zj}^{\rm applied}$ [Eq. (11.89)]. The (shear) forces in the ϕ direction, $T_{z\phi}$ and $T_{z\phi}^{\rm applied}$, vanish because of cylindrical symmetry and thus provide no useful boundary condition. The (shear) force in the ϖ direction, which must vanish at $z=0$ since $T_{z\varpi}^{\rm applied}=0$, is given by [cf. Eq. (2) in Box 11.4]

shear-force boundary condition at $z=0$

$$T_{z\varpi}(z=0) = -2\mu\Sigma_{z\varpi} = -\mu\left(\frac{\partial\xi_z}{\partial\varpi}+\frac{\partial\xi_\varpi}{\partial z}\right)$$
$$= -\mu\int_0^\infty [\beta(k)-\alpha(k)]\,J_1(kz)k dk = 0, \qquad (11.94)$$

which implies that $\beta(k)=\alpha(k)$. The (normal) force in the z direction, which must balance the applied pressure (11.89), is $T_{zz}=-K\Theta-2\mu\Sigma_{zz}$; using Eq. (2) in Box 11.4 and Eqs. (11.39), (11.76), (11.93) and (11.89), this reduces to

longitudinal-force boundary condition at $z=0$

$$T_{zz}(z=0) = 2\mu\int_0^\infty \alpha(k)J_0(k\varpi)k dk = T_{zz}^{\rm applied} = \frac{e^{-\varpi^2/\varpi_o^2}}{\pi\varpi_o^2}F_o\cos(2\pi f t), \qquad (11.95)$$

which can be inverted[11] to give

solution for expansion coefficients

$$\alpha(k)=\beta(k)=\frac{1}{4\pi\mu}e^{-k^2\varpi_o^2/4}F_o\cos(2\pi f t). \qquad (11.96)$$

Inserting this equation into the Eqs. (11.93) for the displacement and then evaluating the expansion $\Theta=\nabla\cdot\boldsymbol{\xi}=\xi_{z,z}+\varpi^{-1}(\varpi\xi_\varpi)_{,\varpi}$, we obtain

$$\Theta = 2(1-2\nu)\int_0^\infty \alpha(k)e^{-kz}J_0(k\varpi)k\,dk. \qquad (11.97)$$

As in electrostatics and magnetostatics, so also in elasticity theory, one can solve an elastostatics problem using Green's functions instead of separation of variables. We explore this option for our applied Gaussian force in Ex. 11.27. For greater detail on

11. The inversion and the subsequent evaluation of the integral of $(\nabla\Theta)^2$ are aided by the following expressions for the Dirac delta function:

$$\delta(k-k') = k\int_0^\infty J_0(k\varpi)J_0(k'\varpi)\varpi d\varpi = k\int_0^\infty J_1(k\varpi)J_1(k'\varpi)\varpi d\varpi.$$

For general queries contact webmaster@press.princeton.edu.

© Copyright Princeton University Press. No part of this book may be distributed, posted, or reproduced in any form by digital or mechanical means without prior written permission of the publisher.

T2 Green's functions in elastostatics and their applications from an engineer's viewpoint, see Johnson (1985). For other commonly used solution techniques, see Box 11.3.

THERMOELASTIC NOISE SPECTRAL DENSITY

Let us return to the mirror-noise problem that motivated our calculation. It is straightforward to compute the gradient of the expansion (11.97), and square and integrate it to get the spectral density $S_q(f)$ [Eq. (11.91)]. The result is (Braginsky, Gorodetsky, and Vyatchanin, 1999; Liu and Thorne, 2000)

$$S_q(f) = \frac{8(1+\nu)^2\kappa\alpha^2 k_B T^2}{\sqrt{2\pi}\, c_V^2 \rho^2 \varpi_o^3 (2\pi f)^2}. \tag{11.98}$$

Early plans for advanced LIGO gravitational wave detectors (Sec. 9.5; LIGO Scientific Collaboration, 2015) called for mirrors made of high-reflectivity dielectric coatings on sapphire crystal substrates. Sapphire was chosen because it can be grown in giant crystals with very low impurities and dislocations, resulting in low thermal noise. However, the thermoelastic noise (11.98) in sapphire turns out to be uncomfortably high. Using sapphire's $\nu = 0.29, \kappa = 40\ \mathrm{W\,m^{-1}\,K^{-1}}, \alpha = 5.0 \times 10^{-6}\ \mathrm{K^{-1}}$, $c_V = 790\ \mathrm{J\,kg^{-1}\,K^{-1}}$, $\rho = 4{,}000\ \mathrm{kg\,m^{-3}}$, and a light-beam radius $\varpi_o = 4\ \mathrm{cm}$ and room temperature $T = 300\ \mathrm{K}$, Eq. (11.98) gives the following for the noise in a bandwidth equal to frequency:

$$\sqrt{f S_q(f)} = 5 \times 10^{-20}\ \mathrm{m} \sqrt{\frac{100\ \mathrm{Hz}}{f}}. \tag{11.99}$$

Because this was uncomfortably high at low frequencies, $f \sim 10$ Hz, and because of the birefringence of sapphire, which could cause technical problems, a decision was made to switch to fused silica for the advanced LIGO mirrors.

EXERCISES

Exercise 11.26 *Derivation and Practice: Evaluation of Elastostatic Force in Cylindrical Coordinates* T2

Derive Eqs. (11.92) for the cylindrical components of the internal elastostatic force per unit volume $\mathbf{f} = (K + \frac{1}{3}\mu)\boldsymbol{\nabla}(\boldsymbol{\nabla}\cdot\boldsymbol{\xi}) + \mu\nabla^2\boldsymbol{\xi}$ in a cylindrically symmetric situation.

Exercise 11.27 ***Example: Green's Function for Normal Force on a Half-Infinite Body* T2

Suppose that a stress $T_{zj}^{\mathrm{applied}}(\mathbf{x}_o)$ is applied on the face $z = 0$ of a half-infinite elastic body (one that fills the region $z > 0$). Then by virtue of the linearity of the elastostatics equation $\mathbf{f} = (K + \frac{1}{3}\mu)\boldsymbol{\nabla}(\boldsymbol{\nabla}\cdot\boldsymbol{\xi}) + \mu\nabla^2\boldsymbol{\xi} = 0$ and the linearity of its boundary conditions, $T_{zj}^{\mathrm{internal}} = T_{zj}^{\mathrm{applied}}$, there must be a Green's function $G_{jk}(\mathbf{x} - \mathbf{x}_o)$ such that the body's internal displacement $\boldsymbol{\xi}(\mathbf{x})$ is given by

$$\boxed{\xi_j(\mathbf{x}) = \int G_{jk}(\mathbf{x} - \mathbf{x}_0) T_{kz}^{\mathrm{applied}}(\mathbf{x}_o) d^2x_o.} \tag{11.100}$$

For general queries contact webmaster@press.princeton.edu.

© Copyright Princeton University Press. No part of this book may be distributed, posted, or reproduced in any form by digital or mechanical means without prior written permission of the publisher.

Here the integral is over all points $\mathbf{x}_o$ on the face of the body ($z = 0$), and $\mathbf{x}$ can be anywhere inside the body, $z \geq 0$.

(a) Show that if a force F_j is applied on the body's surface at a single point (the origin of coordinates), then the displacement inside the body is

$$\xi_j(\mathbf{x}) = G_{jk}(\mathbf{x}) F_k. \tag{11.101}$$

Thus, the Green's function can be thought of as the body's response to a point force on its surface.

(b) As a special case, consider a point force F_z directed perpendicularly into the body. The resulting displacement turns out to have cylindrical components[12]

$$\xi_z = G_{zz}(\varpi, z) F_z = \frac{(1+\nu)}{2\pi E}\left[\frac{2(1-\nu)}{r} + \frac{z^2}{r^3}\right] F_z,$$
$$\xi_\varpi = G_{\varpi z}(\varpi, z) F_z = -\frac{(1+\nu)}{2\pi E}\left[\frac{(1-2\nu)\varpi}{r(r+z)} - \frac{\varpi z}{r^3}\right] F_z, \tag{11.102}$$

where $r = \sqrt{\varpi^2 + z^2}$. It is straightforward to show that this displacement does satisfy the elastostatics equations (11.92). Show that it also satisfies the required boundary condition $T_{z\varpi}(z = 0) = -2\mu\Sigma_{z\varpi} = 0$.

(c) Show that for this displacement [Eq. (11.102)], $T_{zz} = -K\Theta - 2\mu\Sigma_{zz}$ vanishes everywhere on the body's surface $z = 0$ except at the origin $\varpi = 0$ and is infinite there. Show that the integral of this normal stress over the surface is F_z, and therefore, $T_{zz}(z = 0) = F_z\delta_2(\mathbf{x})$, where δ_2 is the 2-dimensional Dirac delta function on the surface. This is the second required boundary condition.

(d) Plot the integral curves of the displacement vector $\boldsymbol{\xi}$ (i.e., the curves to which $\boldsymbol{\xi}$ is parallel) for a reasonable choice of Poisson's ratio ν. Explain physically why the curves have the form you find.

(e) One can use the Green's function (11.102) to compute the displacement $\boldsymbol{\xi}$ induced by the Gaussian-shaped pressure (11.89) applied to the body's face, and to then evaluate the induced expansion and thence the thermoelastic noise; see Braginsky, Gorodetsky, and Vyatchanin (1999) and Liu and Thorne (2000). The results agree with Eqs. (11.97) and (11.98) deduced using separation of variables.

Bibliographic Note

Elasticity theory was developed in the eighteenth, nineteenth, and early twentieth centuries. The classic advanced textbook from that era is Love (1927). An outstanding, somewhat more modern advanced text is Landau and Lifshitz (1986)—originally

12. For the other components of the Green's function, written in Cartesian coordinates (since a non-normal applied force breaks the cylindrical symmetry), see Landau and Lifshitz [1986, Eqs. (8.18)].

For general queries contact webmaster@press.princeton.edu.

© Copyright Princeton University Press. No part of this book may be distributed, posted, or reproduced in any form by digital or mechanical means without prior written permission of the publisher.

written in the 1950s and revised in a third edition shortly before Lifshitz's death. This is among the most readable textbooks that Landau and Lifshitz wrote and is still widely used by physicists in the early twenty-first century.

Some significant new insights, both mathematical and physical, have been developed in recent decades, for example, catastrophe theory and its applications to bifurcations and stability, practical insights from numerical simulations, and practical applications based on new materials (e.g., carbon nanotubes). For a modern treatment that deals with these and much else from an engineering viewpoint, we strongly recommend Ugural and Fenster (2012). For a fairly brief and elementary modern treatment, we recommend Lautrup (2005, Part III). Other good texts that focus particularly on solving the equations for elastostatic equilibrium include Southwell (1941), Timoshenko and Goodier (1970), Gladwell (1980), Johnson (1985), Boresi and Chong (1999), and Slaughter (2002); see also the discussion and references in Box 11.3.

For general queries contact webmaster@press.princeton.edu.

© Copyright Princeton University Press. No part of this book may be distributed, posted, or reproduced in any form by digital or mechanical means without prior written permission of the publisher.

NAME INDEX

Page numbers for entries in boxes are followed by "b," those for epigraphs at the beginning of a chapter by "e," those for figures by "f," and those for notes by "n."

Archimedes of Syracuse, 675e

Bondi, Hermann, 890
Burke, William, 869

Cauchy, Augustin-Louis, 565, 588n
Clough, Ray W., 565

De Laval, Gustaf, 887n

Eddington, Arthur, 835e
Emden, Robert, 688
Euclid, 947n
Euler, Leonhard, 565, 600, 602, 603, 697n

Faraday, Michael, 943n
Feigenbaum, Mitchell, 828
Feynman, Richard P., 729e, 952n, 973

Galileo Galilei, 565
Germain, Marie-Sophie, 565
Gibbs, J. Willard, 943n
Goldreich, Peter, 702

Hamilton, William Rowan, 943n
Heaviside, Oliver, 943n
Heisenberg, Werner, 788n, 917e
Hooke, Robert, 565, 567e

Lagrange, Joseph-Louis, 565, 943n, 952
Lane, Jonathan Homer, 688
Lele, Sanjiva K., 807f
Libchaber, Albert, 830
Lorenz, Edward, 834
Love, Augustus Edward Hugh, 565

Marriotte, Edme, 565
Martin, H. C., 565
Maxwell, James Clerk, 943n
Millikan, Robert, 749

Navier, Claude-Louis, 565, 588n
Nelson, Jerry, 609
Newton, Isaac, 690, 712, 943e, 943n, 952

Oseen, Carl Wilhelm, 754

Rayleigh, Lord (John William Strutt), 899n
Richardson, Lewis, 787e
Richter, Charles, 629e
Ride, Sally, 875e
Rouse, Hunter, 727, 731b

Saint-Venant, Barré de, 590b
Schwarzschild, Karl, 935
Scott-Russell, John, 850, 855
Sedov, Leonid I., 911, 912
Shapiro, Ascher, 731b
Stevenson, David, 816n, 843n
Stewart, Potter, 788n
Stokes, George G., 754, 899n

Taylor, Geoffrey Ingram, 746, 911, 912
Topp, L. J., 565
Turner, M. J., 565

Zel'dovich, Yakov Borisovich, 916

For general queries contact webmaster@press.princeton.edu.

© Copyright Princeton University Press. No part of this book may be distributed, posted, or reproduced in any form by digital or mechanical means without prior written permission of the publisher.

For general queries contact webmaster@press.princeton.edu.

© Copyright Princeton University Press. No part of this book may be distributed, posted, or reproduced in any form by digital or mechanical means without prior written permission of the publisher.

SUBJECT INDEX

Second and third level entries are not ordered alphabetically. Instead, the most important or general entries come first, followed by less important or less general ones, with specific applications last.

Page numbers for entries in boxes are followed by "b," those for epigraphs at the beginning of a chapter by "e," those for figures by "f," for notes by "n," and for tables by "t."

absorption of radiation, 937
accretion disk around spinning black hole, 784
accretion of gas onto neutron star or black hole, 890–891
action principles
  Hamilton's, in analytical mechanics, 953
  for elastic stress, 584
adiabatic index
  definition, 724b
  polytropic, 878
  for ideal gas: ratio of specific heats, 678, 681b, 724b
    influence of molecules' internal degrees of freedom, 879–880
  for air, as function of temperature, 880f
advective (convective) time derivative, 692, 724b, 892, 970
airplane wing or airfoil, lift on, 743f, 743–744, 824
allometry, 587, 609
angular momentum
  and moment of inertia tensor, 944
  of fundamental particles (spin), 960
  in elastodynamics, 644, 661–662
  in fluid mechanics, 702, 729, 732, 733, 784, 826, 849
angular momentum conservation, Newtonian, 952–953
  in circulating water, 729, 732–733
Archimedes law, 675, 684–685, 692
artery, blood flow in, 716–719
atmosphere of Earth. *See also* tornado; winds
  structure of, 683–684, 684f
  and greenhouse effect, 748–749
  storms in, 768, 769b
    excitation of ocean waves by, 783
  billow clouds in, 783, 783f
  sedimentation in, 748–755
  turbulence of
    excitation of earth's normal modes by, 816–817
atomic bomb, 912–914

bacterium, swimming, 747b–748b, 756–757
balls, physics of flight, 817, 823–825
barotropic fluid, 681b, 724b
basis vectors in Euclidean space
  orthogonal transformation of, 958–959
  Cartesian, 954–955
  spherical and Cartesian, orthonormal, 614
BBGKY hierarchy of kinetic equations, 803
bending modulus (flexural rigidity), 594
bending torque, 593f, 594, 596, 600, 602, 603, 608, 611, 612
bent beam, elastostatics of, 592–596
  elastostatic force-balance equation for, 595
  solutions of force-balance equation
    for clamped cantilever pulled by gravity, 596–597
    for Foucault pendulum, 597–598
    for elastica, 600–601, 601f
bent plate, elastostatics of, 609–613
  elastostatic force-balance equation: shape equation, 610
Bernoulli function, 698–700, 702, 721, 722, 724b
Bernoulli's theorem
  most general version: for any ideal fluid, 698
  for steady flow of an ideal fluid, 698, 700

For general queries contact webmaster@press.princeton.edu.

© Copyright Princeton University Press. No part of this book may be distributed, posted, or reproduced in any form by digital or mechanical means without prior written permission of the publisher.

Bernoulli's theorem *(continued)*
for irrotational flow of an ideal, isentropic fluid, 701
relativistic, 722
bifurcation of equilibria
onset of dynamical instability at bifurcation
in general, in absence of dissipation, 648
for beam under compression, 647–648
for convection, Rayleigh-Bénard, 931
for beam under compression, 603–605
for rapidly spinning star, 607
for rotating Couette flow, 826–827
for Venus fly trap, 607
for whirling shaft, 607
biharmonic equation, 589, 610, 754, 756
billow clouds, 783, 783f
binary star system
tidally locked, shapes of stars, 691
bird flight
V-shaped configuration, 744
wingtip vortices, 734f, 739, 744, 744f
black holes
accretion of gas onto, 784, 890–891
Blasius profile for laminar boundary layer, 758–764
blood flow in arteries, 717–719
boat waves, 846–848
boat, stability of, 685–686
boundary layers
laminar, 757–766
Blasius profile, 758–764
sublayer of turbulent boundary layer, 818
Ekman, for rotating flow, 772–777
vorticity creation in, 758
diffusion of vorticity in, 741–742, 741f, 758
instability of, 822–823
in a pipe, 766
near curved surface, 764–765
separation from boundary, 764, 793
turbulent, 817–825
profile of, 818–820, 818f
separation from boundary, 821f, 820–821
thermal, 923
influence on flight of sports balls, 823–825
Boussinesq approximation, 923–925
bow shock around Earth, 876f
Brunt-Väisälä frequency for internal waves in stratified fluid, 941
bubbles
in water, collapse of, 703
in water, rising, 937
soap, 846
buckling of compressed beam or card, 602
onset of buckling at bifurcation of equilibria, 603–605
onset of elastostatic instability at bifurcation of equilibria, 648
elementary theory of, 602–605, 608–609
free energy for, 604
applications
collapse of World Trade Center buildings, 605–607
mountain building, 609
thermal expansion of pipes, 609
bulk modulus, for elasticity, 581
values of, 586t, 651t
atomic origin of, 649f
relation to equation of state, 650

cantilever, 566, 592–593, 596–597
capillary waves, 844–848
Cartesian coordinates, 954, 964, 966
catastrophe theory
applications to buckling of a beam, 606–607
cavitation, 702–703
centrifugal acceleration, 689, 767
chaos in dynamical systems, 832–834
Lyapunov exponent, 833
Lyapunov time, 832
strange attractors, 833–834
examples of, 832
quantum chaos, 832
chaos, onset of in dynamical systems, 825–833. *See also* turbulence, onset of
in idealized equations and mathematical maps
logistic equation and Feigenbaum sequence, 828–831
Lorenz equations, 834
universality of routes to chaos, 830
characteristics of a dynamical fluid flow, 852, 892–893, 893f, 894–896
circulation, 729, 733, 734, 739–740
and lift on airplane wing, 743
as flux of vorticity, 739
evolution equations and Kelvin's theorem, 740
climate change, 748–749, 755. *See also* greenhouse effect
clouds, billow, 783, 783f
Coanda effect, 809f, 809–810, 820, 821f
collective effects in plasmas, 907
collisionless shocks, 907
commutator of two vector fields, 735n
component manipulation rules, 954–957
compressible fluid flow
equations for, 877–879
1-dimensional, time-dependent, 891–897
Riemann invariants for, 891–895

For general queries contact webmaster@press.princeton.edu.

© Copyright Princeton University Press. No part of this book may be distributed, posted, or reproduced in any form by digital or mechanical means without prior written permission of the publisher.

nonlinear sound wave, steepening to form shock, 894, 894f
in shock tube. *See* shock tube, fluid flow in
transonic, quasi-1-dimensional, steady flow, 884f, 880–891
equations in a stream tube, 880–882
properties of, 882–883
relativistic, 890
conductivity, thermal, κ
energy flux for, 714
connection coefficients
for orthonormal bases in Euclidean space, 615
pictorial evaluation of, 616f
used to compute components of gradient, 617
for cylindrical orthonormal basis, 615
for spherical orthonormal basis, 616
conservation laws
differential and integral, 966
continental drift, 932b
contraction of tensors
formal definition, 950–951
in slot-naming index notation, 957
component representation, 955
convection
onset of convection and of convective turbulence, 830–831, 931
Boussinesq approximation for, 924–925
between two horizontal plates at different temperatures: Rayleigh-Bénard convection, 925–933
Boussinesq-approximation analysis, 925–928, 930
critical Rayleigh number for onset, 930, 930f, 933
pattern of convection cells, 930–931, 931f
toy model, 929
in a room, 931
in Earth's mantle, 932
in a star, 933–937
in the solar convection zone, 936
coordinate independence. *See* geometric principle
Coriolis acceleration, 735, 767–768
as restoring force for Rossby waves, 858
critical point of transonic fluid flow, 883, 886, 891
Crocco's theorem, 702, 742
cross product, 963–964
curl, 963–964
curve, 947
cylindrical coordinates
related to Cartesian coordinates, 614
orthonormal basis and connection coefficients for, 614–615
expansion and shear tensor in, 617, 618
d'Alembert's paradox, for potential flow around a cylinder, 765
dam, water flow after breaking, 857–858, 897
De Laval nozzle, 887
decibel, 865
derivatives of scalars, vectors, and tensors
directional derivatives, 960–961
gradients, 617, 961
Lie derivative, 735n
diffusion coefficient
for temperature, in thermally conducting fluid, 920
for vorticity, in viscous fluid, 741
diffusion equation
for temperature in homogenous medium, 920
for vorticity, in viscous fluid, 741
dimensional analysis for functional form of a fluid flow, 790–791
dimensional reduction in elasticity theory, 590b
for bent beam, 592–595
for bent plate, 609–613
directional derivative, 960–961
displacement vector, in elasticity, 570
gradient of, decomposed into expansion, shear, and rotation, 570–571
Navier-Cauchy equation for, 587. *See also* Navier-Cauchy equation for elastostatic equilibrium
dissipation, 724b
divergence, 962
DNA molecule, elastostatics of, 599–600
double diffusion, 937–940
drag force and drag coefficient, 792
at low Reynolds number (Stokes flow), 753–754
influence of turbulence on, 792f, 794, 820–821
on a flat plate, 763–764
on a cylinder, 792–794, 792f
on an airplane wing, 820–821
on sports balls, 825
on fish of various shapes, 797–798

Earth. *See also* atmosphere of Earth; elastodynamic waves in Earth
internal structure of, 651t
pressure at center of, 649
Moho discontinuity, 650
mantle viscosity, 755–756
mantle convection, 932
continental drift, 932
normal modes excited by atmospheric turbulence, 816
eddies
in flow past a cylinder, 791f, 793–794
in turbulence, 798–800, 802, 804–807, 811–814

For general queries contact webmaster@press.princeton.edu.

© Copyright Princeton University Press. No part of this book may be distributed, posted, or reproduced in any form by digital or mechanical means without prior written permission of the publisher.

Einstein summation convention, 954
Ekman boundary layer, 772–777
Ekman number, 768
Ekman pumping, 773
elastic energy density, 583–584
  elastic physical free energy density, 584
elastic limit, 580, 581f
elastic moduli, 580–582
  physical origin of, and magnitudes, 585–586, 586t
  for anisotropic solid, 580
  for isotropic solid
    shear and bulk, 581–582
    Young's, 591
    numerical values, 586t
  in Earth, 651t
elastodynamic waves in a homogeneous, isotropic medium, 630–642
  influence of gravity at ultralow frequencies, 639
  wave equation, 635–636
  energy density, energy flux, and Lagrangian for, 641–642
  decomposition into longitudinal and transverse, 636, 637f, 640
  Heaviside Green's functions for, 658–660
  longitudinal waves, 637–638
    displacement is gradient of scalar, 637, 639–640
    sound speed, dispersion relation, group and phase velocities, 637–638
  transverse waves, 638–639
    displacement is curl of a vector, 637, 639–640
    sound speed, dispersion relation, group and phase velocities, 638–639
  Rayleigh waves at surface, 654–657
elastodynamic waves in Earth
  body waves, 650–654
    P-modes and S-modes, 650
    wave speeds at different depths, 651t
    geometric optics ray equation, 652
    junction conditions and mixing of, at discontinuities, 651–654, 651f, 653f
    rays inside Earth, 653f
  edge waves, 654
    Rayleigh wave at Earth's surface, 654–657
    Love waves at Earth's surface, 658
    internal waves, 941
elastodynamic waves in rods, strings and beams, 642–648
  waves on a string under tension, 644–645
  flexural waves in a stretched or compressed beam, 645–646
  torsion waves in a circular rod, 643–644
elastodynamics. *See also* elastodynamic waves in Earth; elastodynamic waves in a homogeneous, isotropic medium; elastodynamic waves in rods, strings and beams
  force density, 587
    in cylindrical coordinates, 624
  when gravity can be ignored, 631
  momentum conservation, 631
  wave equation for displacement vector, 635–636
  quantization of, 667–670
elastostatic force balance. *See* Navier-Cauchy equation for elastostatic equilibrium
electromagnetic field
  stress tensor, 971
energy conservation, Newtonian, 695
energy, relativistic, 972
  kinetic, 972
  Newtonian limit, 972
entrainment of one fluid by another
  laminar, 796–797
  turbulent, 806, 809–810
equations of state
  polytropic, 681b, 687, 726b, 878
    thermodynamic quantities in terms of sound speed, 878–879
  for ideal or perfect gas, 675n
  for fluids, 680b–681b, 725b
Euler equation of fluid dynamics, 697, 725b
Eulerian changes, 725b
evanescent wave, 654
expansion, in elasticity theory, Θ, 571, 572b, 574, 577
  temperature change during, 585
expansion rate of fluid, θ, 693, 725b
explosions and blast waves
  in atmosphere or interstellar space, 908–914
  into stellar wind, 915–916
  underwater, 914–915

Feigenbaum sequence and number, 828–831
finite-element methods, 565, 590b, 606f
fish
  streamlining and drag coefficients, 797–798
  swimming, 744, 747b–748b
flexural rigidity (bending modulus), 594
flexural waves on a beam or rod, 645–646
flows, fluid. *See* fluid flows
fluid, 677. *See also* fluid dynamics, fundamental equations; fluid dynamics, relativistic; fluid flows; fluid-flow instabilities
  thermodynamics for, 679b–681b
  perfect (ideal), 675, 675n
  Newtonian, 712, 726b
  non-Newtonian, 712f

For general queries contact webmaster@press.princeton.edu.

© Copyright Princeton University Press. No part of this book may be distributed, posted, or reproduced in any form by digital or mechanical means without prior written permission of the publisher.

fluid dynamics, fundamental equations. *See also* fluid dynamics, relativistic
terminology, 724b–726b
mass density and flux, 708t
mass conservation, 692–693, 970–971
for ideal fluid in external gravitational field
momentum density and flux, 708t
Euler equation (momentum conservation), 696–697
energy density and flux, 704, 708t
energy conservation, 707
entropy conservation, 697, 707
for self-gravitating ideal fluid, 705b–707b, 709
for viscous, heat-conducting fluid in external gravitational field, 710–719, 919–920
momentum and energy densities and stress tensor, 715t
viscous stress tensor, 712
Navier-Stokes equation (momentum conservation), 712–713. *See also* Navier-Stokes equation
total energy flux, 715t
viscous and thermal-conductive energy flux, 714
entropy evolution (dissipative heating), 715–716
for viscous, heat-conducting, incompressible flow with negligible dissipation, 919–920
Boussinesq approximation, 924–925. *See also* convection
in rotating reference frame, 767–768, 770
fluid dynamics, relativistic, 719–724
fundamental equations, 719–720
nonrelativistic limit, 723–724
relativistic Bernoulli equation and theorem, 721–722
application to steady, relativistic jet, 721–722
application to relativistic shock wave, 902–903
fluid flows. *See also* fluid-flow instabilities; fluid dynamics, fundamental equations; fluid dynamics, relativistic
between two plates, steady, 718
through a pipe
laminar, 716–717, 766
onset of turbulence, 787
around a body at low Reynolds number: Stokes flow, 749–754, 749f
around a cylinder: high-Reynolds-number, potential flow, 765, 789–794
types of
barotropic, inviscid, 736–738, 740
viscous, 710–716
high-Reynolds-number, 757–766
low-Reynolds-number, 746–757. *See also* low-Reynolds-number flow
irrotational (potential), 701
irrotational, incompressible, 837
incompressible, 709–710
compressible, 875–916. *See also* compressible fluid flow
laminar, 716–717. *See also under* boundary layers; jets; wakes
turbulent, 787–834. *See also under* boundary layers; jets; wakes
nearly rigidly rotating, 766–768
geostrophic, 770–777
self-similar, 759. *See* self-similar flows
fluid-flow instabilities. *See also* fluid flows
convective. *See* convection
density inversion: Rayleigh-Taylor instability, 783–784
shear flows
Kelvin-Helmholtz instability, 778–782
influence of gravity and density stratification, 782–783, 784–786
laminar boundary layer, 822–823
rotating Couette flow, 784, 785f, 825–828
force density, as divergence of stress tensor, 578
Foucault pendulum, 597–598
fracture, criterion for safety against, 621
free energy
physical (Helmholtz) free energy
for elastic medium, 584, 603–604
fundamental thermodynamic potentials. *See also under* thermodynamics
physical-free-energy potential
for elastic medium, 584, 603–604

g modes of sun, 837, 849–850
gas, 678, 725b
perfect gas, nonrelativistic, 726b
ideal, 725b
Gauss's theorem, 965
geometric object, 943
geometric principle, 944–945, 948
examples, 966, 967
geometrized units, 971–972, 973
geostrophic flow, 770–777
global warming, 748–749, 755
gradient operator, 617, 961
Gran Telescopio Canarias, 609
gravity, Newtonian
gravitational potential, Φ, 682
field equation for Φ, 682
gravitational acceleration $\mathbf{g}$, 682
gravitational stress tensor, 705b
gravitational energy density, 706b
gravitational energy flux, 706b
total gravitational energy, 709
gravity waves on water, 837–843
arbitrary depth, 837–840

For general queries contact webmaster@press.princeton.edu.

© Copyright Princeton University Press. No part of this book may be distributed, posted, or reproduced in any form by digital or mechanical means without prior written permission of the publisher.

gravity waves on water *(continued)*
shallow water, 840–843
dam breaking: water flow after, 857
nonlinear, 840–841, 843, 850–858, 897
solitary waves (solitons) and KdV equation, 850–858
deep water, 840
viscous damping of, 842
capillary (with surface tension), 844–848
Green's functions
for elasticity theory, 590b
for elastostatic displacement, 626–627
for elastodynamic waves, 658–661, 660f
greenhouse effect, 748. *See also* climate change
gyre, 773, 775–776, 805

heat conduction, diffusive. *See also* diffusion equation
in the sun, 937
in a flowing fluid, 920
Heaviside Green's functions, 658–660, 660f
helioseismology, 848–850
high-Reynolds-number flow, 757–766
boundary layers in. *See* boundary layers
Hilbert space, 956b
Hooke's law, 568f, 591
realm of validity and breakdown of, 580, 581f
hydraulic jump, 903–904, 904f
hydrostatic equilibrium
in uniform gravitational field
equation of, 681
theorems about, 682–683
of nonrotating stars and planets, 686–689
of rotating stars and planets, 689–691
barotropic: von Zeipel's theorem, 702
centrifugal flattening, 690, 691
hydrostatics, 681–691

ideal gas. *See* gas, ideal
impedance
acoustic, 654
incompressible approximation for fluid dynamics, 709–710, 725b
index gymnastics. *See* component manipulation rules
index of refraction
for Earth's atmosphere, 814–815
for seismic waves in Earth, 652
inner product
in Euclidean space, 948–950, 955
in quantum theory, 956b
instabilities in fluid flows. *See* fluid-flow instabilities
integrals in Euclidean space
over 2-surface, 965
over 3–volume, 965
Gauss's theorem, 965
intermittency in turbulence, 798–799, 807
internal waves in a stratified fluid, 941
interstellar medium, 891, 914–916
inviscid, 725b
irreducible tensorial parts of second-rank tensor, 572b–574b, 577, 711
irrotational flow (vorticity-free), 701, 725b, 837
isentropic, 725b
isobar, 725b

jets
laminar, 796–797
turbulent, 809f, 810
Joukowski's (Kutta-Joukowski's) theorem, 743
Joule-Kelvin cooling, 708, 708f
junction conditions
elastodynamic, 588–589, 651, 654
hydraulic jump, 903–904
shock front. *See* Rankine-Hugoniot relations for a shock wave
Jupiter, 687, 689, 702, 801b

Kármán vortex street, 791f, 794
Keck telescopes, 609–611
Kelvin-Helmholtz instability in shear flow, 778–782
influence of gravity on, 782–783
onset of turbulence in, 801b
Kelvin's theorem for circulation, 740, 746, 824
Kepler's laws, 691, 784, 952
Knudsen number, 755n
Kolmogorov spectrum for turbulence, 810–815
phenomena missed by, 814
derivation of, 810–812
for transported quantities, 814–816
Korteweg–de Vries equation and soliton solutions, 850–856, 858
Kutta-Joukowski's theorem, 743

Lagrangian changes, 725b
lagrangian methods for dynamics
lagrangian density
energy density and flux in terms of, 642
for elastodynamic waves, 642
Lamé coefficients, 582
laminar flow, 716–717. *See also under* boundary layers; jets; wakes
laplacian, 665, 962
Levi-Civita tensor in Euclidean space, 962–964
product of two, 963

For general queries contact webmaster@press.princeton.edu.

© Copyright Princeton University Press. No part of this book may be distributed, posted, or reproduced in any form by digital or mechanical means without prior written permission of the publisher.

Lie derivative, 735n
LIGO (Laser Interferometer Gravitational-Wave Observatory), noise in, 626
liquid, 678, 726b
  bulk modulus for, 678
liquid crystals and LCDs, 712
logistic equation, 828–831
Lorentz contraction
  of rest-mass density, 723
Lorentz force
  in terms of electric and magnetic fields, 944, 952
Lorenz equations for chaotic dynamics, 834
Lorenz gauge, 760
low-Reynolds-number flow, 746–757
  nearly reversible, 746
  pressure gradient balances viscous stress, 746
  regimes of: small-scale flow, or very viscous large-scale flow, 746
Lyapunov time and exponent, 832–833

Mach number, 882
Maple, 619, 647, 691, 858
mass conservation, 692–693, 970–971
matched asymptotic expansions, 874
  in Stokes flow, 753–754
  in theory of radiation reaction, 869–871, 872f
Mathematica, 619, 647, 691, 858
Matlab, 619, 647, 691, 858
mean molecular weight, 680b, 726b
method of moments. *See* moments, method of
metric tensor
  geometric definition, 949–950
  components in orthonormal basis, 955
microcantilever, 597
mixing length for convection in a star, 935–936
Moho discontinuity, 648, 650
moments, method of: applications
  dimensional reduction in elasticity theory, 594–595, 612–613
momentum, relativistic, 972
  Newtonian limit, 972
momentum conservation, Newtonian
  differential, 694–695, 970
  integral, 970
multipole moments
  in sound generation, 865–867

National Ignition Facility, 664
Navier-Cauchy equation for elastostatic equilibrium, 588
  in cylindrical coordinates, 624
  displacement is biharmonic, 589
  boundary conditions for, 588–589
  methods for solving, 590b
    simple methods, 619–622
    separation of variables, 624–626
    Green's function, 626–627
Navier-Stokes equation
  general form, 712
  for incompressible flow, 713, 726b
  in rotating reference frame, 767
neutral surface, in elasticity theory, 592–593
neutrinos
  from supernovae, 914
neutron stars
  birth in supernovae, 914
  structures of, 579, 734
  r-modes of oscillation, 860
  accretion of gas onto, 784, 890–891
noise
  thermal noise, 598, 622–623, 626
normal modes
  of elastic bodies, 661–662, 664–668
    quantization of, 668–669
  of elastic, homogeneous sphere, 661–662, 664–667
    radial, 661, 664–665
    ellipsoidal, 662, 666–667
    torsional, 661–662, 665–666
  of sun, 848–850
nuclear reactor
  cooling of, 922–923

ocean currents
  surface currents driven by winds, 775–776
  deep currents driven by gyre pressure, 768, 775–776
ocean waves
  generation by atmospheric pressure fluctuations in storms, 783
  damping by turbulent viscosity, 842
  breaking near shore, 903–904
orthogonal transformation, 958–959

p modes of sun, 849–850
Parseval's theorem, 811
particle conservation law, 966
particle kinetics
  geometric form, 951–953
  in index notation, 957–958
Pascal, unit of stress, 578
path of particle (Newtonian analog of world line), 947–948
paths, for visualizing fluid flows, 699b
Péclet number, 921

For general queries contact webmaster@press.princeton.edu.

© Copyright Princeton University Press. No part of this book may be distributed, posted, or reproduced in any form by digital or mechanical means without prior written permission of the publisher.

perfect fluid (ideal fluid), 675, 675n, 968
  Euler equation for, 697, 971
  stress tensor for, 968–969, 970
phonons for modes of an elastic solid, 667–670
physical laws, geometric formulation of. *See* geometric principle
piezoelectric fields, 586
pipe
  stressed, elastostatics of, 619–621
  fluid flow in, 716–717, 766, 787
Pitot tube, 700, 701f
Planck energy, 580
Planck length, 579, 580
Poiseuille flow (confined laminar, viscous flow)
  between two plates, 718–719
  down a pipe, 717, 922
Poiseuille's law, for laminar fluid flow in a pipe, 717
Poisson's equation, 686, 705
Poisson's ratio, 591–592, 586t
polytrope, 687–689
potential flow (irrotational flow), 701
Prandtl number, 920, 921t
pressure, 968
  as component of stress tensor, 968–969
pressure self-adjustment in fluid dynamics, 742
proportionality limit, in elasticity, 580, 581f

radiation reaction, theory of
  slow-motion approximation, 871
  matched asymptotic expansion, 871
  radiation-reaction potential, 871
  damping and energy conservation, 872, 873
  runaway solutions, their origin and invalidity, 872–873
  examples
    electromagnetic waves from accelerated, charged particle, 873
    sound waves from oscillating ball, 869–874
radiative processes
  Thomson scattering, 937
rank of tensor, 949
Rankine-Hugoniot relations for a shock wave, 900
  derivation from conservation laws, 898–900
  physical implications of, 900–902
  for polytropic equation of state, 905
  for strong polytropic shock, 905
  relativistic, 902–903
rarefaction wave, 895f, 896
Rayleigh criterion for instability of rotating flows, 784
Rayleigh number, 928
Rayleigh waves at surface of a homogeneous solid, 654–657, 659, 661, 839–840, 941
Rayleigh-Taylor instability, 783–784
renormalization group
  applied to the onset of chaos in the logistic equation, 831
resistance in Stokes fluid flow, 753
rest frame, local, 677, 719–720
rest mass, 972
Reynolds number, 716, 726b
  as ratio of inertial to viscous acceleration, 746
Reynolds stress for turbulence, 802
  and turbulent viscosity, 804
Richardson criterion for instability of shear flows, 785–786
Richardson number, 785–786
Riemann invariants, 852, 891–897, 901–902
rocket engines, fluid flow through, 887–890
rod. *See* bent beam, elastostatics of
Rossby number, 768
Rossby waves in rotating fluid, 858–861
rotating reference frame, fluid dynamics in, 766–777
rotation, rate of, in fluid mechanics, 711, 726b
  as vorticity in disguise, 711
rotation group, 572b–574b, 959
rotation matrix, 959
rotation tensor and vector, in elasticity theory, 571, 573b–574b, 575–576, 577
rupture point, in elasticity, 580, 581f

Saint-Venant's principle, for elastostatic equilibrium, 590b
salt fingers due to double diffusion of salt and heat, 937–940
scaling relations in fluid flows
  between similar flows, 791–792
  for drag force on an object, 765
  for Kolmogorov turbulence spectrum, 789, 810–814
Schrödinger equation
  energy eigenstates (modes) of, 848–849
  nonlinear variant of, and solitons, 856–857
Schwarzschild criterion for onset of convection in a star, 935, 935f
secondary fluid flows, 775–776
sedimentation, 749, 754–755
Sedov-Taylor blast wave, 909–912
seismic waves. *See* elastodynamic waves in Earth
self-gravity, in fluid dynamics, 705b–706b, 709
self-similar flows
  boundary layer near flat plate: Blasius profile, 758–763
  Sedov-Taylor blast wave, 909–912
  underwater blast wave, 914–915
  flow in shock tube, 916
  stellar wind, 915–916
  water flow when dam breaks, 857–858
separation of variables for Navier-Cauchy equation, 590b, 624–625

For general queries contact webmaster@press.princeton.edu.

© Copyright Princeton University Press. No part of this book may be distributed, posted, or reproduced in any form by digital or mechanical means without prior written permission of the publisher.

shear, rate of, 711, 726b
shear modulus, for elasticity, 581, 586t, 651t
shear tensor, in elasticity theory, 571, 572b–574b, 574–577
  stretch and squeeze along principal axes, 574–575, 575f
shock tube, fluid flow in
  analyzed using similarity methods, 916
  analyzed using Riemann invariants, 895–896
  shock front in, 906
shock waves (shock fronts) in a fluid, adiabatic
  terminology for, 898, 900f
  inevitability of, 897
  Rankine-Hugoniot relations for, 900. *See also* Rankine-Hugoniot relations for a shock wave
  shock adiabat, 900–901, 901f
  properties of, 900–901
  internal structure of, 898, 906–907
    role of viscosity in, 898
  patterns of
    around a supersonic aircraft, 876f
    bow shock in solar wind around Earth, 876f
    Mach cone, 907–908, 907f
    Sedov-Taylor blast wave, 909–912
  sonic boom, 908, 908f
shock waves in an elastic medium, 663–664
shock waves in a plasma, collisionless, 907
similarity methods in fluid mechanics. *See* self-similar flows
slot-naming index notation, 957–958, 961, 963
smoke rings, 744f
soap film, shapes of, 846
solar wind, 875, 876f
  collisionless shocks in, 907
  bow shock at interface with Earth, 876f
solid-body normal modes. *See* normal modes, of elastic bodies
solitons
  balance of nonlinearity against dispersion in, 853–854
  equations exhibiting, 856–857
  Korteweg–de Vries equation and solutions, 852–856, 858
  venues for, 856–857
    in nonlinear gravity waves on water, 852–856, 858
sonic boom, 889b, 907–908
sound speed in elastic solid, C_L, 586t, 638
sound waves in a fluid
  wave equation, 862
  sound speed, 862
  analysis of, 862–865
  energy density, 864
  energy flux, 865
  in inhomogeneous fluid: example of prototypical wave equation, 863
  generation of, 865–869
    radiation reaction on source, 869–874
  attenuation of, 868
  nonlinearity of, and shock formation, 894
space shuttle, 889b–890b
  sonic boom from, 889b, 907–908
specific heats, C_p, c_p, C_V, and c_V, 678. *See also* adiabatic index
  for ideal gas with internal degrees of freedom, 879–880
speed of light
  constancy of, 972
  in geometrized units, 972
spherical coordinates
  related to Cartesian coordinates, 614
  orthonormal bases and connection coefficients, 614, 616
    expansion and shear tensor in, 617, 618b
sports, physics of, 823–825
stagnation pressure, 700, 792
steady fluid flow, 726b
Stokes flow, 749–754, 749f, 766
  drag force in: Stokes' law, 753
Stokes' paradox for fluid flow past a cylinder, 754
Stokes' theorem for integrals, 965
storms, fluid dynamics of, 768, 769b, 842
strain tensor, in elasticity theory, 576
strange attractors, 833–834
stratosphere, 683, 684f, 731, 748, 755, 784–786
streaks, for visualizing fluid flows, 699b
stream function for 2-dimensional incompressible flow
  in Cartesian coordinates, 759
  in any orthogonal coordinate system, 760b–761b, 766
stream tube, in fluid dynamics, 699–700, 700f, 721–722, 721f
streamlines, for visualizing fluid flows, 698, 699f
stress polishing mirrors, 609–611, 611f, 613
stress tensor
  geometric definition of, 577, 967
  components, meaning of, 968
  symmetry of, 968
  for specific entities
    electromagnetic field, 971
    perfect fluid, 696, 968–969, 970
    strained elastic solid, 581, 584
    strained and heated elastic solid, 584
  magnitudes of, 578–580
stress-energy tensor
  for perfect fluid, 720
    nonrelativistic limit, 723–724
structure function, for fluctuations, 815
sun. *See also* solar wind
  core of, 933f, 937
  convection zone, 933f, 936
  normal modes of, 848–850. *See also* normal modes

For general queries contact webmaster@press.princeton.edu.

© Copyright Princeton University Press. No part of this book may be distributed, posted, or reproduced in any form by digital or mechanical means without prior written permission of the publisher.

superfluid, rotating, 733–734
supernovae
  neutron stars produced in, 914
  Sedov-Taylor blast wave from, 914–915
surface tension, 844b–845b
  force balance at interface between two fluids, 846
swimming mechanisms, 744, 747b–748b, 756–757

tangent space, 947
tangent vector, 947
Taylor rolls, in rotating Couette flow, 826, 826f
Taylor-Proudman theorem for geostrophic flow, 771
tea cup: circulating flow and Ekman boundary layer, 776–777
temperature diffusion equation, 920
tensor in Euclidean space
  definition and rank, 949
  algebra of without coordinates or bases, 949–951
  expanded in basis, 954
  component representation, 955–957
tensor in quantum theory, 956b
tensor product, 950
thermal diffusivity, 920, 921t
thermal plume, 933
thermodynamics. *See also* equations of state; fundamental thermodynamic potentials
  first law of for fluid, 679b–680b
thermoelastic noise in mirrors, 623, 626
thermoelasticity, 584–585
Thomson scattering of photons by electrons, 937
time derivative
  advective (convective), 692, 724b, 892, 970
  fluid, 736
Tollmien-Schlichting waves, 823
tomography, seismic, 663
tornado, 738, 739f
  pressure differential in, 702, 738
torsion pendulum, elastostatics of, 621–622
transformation matrices between orthogonal bases, 958–959
trumpet, sound generation by, 868
tsunamis, 841b, 843, 922
turbulence, 787–834
  weak and strong, 800
  characteristics of
    3-dimensional, 794
    disorder, 798
    irregularly distributed vorticity, 799
    wide range of interacting scales, 798–799
    eddies, 798–800, 802, 804–807, 811–814
    efficient mixing and transport, 799
    large dissipation, 799
    intermittency, 798–799, 807, 814, 831
  onset of. *See* turbulence, onset of
  vorticity in, 799–800
    drives energy from large scales to small, 799f
  semiquantitative analysis of, 800–817
    Kolmogorov spectrum, 810–813, 813f, 815. *See also* Kolmogorov spectrum for turbulence
    weak turbulence formalism, 800–810. *See also* weak turbulence formalism
  generation of sound by, 869
turbulence, 2-dimensional analog of, 801b
  inverse cascade of energy, 799n
  transition to (3-dimensional) turbulence, 800
turbulence, onset of. *See also* chaos, onset of in dynamical systems
  critical Reynolds number for, 787, 794, 822, 826
  in convection, 830, 831
  in flow past a cylinder, 789–794, 800
  in rotating Couette flow, 825–828
  routes to turbulence
    one frequency, two frequencies, turbulence, 825–828
    one frequency, two frequencies, phase locking, turbulence, 831
    one frequency, two frequencies, three frequencies, turbulence, 831
    period doubling sequence, 830–831
    intermittency, 831

ultrasound, 663–664

vector
  as arrow, 946
  as derivative of a point, 947
vector components, 954
vector in quantum theory, 956b
velocity, 947
velocity potential for irrotational flow, 701
violin string, sound generation by, 868
viscosity, bulk, coefficient of, 712, 724b
viscosity, molecular origin of, 713–714
viscosity, shear, coefficient of, 712, 726b
  dynamic, η, 713, 724b
  kinematic, ν, 713, 725b
  values of, for various fluids, 713t, 921t
  for monatomic gas, 714
volcanic explosions, 748, 755
volume in Euclidean space
  2–volume (area), 964
  vectorial surface area in 3-space, 965
  3–volume, 965
  n-volume, 962
  differential volume elements, 966

For general queries contact webmaster@press.princeton.edu.

© Copyright Princeton University Press. No part of this book may be distributed, posted, or reproduced in any form by digital or mechanical means without prior written permission of the publisher.

von Zeipel's theorem, 702
vortex. *See also* vortex lines; vorticity
  diffusive expansion of, 742
  above a water drain, 729, 732, 777
  vortex sheet, 782, 801b
  vortex ring, 744
  starting vortex, 824, 825f
  vortex street, Kármán, 791f, 794
  wingtip vortex, 734f, 739, 744, 744f
  tornado, 702, 732, 738, 739f
  vortex generated by spatula, 745–746
  vortex generators, on airplane wing, 821–822, 821f
vortex cores, in superfluid, 733–734
vortex generator on airplane wing, 821–822, 821f
vortex lines, 734, 734f
  diffuse due to viscosity, 741–742
  frozen into fluid, for barotropic, inviscid flows, 736–738, 737f
vortex rings, 744, 744f
vorticity, 697, 731–732, 732f
  relation to angular velocity of a fluid element, 697–698
  measured by a vane with orthogonal fins, 732
  sources of, 744–746
  evolution equations for, 735–738, 741
    diffusion of vorticity, 741
    frozen into an inviscid, barotropic flow, 736–737
  delta-function: constant-angular-momentum flow, 732–733

wakes
  2-dimensional, behind cylinder
    laminar, 794–795
    turbulent, 805–810
  3-dimensional, behind sphere
    laminar, 796
    turbulent, 810
water waves. *See* gravity waves on water; sound waves in a fluid
wave equations
  for elastodynamic waves, 635
  for sound waves, 862, 863
weak turbulence formalism, 800–810
  Reynolds stress and turbulent viscosity, 802, 803–804
  turbulent diffusion coefficient, 805
  turbulent thermal conductivity, 805
  correlation functions in, 802–803
  spatial evolution of turbulent energy, 804, 808f, 808–809
winds
  around low-pressure region, 770
  drive ocean's surface currents, 772–776, 805
  in stratosphere, 784–785
  lee waves in, 821n
wingtip vortices, 734f, 739, 744, 744f
Womersley number, 719
World Trade Center buildings, collapse of, 605–607

yield point, in elasticity, 580, 581f
  origin of yield: dislocations, 586, 587f
  yield strains for various materials, 586t
Young's modulus, 582, 589–592
  values of, for specific materials, 586t

zero point energy, 669

For general queries contact webmaster@press.princeton.edu.